Research Center Borstel
Leibniz-Center for Medicine and Biosciences
Managing Director: Prof. Dr. S. Ehlers

Division of Structural Biochemistry

Head: Prof. Dr. O. Holst

‡

Immunochemical investigations of the cell envelope components isolated from *Streptococcus uberis*

‡

Dissertation

for

Fulfillment of Requirements

for the Doctoral Degree

of the University of Lübeck

from the Department of Natural Sciences

Submitted by

Anna Czabanska

from Zabrze, Poland

Borstel, March 2013

First referee: Prof. Dr. rer. nat. Otto Holst

Second referee: Prof. Dr. rer. nat. Tamas Laskay

Date of oral examination: 28.06.2013

Approved for printing. Lübeck, 04.12.2013

‘Structure without function
is a dead corpse
and function without structure
is a ghost.’

(Vogel and Wainwright, 1969)

TABLE OF CONTENTS

Abreviations

Ala	Alanine
bo TLR2	Bovine Toll-like receptor 2
CPS	Capsular polysaccharide
DGlcDAG	Diglucosyldiacylglycerol
EPS	Exopolysaccharide
Ery	Erytromycin
Fuc	Fucose
G1, G2, G3	Glycolipid 1, 2 and 3
Gal	Galactose
GalN	Galactosamine
GC	Gas chromatography
Glc	Glucose
GlcA	Glucuronic acid
GlcN	Glucosamine
GlcNAc	*N*-Acetylglucosamine
HEK293	Human Embryonic Kidney 293 cells
IL-1,- 6,- 8	Interleukin-1, -6, -8
LTA	Lipoteichoic acid
Man	Mannose
ManNAc	*N*-Acetylmannosamine
MGlcDAG	Monoglucosyldiacylglycerol
MNC	Mononuclear cell
MS	Mass spectroscopy
MurNAc	*N*-Acetylmuramic acid
NMR	Nuclear magnetic resonance

PAMP	Pathogen-associated molecular pattern
pbMEC	Primery bovine mammary epithelial cells
RAW 264.7	Mouse leukaemic monocyte macrophage cell line
Rha	Rhamnose
SCWP	Secondary cell wall polymer
TLC	Thin-layer chromatography
TLR2	Toll-like receptor 2
TNF-α	Tumor necrosis factor α
WTA	Wall teichoic acid

1. Introduction

1.1. Mastitis

Bovine mastitis is defined as inflammation of the mammary glands and usually arises as a result of bacterial infection (Leigh, 1999). The disease can be caused by over 135 different pro- and eukaryotic organisms as diverse as bacteria, mycoplasma, yeast and algae (Watts, 1988). The majority of cases are, however, due to infection with one of five bacterial species: *Streptococcus uberis*, *Escherichia coli*, *Staphylococcus aureus*, *Streptococcus dysgalactiae* and *S. agalactiae* (Bradley, 2002). The mastitis pathogens can be classified as environmental or contagious. The incidences caused by contagious pathogens (e.g. *S. aureus, S. dysgalactiae, S. agalactiae*), due to the hygiene education, have decreased over last decade (Blowey and Edmondson, 2010). The amount of mastitis cases caused by environmental pathogens (*S. uberis, E. coli*) remains unchanged (Zadoks and Fitzpatrick, 2009).

Depending on factors in the host and the invading pathogen, the signs of mastitis are different and the infection may result in sub-clinical or clinical disease. Sub-clinical mastitis, showing no obvious signs of disease, proceeds often unnoticed and untreated, and may result in long duration of the infection. The symptoms of the clinical disease can range from visible abnormalities in the milk (protein aggregates or clots) accompanied by pain and swelling in the affected gland to production of a secretion which is composed solely of aggregated proteins in a serous fluid. In severe cases there may be systemic signs such as elevated temperature and loss of appetite which may develop to bacteraemia, septicaemia and eventually death of the animal (Leigh, 1999).

The diagnosis of mastitis is based on the somatic cell count in milk. Leukocytes, including macrophages, neutrophils and lymphocytes are typical ingredients of the milk. As long as their number is below 200,000 cells/ml the cow is considered healthy. Increase in cell count, primarily due to the influx of neutrophils is a result of immune response on the pathogen. Milk from sub-clinically infected quarters usually contains about 250,000 cells/ml (but this figure may vary widely), and that from clinically infected gland usually contains in excess of 2,000,000 cells/ml (Akers and Nickerson, 2011). The inflammatory reaction followed by increase in the numbers of neutrophils in the gland results in a lower

rate of milk production and quality of the secretion. Such milk is unmarketable (Leigh, 1999).

Mastitis is treated with antibiotics. Despite the fact, that it is strongly recommended to make a treatment decision based on culture results (there is no rapid test so far), only every second farmer in U.S. follows the recommendations. Also, the prevention of infection is based on the administration of antibiotics to the glands during the dry period – when the cow is the most susceptible to infection (Barlow, 2011). Since there are neither good working vaccines against mastitis available nor rapid diagnostic tests and alternative medicaments or antibiotics, the research on this disease is very important.

1.2. *Streptococcus uberis*

Streptococcus uberis is an important pathogen of the udder in the modern dairy industry. It ranks among the main causes of mastitis in countries around the world. The bacterium is classified as environmental pathogen, since it was found in body sites, manure, pasture and bedding material. New infections with *S. uberis* occur most often during dry period and in heifers before calving (Zadoks et al., 2003). In experimental infections models, it was shown that *S. uberis* rapidly colonizes the mammary gland, induce neutrophils diapedesis, and cause the acute inflammation of the mammary gland, during which the quarter becomes swallowed and painful, and milk denaturated. Next to the acute form of mastitis, *S. uberis* can cause clinical chronic and recurrent, and a subclinical form of disease (Leigh et al., 2010).

Many efforts have been invested into designing an effective vaccine against *S. uberis*. The immunization against *S. uberis* mastitis was initially demonstrated in early 1990s. It was shown that the treatment of the cattle with *S. uberis via* the teat canal reduces the number of bacteria present in the milk, after the challenge with the same strain. Subsequent studies using crude vaccines have shown that neither heat-killed *S. uberis* nor live bacteria administered locally to the mammary gland could increase resistance against homologous challenge, i.e. the same strain as the vaccine (Finch et al., 1997).
The later attempts at protection against *S. uberis* consisted of using cloned Gap C molecule and plasminogen activator, PauA (Schukken et al., 2011). The vaccination with Gap C resulted in less severe inflammatory response (Fontaine et al., 2002) and in the case of

PauA, the vaccination protected against *S. uberis* strains that possess this gene, but *S. uberis* isolates with alternative pathways have been shown to exist on commercial dairies.

During the last decades several potential virulence factors of *S. uberis* have been proposed. Potential antiphagocytic factors include: capsule, neutrophil toxin, R-like protein and M-like protein. Proposed virulence factors which are secreted outside the cell wall are hyaluronidase and uberis factor. Furthermore, the activation of plasminogen by *S. uberis* seems to be an important mechanism to obtain nutritions for optimal growth (Oliver et al., 1998).

1.3. The Gram-positive cell envelope

The cell envelope of bacteria possesses a complex structure that serves to protect these organisms from their environment, unpredictable and often hostile. The main constituent of the Gram-positive cell wall is peptidoglycan (PG) which consists of β-(1→4) linked *N*-acetylmuramic acid (MurNAc) and *N*-acetylglucosamine (GlcNAc) (Silhavy et al., 2010). The D-lactyl carboxyl group of MurNAc binds the pentapeptide composed of L-alanine, D-*iso*-glutamine, *meso*-diaminopimelic acid or L-lysine and two D-alanines. In bacteria of the class *Bacilli* L-ornitine or L-5-hydroxylysine can take the central position and D-alanine at position 5 can be replaced by D-serine or D-lactate (Vollmer et al., 2008). Cross-linking of the polymer strands generally occurs between the carboxyl group of D-Ala at position 4 and the amino group of the diaminoacid at position 3, either directly or through a short peptide bridge (Schleifer and Kandler, 1972). The modifications can occur in PG strands as well. *N*-Deacetylation of GlcNAc and MurNAc seems to be very common. The presence of nonacetylated amino sugars determines the resistance of PG against lysozyme (Amano et al., 1980). Also PG with *O*-acetylated MurNAc at C-6 was shown to be resistant against actions of muramidases. Muramic acid δ-lactams residues are ubiquitous in spores whereas the *N*-glycosylation of MurNAc is a common modification within *Actinomycetales* (Vollmer, 2008).

The Gram-positive cell envelope is additionally decorated with a diversity of polysaccharides called secondary cell wall polymers (SCWPs – described below). Some of them – lipoteichoic acid (LTA) – are anchored in the lipid membrane (Reichmann and

Gründling, 2011), and others – wall teichoic acid (WTA) and other cell wall polysaccharides – are bound at position 6 of MurNAc *via* phosphoester (Ward, 1981) or pyrophosphate linkage (Schäffer et al., 2000).

Besides the polysaccharides, surface layer proteins (S-layer) can be found on the peptidoglycan. In case of *Bacilli* these proteins are often glycosylated. S-layers are monomolecular, regular arrays, covering the cell surface and when present, are the most abundant from cellular proteins. They are composed of one protein or glycoprotein (Schäffer and Messner, 2001). Previous studies revealed that the S-layer is produced by important pathogens including *Streptococcus*, and plays an important role in pathogenicity (Tuomanen, 1996).

The bacterial cell envelope can, but does not have to be covered by a capsular polysaccharide (CPS). Some of bacteria produce also an exopolysaccharide (EPS), which is secreted outside the cell (Delcour et al., 1999). The structure of Gram-positive cell envelope is schematically depicted in Fig. 1.

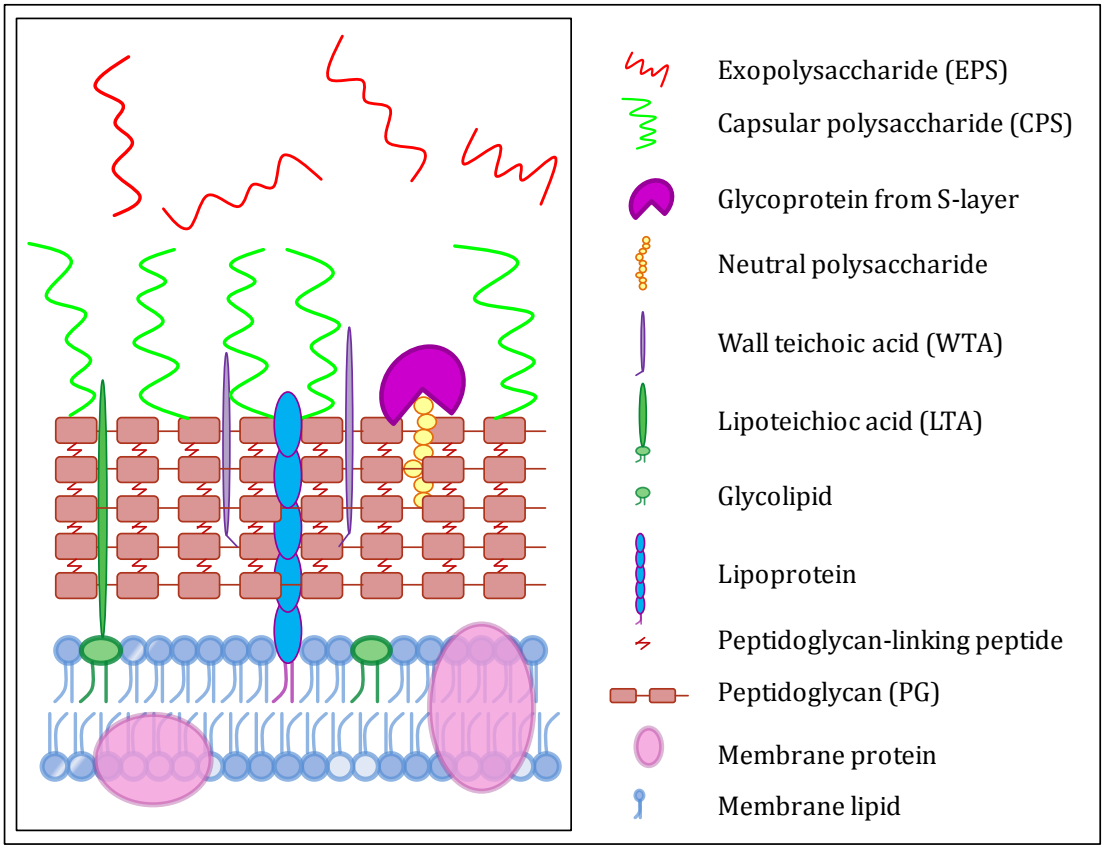

Fig. 1. Schematic view on the cell envelope of Gram-positive bacteria. The bilayer plasma membrane with intercalated proteins and glycolipids is covered by a multilayer peptidoglycan decorated with secondary cell wall polysaccharides and lipoproteins, and surrounded by S-layer glycoproteins (for the clarity of the picture, only one glycoprotein was drawn). Additionally, capsular polysaccharide can be bound to the cell wall and exopolysaccharide can be released outside the whole complex. According to Delcour et al., 1999.

1.3.1. Glycolipids

Glycolipids are small molecules of bacterial membranes. In Gram-positive bacteria they often serve as the lipid anchor for lipoteichoic acids (Hölzl and Dörmann, 2007). Their biosynthesis in the phylum *Firmicutes* occurs in the cytoplasm. They are produced by either a single processive glucosyltransferase or two separate enzymes (Reichmann and Gründling, 2011), from which one is responsible for the synthesis of mono- and the other for that of diglycolipids with diacylglycerol (DAG) as a primary acceptor (Jorasch et al., 2000). However, in the membrane a significant amount of monoglucosyldiacylglycerol (MGlcDAG) can be found but the main glycolipid is the diglucosyldiacylglycerol (DGlcDAG). In *Bacillus subtilis* the sugar backbone of the main glycolipid consists of two β-(1→6)-linked Glc residues (Hölzl and Dörmann, 2007). In *S. aureus* gentobiose is present (Morath, 2001), and for *L. lactis* (Fischer et al., 2011), *E. faecalis* (Theilacker et al., 2009) and *S. agalictiae* (Doran et al., 2005) it is kojibiose, which is the most abundant substituent of DAG.

Recent studies demonstrated the important role of membrane glycolipids in bacterial virulence. These molecules are involved in the formation of a permeable layer between the cytoplasm and the environment. They are involved in crossing the blood-brain barrier (Doran et al., 2005), biofilm formation and adhesion to epithelial cells (Theilacker et al., 2009). The DGIcDAG-deficient mutant (Δ*bgsA*) of *E. feacalis* administered intravenous to mice was cleared from their bloodstream within 72 h after challenge, whereas mice challenged with wild type strain were still bacteremic at that time p. ch. (Sava et al., 2009).

Furthermore, it was shown that bacterial glycolipids can act as antigens presented by CD1d to natural killer T (NKT) cells. In response, NKT cells produce a number of pro- and anti-inflamatory cytokines, among of which interferon γ (IFN-γ) and interleukin (IL)-4 are the best characterized. This results in activation of other cells in the immune system, e.g. natural killer (NK) cells, dendritic cells (DC), macrophages, B cells, and T cells. These cells secrete other immune modulating cytokines (e.g. TNF-α and IL-8), release of which is responsible for mobilizing the immune system, and in effect eliminating the pathogen (Kinjo et al., 2011; Zajonc and Kronenberg, 2009; Wu et al., 2008).

1.3.2. Secondary cell wall polymers (SCWPs)

The cell wall of Gram-positive bacteria is decorated with a variety of polysaccharides. Based on their structural character, they can be classified into three groups: 1) teichoic acids, 2) teichuronic acids and 3) other polysaccharides, neutral or acidic, which do not belong to any of the other groups (Schäffer and Messner, 2005).

Teichoic acids (TAs, LTA and WTA) are phosphate-rich polysaccharides which were shown to contribute to resistance to environmental stresses, such as heat (Vergara-Irigaray et al., 2008) or low osmolarity (Oku et al., 2009), to antimicrobial peptides (Peschel, 1999) and fatty acids (Kohler et al., 2009), cationic antibiotics and lytic enzymes produced by the host (Peschel et al., 2000), including lysozymes (Bera et al., 2007). Together, TAs and PG make up a 'continuum of anionic charge' that provides the rigidity and porosity of the cell envelope (Clarke-Sturman et al., 1989). They bind cations (in particular magnesium), providing an important ions reservoir for the activity of different enzymes (Atilano et al., 2010). It was shown that mutants impaired in either LTA or WTA synthesis have cell division and morphology defects, and that deletion of both polymers is lethal (D'Elia et al., 2006).

The teichuronic acids are synthesized under phosphate limited-conditions. The phosphate is then replaced by uronic acids, so that the 'continuum of negative charge' of the molecule is extant (Ward, 1981).

The last group of cell wall polysaccharides is not well described. Till now nothing is known about their biosynthesis, but they seem to be involved in the attachment of the S-layer to the underlying peptidoglycan (Cava et al., 2004; see 1.3.2.3).

1.3.2.1. Lipoteichoic acid (LTA)

On the search for a 'Gram-positive endotoxin' LTA used to be considered as a safe candidate for this title (Morath, 2001). Furthermore, it was postulated that the recognition of LTA in host cells occurs *via* Toll-like receptor 2 (TLR2). The recent studies with synthetic LTAs of all types (I-IV; described below) revealed, that the activation of cells is TLR2-independent, and that previous results were obtained due to the contamination with

lipoproteins (Schmidt et al., 2011). Additionally, it was proven that the stimulation of cells with LTA is not as effective as with LPS from Gram-negative bacteria.

LTAs are amphifilic polymers found in the cell walls of many Gram-positive bacteria. Their polyaliditolphosphate chain is anchored to the bacterial membrane *via* a glycolipid linker (1.3.1). Till now all discovered LTAs are classified in four groups. LTA type I is the most popular among bacteria. Those LTAs' repeating units are composed of unbranched (1→3)-linked polyglycerophosphate, which vary in length from 18 to 40 units. The position 2 of the glycerol can be substituted with D-alanine or/and a glucosyl residue (Greenberg et al., 1996). As an example, the structure of *S. aureus* LTA, representing LTA type I, is depicted in Fig. 2.

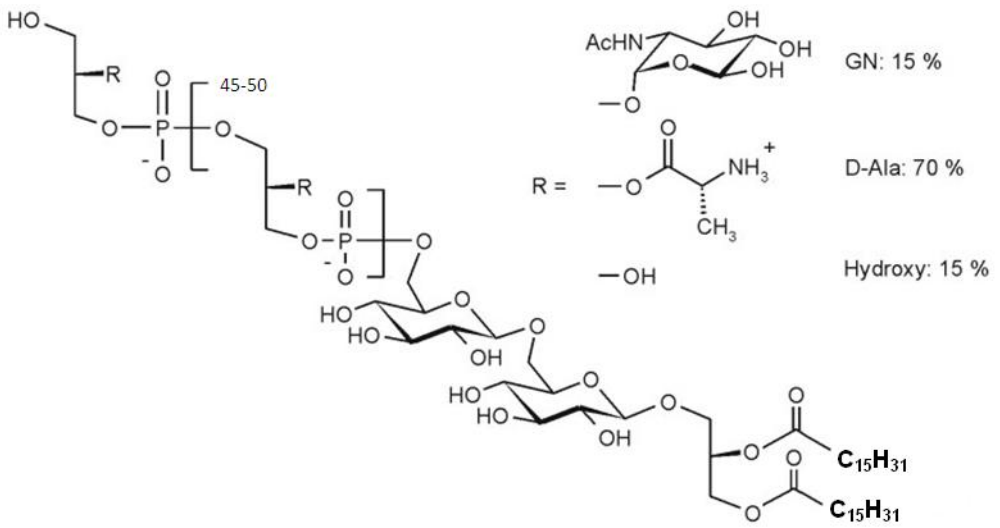

Fig. 2. The structure of *S. aureus* LTA (Morath et al., 2001. Originally published in The Rockefeller University Press, doi: 10.1084/jem.193.3.393).

The LTA type II possesses a digalactosyl residue intercalated between glycerophosphate, and position 2 of the Gro is consistently substituted with a monogalactosyl residue. This type of LTA was found so far only in *Lactococcus garvieae* (Koch and Fischer, 1978). Type III is represented by the LTA isolated from *Clostridium innocuum*. In its polygalactosylglycerophosphate chain C-2 of Gro is either not substituted or substituted nonstoichiometrically with *N*-acetylglucosamine or/and *N*-acetylglucosamine. Type IV LTA was found and described for *Streptococcus pneumoniae* (Fischer, 1988). Its repeating unit is the most complex one from all LTAs known so far and consists of one glucose, two

galactosamine and one 2-acetamido-4-amino-2,4,6-trideoxygalactose residues that are differently linked, and one ribitol (Pedersen et al., 2010).

1.3.2.2. Wall teichoic acid (WTA)

A review of the literature reveals a wide structural diversity of WTAs in Gram-positive bacteria. The WTAs are bound covalently to C-6 of MurNAc of PG *via* a phosphodiester bond (Araki and Ito, 1989). Their repeating unit can possess the same structure as those originating from LTA – polyglycerol- or polyribitolphosphate substituted nonstoichiometrically with alanine or glycosyl residues (Sánchez Carballo et al., 2010; Endl et al., 1983). The structure can also considerably differ from this scheme. Phosphoglycerol or phosphorybitol is, however, always a part of the repeating unit. For instance the repeating unit of WTA isolated from *E. feacalis* (Fig. 3) was composed of 1 Glc, 2 Gal, 1 GalNAc, 1 GlcNAc, 1 ribitol, and 1 phosphate (Theilacker et al., 2012).

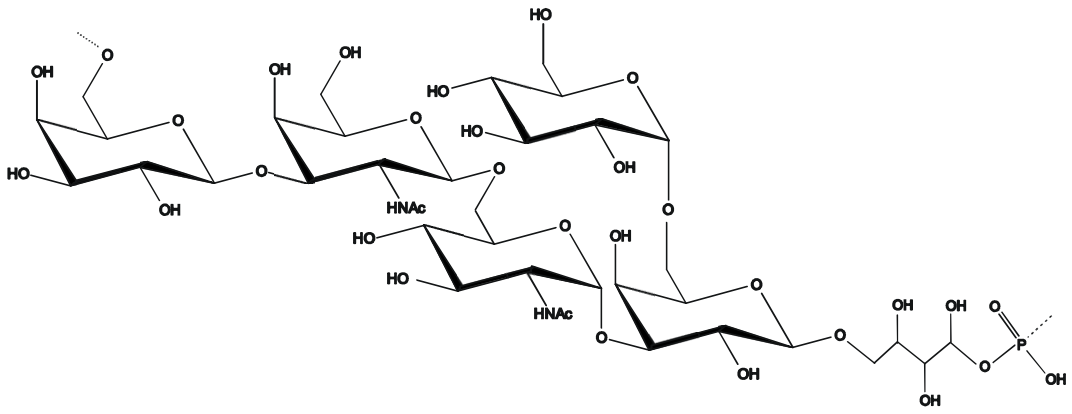

Fig. 3. The structure of *E. feacalis* WTA (Theilacker et al., 2012. Originally published in Carbohydrate Research http://dx.doi.org/10.1016/j.carres.2012.03.031).

In regard to the biological activity of the WTAs, it was reported that HEK293 cells transfected with TLR2, TLR4, NOD1 and NOD2, and challenged with WTA of *L. lactis* do not activate the NF-κB pathway (Fischer et al., 2012). WTA showed also no pro-inflammatory activity in monocytes (THP1) or murine macrophages (RAW 264.7), but stimulated CD4+ T-cells proliferation *in vitro*. The mechanisms that lead to WTA-mediated activation of T-cells are not yet understood (Weidenmaier et al., 2010).

1.3.2.3. 'Non classical' secondary cell wall polysaccharides

The 'non classical' cell wall polymers were discovered during work on S-layer glycoproteins. In course of the purification, they were co-isolated and for some time considered as a second set of glycan chains in S-layer glycoprotein (Altman et al., 1996; Steindl et al., 2002). Finally, thanks to improved purification procedures, they were assigned to the SCWPs which comprise 7-15% (w/w) of the bacterial cell wall (Schäffer et al., 2001). Although the structural analyses of those polymers are not as advanced as for teichoic acids, the comparison of known structures revealed several common features. SCWPs are either charged (Schäffer et al., 1999) or neutral (Steindl et al., 2002) heteropolysaccharides covalently bound to PG *via* a phosphodiester (Steindl et al., 2005) or pyrophosphate linkage (Schäffer et al., 2000). Up to date analyzed 'non classical' SCWPs were composed of some of the following sugars: *N*-acetylglucosamine (GlcNAc), *N*-acetylmannosamine (ManNAc), *N*-acetylgalactosamine (GalNAc), 2,3-diacetamido-mannouronic acid (Man-2,3-diNAcA), Glc, and ribose (Rib), with possible modifications like pyruvate, phosphate or acetate (Schäffer and Messner, 2005).

These polysaccharides have been proven to play a role in non-covalent attachment of the S-layer to the underlying PG (Schäffer and Messner, 2005). The binding of the S-layer to the polysaccharide can occur through different mechanisms. The first to be proposed was that the S-layer homology (SLH) domain of the glycoprotein interacts with the pyruvate group of the polysaccharide (Cava et al., 2004; Mesnage et al., 2000). Then, it was observed that not all bacterial S-layer glycoproteins posses the SLH domain, and that cell wall polymers of those organisms are not substituted with pyruvyl residues. For those bacteria two different mechanisms were postulated. The first proposes basic amino acids of the cell wall-targeted region of protein to interact with negatively charged polysaccharide (Jarosch et al., 2000), and the second is based on the hypothesis that the binding could occur through a highly specific lectin interaction (Sára, 2001).

1.3.3. Capsular polysaccharide (CPS) and exopolysaccharide (EPS)

The CPSs form a thick shell around the bacterial cell, and may be or not covalently bound to the PG. EPSs are another group of bacterial polymers, which in contrast to CPSs are not

attached to the cell, but are released to the environment (Delcour et al., 1999). The distinction can be sometimes problematic, since bacteria producing a lot of CPS may release some of this material to the culture medium, and on the other hand EPS, when transported from the cytoplasm, where it is synthesized, through a thick Gram-positive cell wall may mistakenly be taken as a loose associated material. Most bacteria produce only one of those polysaccharides (if any), but there are also strains, which are able to produce both at one time, and their structure can be the same or different (Whitfield, 1988). Polymer diversity is defined by serology and chemistry, and can range in one bacterial species from one, as for *Streptococcus pyogenes*, to a few, as for *Streptococcus agalactiae* or 93 for *S. pneumoniae* (Yother, 2011). As an example, structures of CPSs repeat units of some representative bacteria genus *Streptococcus* are presented in Table 1.

Table 1. Structures of CPSs repeat units of some representative bacteria genus *Streptococcus.*

Hemolysis	Group	Species	Structure of CPS	Reference
α	–	*S. pneumoniae*	TypeII →3)-[α-GlcA-(1→6)-α-Glc(1→2)]α-Rha-(1→3)-β-Rha-(1→4)-β-Glc-(1→	(Yother, 2011)
α	–	*S. suis*	Type II →4) [α-Neu5Ac-(2→6)-β-Gal(1→4)-β-GlcNAc-(1→3)]β-Gal-(1→4)[α-Gal(1→3)]-β-Rha(1→4)-β-Glc-(1→	(Van Calsteren et al., 2010)
β	A	*S. pyogenes*	→4)-β-Glc*p*A-(1→3)β-Glc*p*NAc-(1→	(DeAngelis et al., 1993)
β	B	*S. agalactiae*	Type Ia →4)-β-Glc*p*NAc-(1→4)-β-Gal*p*-(1→	(Cieslewicz et al., 2005)
γ	D	*E. faecalis*	→6)-[α-Glc-(1→2)]α-Glc-(1→2)-(PO_4→1)Gro-3→PO_4→	(Huebner et al., 1999)

The production of CPS is associated with the pathogenicity of bacteria. The capsule is of a great advantage for a pathogen, since those molecules do not activate the complement themselves but effectively mask the components of the cell wall which do so (Yother, 2011). The opsonization of encapsulated bacteria is not efficient, thus the phagocytosis is also very poor (Koskiniemi et al., 1998). The recent data on a capsule isolated from *S. suis* show, that the capsule cannot only mask the pathogen, but also actively inhibit phagocytosis through the destabilization of lipid rafts (Houde et al., 2011).

Many other protective functions of capsules have been reported. The presence of this highly hydrated layer can protect cells from desiccation, antibiotics (Fernebro et al., 2004) and toxic metals (Bitton and Freihofer, 1977). On the other hand, since many CPSs are negatively charged, they bind positive ions and serve as a reservoir of useful metals (Uhlinger and White, 1983). The role of CPS in adhesion of bacteria to epithelial cells and biofilm formation has been also described (Vu et al., 2009).

The EPSs seem to be expendable under laboratory conditions and their function is not clear (Whitfield, 1988). Extracellular mannan isolated from *Pseudomonas syringae*, which is a pathogen of a carob plant, had a phytotoxic effect on tobacco leaves (Corsaro et al., 2001). The galactomannan produced by *Histophilus somni* – an opportunistic pathogen of bovine airways – was suggested to be involved in biofilm formation, since it could be detected only upon biofilm growth (Sandal et al., 2011).

CPSs are intensively examined as antigens for vaccine production. The most popular polysaccharide vaccines protect against *Streptococcus pneumoniae* (Cartwright, 2002), *Neisseria meningitidis* (Nolan et al., 2011) and *Haemophilus influenza* (Eskola et al., 1987). Antibodies against the CPSs are widely used as selective and sensitive diagnostic tools (Fournier et al., 1993; Karakawa et al., 1988) and utilization of EPS in the same manner has been proposed (Sandal et al., 2011).

1.4. Characterization of HEK293, RAW 264.7, pbMEC

HEK293 cells were originally isolated from primary human embryo kidney cells (HEK) and transformed with sheared DNA of adenovirus 5 in the early 1970s (Graham et al., 1977). The latest reports revealed that HEK293 originated most probably from a neuronal lineage cell (Shaw et al., 2002). Since they are easy to transfect and cultivate they became widely spread in cell biology research and biotechnology industry. Like all cell lines, they do not represent a model of normal cells, but are good experimental object when the behavior of a cell itself is not important; for instance when studying the activation *via* immune receptors. In such studies, HEK293 are transfected with a particular receptor (or receptors) which is/are then overproduced, and the transduction of the signal upon certain stimuli can be investigated (Schröder et al., 2004).

RAW 264.7 (a mouse leukaemic monocyte macrophage cell line) cell line was established from a tumor induced by the Abelson murine leukemia virus (Raschke, 1980). The cell line is widely used model for studying phagocytosis (Rosenberger et al., 2000) and cellular responses to microbes and their products. It was shown that such cells closely mimic bone marrow-derived macrophages in terms of cell surface receptors and response to microbial ligands (Berghaus et al., 2010).

pbMEC (primary bovine mammary epithelial cells) are isolated from the udder of healthy, lactating cows (Yang et al., 2006) and serve as a bovine model of lower complexity than udders to study the host-pathogen interaction. Their immune relevance has been just recently appreciated (Lahouassa et al., 2007; Günther et al., 2009). Despite the fact, that the main function of mammary epithelial cells is milk formation during the lactation, they were shown to be immunologically active against pathogens (Strandberg et al., 2005; Günther et al., 2011). They express transcripts of genes encoding for TLR1, 2, 3, 4, 6, NOD1 and NOD2, and CD36 (Bougarn et al., 2010), and when stimulated, a strong activation of NF-κB occurs (Yang et al., 2006).

1.5. Pattern-recognition receptors and immune response

The immune response consists of an innate and adaptive part, the letter of which represents the specific response to antigens. The innate immune system uses – more generally – either passive barriers or receptors recognizing conserved microbial molecules (Schukken et al., 2011). The innate immune response is the first line of defense against microbes. The function of the cells belonging to the innate defense system (macrophages and other white blood cells that are not B lymphocytes or T lymphocytes) is an immediate, defensive response to invading microbes (Riollet et al., 2001). The recognition of microbial molecules is ensured by a group of proteins that comprise e.g. the family of Toll-like receptors.

The perception of a pathogen is the first and obligatory step in the immune defense against the intruder. Mammalian cells are equipped with trans-membrane receptors, which are capable to recognize molecular components of pathogens. The 13 different Toll-like-receptors (TLRs) represent the best-described family of such ‘pattern recognition

receptors' (PPRs) (Kumar et al., 2011). These receptors are intercalated in the cell membrane and bind bacterial ligands with their extracellular domains (Kumar et al., 2009). TLR4, for example, is known to bind lipopolysaccharide from Gram-negative bacteria (Hirschfeld et al., 2001). TLR2 was reported to bind conserved components of Gram-positive bacteria such as lipoproteins and lipopeptides, LTA, PG, phosphatidyl myoinositol mannosides (PIM) or lipoarabinomannan (LAM) from mycobacteria (Aderem and Ulevitch, 2000; Akira et al., 2006). After recognition of ligands, TLR2 heterodimerizes with co-receptors TLR1 or TLR6, and this step is essential for the signal transduction (Botos et al., 2011). The latest reports, based on crystal structure analysis, provided evidence that the heterodimerization of TLR2/1 and TLR2/6 occurs only after binding lipopeptides or lipoproteins (Kang et al., 2009). Thus, all other TLR2 ligands published before, such as PG or LTA are currently controversially discussed. The presence of CD36, TLR2 and TLR4 on the surface of mammary epithelial cells suggests their direct role in pathogen detection (Bougarn et al., 2010). All TLRs signal transduction pathways eventually activate nuclear factor kappa B (NF-κB) (Akira and Takeda, 2004).

Agonist binding-induced dimerization of TLRs with their co-receptors results in recruiting different adapter proteins. Myeloid differentiation primary response gene 88 (MyD88) is one of adapter proteins which mediate signaling cascades, and is recruited by all TLRs, except for TLR3. In case of TLR2 and TLR4, another adapter protein – TIRAP (also known as MAL) – is required for recruiting MyD88 to the receptor. During signalling, MyD88 oligomerize and recruit IRAK4 and IRAK2 forming the so called 'Myddosome'. This complex is the single-stranded helix, composed of 6 molecules of MyD88, followed with 4 molecules of IRAK4, and ended with 4 molecules of IRAK2 (Lin at al., 2010). Myddosome formation is a crutial step in signal transduction, since only this complex can interact with TNF receptor-associated factor 6 (TRAF6). The latter, further activates TGF-β-activated kinase 1 (TAK1) and TAK1 binding proteins (TAB) 1-3 which then phosphorylate IkappaB kinase (IKK)-β subunit of IKK complex composed of IKKα, -β and –γ. This activation modulates the induction of NF-κB factors (Akira et al., 2006).

The genes encoding for pro-inflammatory factors need binding the NF-κB sites in their promoter region. Cytokine expression in cows with mastitis has been shown to correlate with NF-κB activation (Schukken et al., 2011).

The cytokines are proteins playing a crucial role in intercellular communication during stress, inflammation and regeneration (Alluwaimi, 2004; Belardelli and Ferrantini, 2002).

Some cytokines promote inflammation, others have anti-inflammatory properties. The most important pro-inflammatory cytokines, called often the master cytokines, are tumour necrosis factor (TNF)-α, interleukin (IL)-1 and interleukin (IL)-6. TNF-α and IL-1 trigger an inflammatory cascade, causing fever, inflammation, tissue damage, and, in some cases, toxic shock and death (Dinarello, 2000). IL-6 is a third key pro-inflammatory cytokine. It is one of the most important mediators of the "acute-phase response" in inflammation, but has also anti-inflammatory properties (Heinrich et al., 2003).

Chemokines are a specific class of cytokines which recruit the immune effector cells to the site of inflammation. CXCL8 (IL-8) is the best examined chemokine in udder immune response. A significant increase of the CXCL8 mRNA in udder tissue and of the CXCL8 protein in milk after challenge with various mastitis pathogens was reported (Bannerman, 2009). CXCL8 preferentially mediate the recruitment of neutrophils and to a lesser extent T lymphocytes by interaction with CXC chemokine receptor 1 (CXCR1) and CXCR2 (Harada et al., 1994). Neutrophil granulocytes constitute a first line of cellular immune defence and are recruited early after infection (Riollet et al., 2002). It was found that the CXCL8-encoding gene is one of the first genes revealing induced expression in MEC after an inflammatory stimulus.

CCL5 is another chemokine, known to induce eosinophil recruitment through binding to the CCR3 receptor which is highly expressed in these cells. This chemokine is strongly expressed in the infected udder as well as in inflammatory stimulated MEC (Griesbeck-Zilch et al., 2008).

In addition to cytokines and chemokines changes in the expression of other mediators of inflammation have been characterized in the setting of bovine mastitis. Increases in milk and blood concentrations of serum amyloid A (SAA3), β-defensins (e.g. LAP) and other innate immune effectors like inducible nitric oxide synthase (iNOS) have been reported in response to naturally acquired and experimentally induced intramammary infections (Günther et al., 2009; Bannerman et al., 2004).

2. Aim of the thesis

Bovine mastitis, namely infection and inflammation of the udder in cattle, is of prime economic importance in dairy industry. Over 135 different organisms have been reported to cause mastitis. *S. uberis*, a Gram-positive, non-haemolitic coccus is responsible for a significant proportion of clinical mastitis worldwide. The infection with *S. uberis* occurs mostly in the dry period and in heifers before calving. Intramammary infections caused by *S. uberis* may be clinical or subclinical with different duration. The response to a conventional treatment with pirlimycin – about 50 % (Milne et al., 2005) – is not sufficient. Also the diagnostic methods leave much to be desired.

The overall goal of this work was to isolate, purify and identify the cell envelope components from various *S. uberis* strains and to examine their biological activity. Components that are capable to activate the adaptive response in the udder could be used as novel drug candidates in therapy by increasing the immune status of the udder (e.g. in dry period, preventing from *S. uberis* infections). Components with unique structure could be used for diagnostic and vaccine purposes. Finally, newly discovered important virulent factors could serve as a target for novel inhibitors, decreasing the virulence of the pathogen.

3. Materials and methods

3.1. Materials

3.1.1. Bacterial cells and their culture media

Table 2. Bacterial strains.

Species	Strain	Country of isolation	Year of isolation	Description
S. uberis	233	New Zealand		Mastitis (clinical or subclinical)
	0140J	UK		Virulent strain
	T1-18	UK		Mastitis (clinical or subclinical)
	EF20	UK		Avirulent strain
	C6344	UK	2002	Mastitis (clinical)
	C5072	UK	2002	Mastitis (clinical)
	S6261	UK	2002	Mastitis (clinical)
	C9359	UK	2002	Mastitis (clinical)
	Ab71	UK	2002	Mastitis (clinical)
	4428	UK	1999	Mastitis (clinical)
	5291	UK	2000	Mastitis (clinical)
	5130	UK	1999	Mastitis (clinical)
	6780	UK	2000	Mastitis (clinical)
	Ab1947	UK	2002	Mastitis (clinical)
	C8329	UK	2002	Mastitis (subclinical)
	C5388	UK	2002	Mastitis (subclinical)
	B190	UK	2000	Mastitis (subclinical)
	6736	UK	1999	Mastitis (subclinical)
	C7131	UK	2002	Mastitis (subclinical)
	S7010	UK	2002	Mastitis (subclinical)
	B362	UK	2000	Mastitis (subclinical)
	6707	UK	2000	Mastitis (subclinical)
	4244	UK	1999	Mastitis (subclinical)
	3448	UK	1999	Mastitis (subclinical)

Species	Strain	Country of isolation	Year of isolation	Description
E. coli	1303	UK		Mastitis (clinical, acute)
	–	(Institute of Veterinary Microbiology, Hannover, Germany)		Mastitis (clinical)
S. aureus	–	Pansorbin, Calbiochem, Merck, Nottingham, UK		–

- *S. uberis* was cultivated in:
  - Brain Heart Infusion (BHI), BD Bacto
  - Todd Hewitt Broth (THB), BD Difco

- *E. coli* was grown in:
  - Brain Heart Infusion (BHI), BD Bacto

Brain-heart infusion broth (BHI broth) is a highly nutritious growth medium for cultivation of fastidious and nonfastidious microorganisms. It is made from boiled bovine or porcine brains and hearts. Its exact chemical composition is unknown.

Todd-Hewitt Broth (THB) is a highly nutritious culture medium intended for the cultivation and serological typing of Group A hemolytic streptococci. It is composed of beef heart infusion, peptone, dextrose and salts. Disodium phosphate and sodium carbonate provide buffering action to counteract the acidity produced during the fermentation of the dextrose (Updyke and Nickle, 1954).

3.1.2. Eukaryotic cells and their culture media

Table 3. Eukaryotic cells and their culture media.

Cell type	Abbreviation	Culture medium
Bovine mononuclear cells	MNC	RPMI 1640 PAA, Pasching, Austria
Embryonic human kidney cell line	HEK293	RPMI 1640 Biochrom AG, Berlin, Germany
Mouse leukaemic monocyte macrophage cell line	RAW 264.7	RPMI 1640 Biochrom AG, Berlin, Germany
Primary bovine mammary epithelial cells	pbMEC	RPMI 1640 Biochrom AG, Berlin, Germany

RPMI 1640 culture medium:

Roswell Park Memorial Institute medium is chemically defined culture medium commonly used in cell culture and tissue culture. This medium contains phosphate and uses a bicarbonate buffering system. It is formulated for use in a 5% CO_2 atmosphere (Moore and Woods, 1977).

3.1.3. Plasmids, primers and probes

- **Plasmids**

Table 4. Plasmids used for transfection of eukaryotic cells.

Plasmid	Characterization
pFLAG-CMV-1	The gene encoding for the bovine TLR2 was cloned into this plasmid. Plasmid was used for transient transfection of HEK293 cells
pELAM-*Renilla*	This vector harbors the widely used ELAM promoter engineered with five NF-κB attachment sites and gene encoding for luciferase.

- **Primers for eukaryotic cells**

  - For real-time qRT-PCR quantification of messenger RNA copy numbers in eukaryotic cells, **Sybr Green Fast Start, Roche** was used.

Table 5. Primers of genes expression of which was measured in eukaryotic cells.

Gene	GenBank no.	Primer sequence (5´–3´)	Amplicon size (bp)
IL1A	NM_174092	GGCCAAAGTCCCTGACCTCT CTGCCACCATCACCACATTC	224
IL6	NM_000600.3	GGAGGAAAAGGACGGATGCT GGTCAGTGTTTGTGGCTGGA	227
IL8	NM_173925	CCTCTTGTTCAATATGACTTCCA GGCCCACTCTCAATAACTCTC	170
CXCL2	NM_001048165.1	GCCAAACCGAAGTCATAGCC TGGAAACCAGCCATTCTCTTC	213
TNF-α	NM_173966.2	CTTCTGCCTGCTGCACTTCG GAGTTGATGTCGGCTACAACG	156
iNOS	NM_001076799	ACAGGATGACCCCAAACGTC TCTGGTGAAGCGTGTCTTGG	188

Gene	GenBank no.	Primer sequence (5´–3´)	Amplicon size (bp)
LAP	NM_203435	AGGCTCCATCACCTGCTCCTT CCTGCAGCATTTTACTTGGGCT	182
SAA3		CTTTCCACGGGCATCATTTT CTTCGGGCAGCGTCATAGTT	
CCL5	NM_175827	TCCCCATATGCCTCGGAC TCGCACCCACTTCTTCTCTG	229

- **Primers and probes for *S. uberis***

Table 6. Primers used for screening of the mutant bank, complementary to the *S. uberis* genome (p800 and p801) and to inserted sequence IS*S1* (p613 and p614).

Gene	Gene ID	Primer sequence (5´–3´)	Description	Amplicon size (bp)
sub0538	7392282	TTTGTGGATTACCTTGG ACATTG	**p800** – sense – 193 bp from SUB0538 start codon	1 487
		CCCTAAGCTGAACTCTGT TTGTGT	**p801-**antisense – 271 bp from sub0538 stop codon	
IS*S1*	-	GCTCTTCGGATTTTCGGT ATC	**p613** - sense	
		CATTTTCCACGAATAGAA GGACTGTC	**p614** - antisense	

- **Probes:** TaqMan® probes, Universal ProbeLibrary, ROCHE APPLIED SCIENCE, Mannheim, Germany
- **Primer pairs**: were obtained from MWG BIOTECH, Ebersberg, Germany

Table 7. Primers and probes of the genes, expression of which was measured in *S. uberis*.

Gene	Gene ID	Primer sequence (5´–3´)	Probe	Ampl. size (bp)
sub0538	7392282	CTGGTTGGGTAAATCAAGATAGC TCCGTAATGCCTTAACAAATCC	**#135**	69
sub0888	7391365	GCCAAAGAAAAAGAGGGTGA AGCTGTGCTAATAAGTGCAGAAAA	**#69**	96

3.1.4. Enzymes, their buffers, molecular markers and kits

- **Enzymes and their buffers**

Table 8. The enzymes and their buffers used in the experiments.

Enzyme	Buffer	Provider
Phusion® High-Fidelity DNA Polymerase	Phusion® HF Reaction Buffer (5 x)	Biolabs
SuperScript™ II Reverse Transcriptase	5 x First-Strand Buffer	Invitrogen
Proteinase K	water	Roche
DNase I, RNase-free		Ambion
DNase	Used with buffer for enzymatic treatment*	Roche
RNase	Used with buffer for enzymatic treatment*	Roche
Lysozyme	water	Sigma-Aldrich
Mutanolysin	water	Sigma-Aldrich
α-Mannosidase	water	Sigma-Aldrich

***Buffer for enzymatic treatment with DNaseI and RNase:**

0.10 M Tris/HCl
0.05 M NaCl
0.01 M $MgCl_2$
pH 7.5

- **Molecular marker**

HyperLadder™ 1kb (HyperLadder I), Bioline used with its 5x sample loading buffer – used for isolation of mutant

- **Kits**

- QIAquick PCR Purification Kit, Quiagen
- TRIzol RNA isolation reagent, Invitrogen
- High Pure RNA Isolation Kit, Roche
- Maxima® First Strand cDNA Synthesis Kit for RT-qPCR, FERMENTAS
- LightCycler® 480 Probe Master Kit
- Direct-Zol-RNA Miniprep Kit, ZymoResearch

3.1.5. Chemicals

Table 9. List of chemicals.

Name	Formula or comment	Provider
Acetic acid	CH_3COOH	Baker
Acetic anhydrite	Ac_2O	Fulca
Aceton	C_3H_6O	Merck
Agarose	Agarose for electrophoresis	Web Scientific
Ammoniac 25%	$NH_3 \cdot H_2O$	Merck
Ammonium acetate	CH_3COONH_4	Merck
Ammonium molybdate monohydrat	$(NH_4)_6MO_7O_{24} \cdot H_2O$	Fulca
Ammonium oxalate	$C_2H_8N_2O_4$	Merck
Ascorbic acid	$C_6H_8O_6$	Fulca
n-Butanol	C_4H_9OH	Merck
(*S*)- Butanol	C_4H_9OH	Merck
Cerium sulphate tetrahydrate	$Ce(SO_4)_2 \cdot 4\ H_2O$	Merck
Chloroform	$CHCl_3$	Merck
Chloroform D1, 99,96% + 0,03% TMS	$CDCl_3$ + TMS 0.03%	Euiso-top
Citric acid monohydrate	$C_3H_4OH(COOH)_3 \cdot H_2O$	Merck
Crystal violet		Merck
Deuteroxide 99.9%	D_2O	Deutero

Name	Formula or comment	Provider
Deuteroxide 99.98%	D_2O	Deutero
Diazomethane	CH_2N_2	
DMSO	C_2H_6OS	Merck
EDTA	$C_{10}H_{16}N_2O_8$	Roth
Ethanol	CH_3CH_2OH	Merck
Ethidium bromide	Final concentration 1%	Bio-Rad
Hexane	C_6H_{12}	Merck
Hydrazine	N_2H_4	Kodak
Hydrochloric acid 37%	HCl	Merck
Hydrofluoric acid	HF	Merck
Hydrogen peroxide 30%	H_2O_2	Merck
Iodomethane	MeI	Fulca
Methanol	CH_3OH	Merck
Methanol D4 99.8%	CD_3OD	Deutero
Methanol Seccosolv	CH_3OH	Merck
α-Naphthol	$C_{10}H_8O$	Sigma-Aldrich
dNTPs	Nucleotides: ATP, CTP, GTP and TTP in conc. 10 mM each	Sigma-Aldrich
Perchloric acid 70%	$HClO_4$	Merck
Phenol	C_6H_5OH	Sigma-Aldrich
phenol/chloroform/ isoamylalcohol	25:24:1; for molecular biology	Sigma-Aldrich
2-Propanol	C_3H_7OH	Merck
Pyridine	C_5H_5N	Fulca
Sodium acetate	CH_3COONa	Merck
Sodium azide	NaN_3	Sigma-Aldrich
Sodium borodeuteride	$NaBD_4$	Sigma-Aldrich
Sodium borohydride	$NaBH_4$	Merck
Sodium chloride	NaCl	Merck

Name	Formula or comment	Provider
Sodium citrate dihydrate	$C_3H_4OH(COOH)_2COONa \cdot 2H_2O$	Merck
Sodium dihydrohen phosphate	NaH_2PO_4	Roth
Sodium dodecyl sulfate	SDS	Bio-Rad
Sodium hydroxide	NaOH	Merck
Sulfuric acid 98%	H_2SO_4	Merck
TAE buffer 10x	Ultra pure	Gibco, Invitrogene
Trifluoroacetic acid	TFA, $C_2HF_3O_2$	Merck
Tris		Sigma-Aldrich
Water	Pyrogen-free from Milipore system – used for isolation and isolated material	Milipore
Water	Molecular biology reagent – used in the experiments leading to isolate the *S. uberis* mutant	Sigma-Aldrich

3.1.6. Equipment and other materials

- **Equipment and materials for chromatography**

  - **Thin layer chromatography (TLC)**

    TLC Silica Gel 60W $F_{254}S$, aluminum sheets 20 x 20 cm, MERCK, Germany

    TLC Silica Gel 60 F_{254}, glass plates 20 x 20 cm, MERCK, Germany

  - **Polar interaction chromatography**

    Silica Gel 60, particle size 0.040-0.063 mm, MERCK, Germany

  - **Gel filtration**

    - Matrices:

      BioGel P2, P10, P60, fine, Bio-Rad

      Sephadex G10, GE Healthcare Life Science

- Detection :
  RI Detector K-2301 KNAUER
  Smartline RI Detector 230 KNAUER

- Software:
  Clarity Chromatography station for Windows

- **Hydrophobic interaction chromatography (HIC)**

  - Column:
    HiPrep column (16 x 100 mm, bed volume 20 ml) of octyl-sepharose, GE Healthcare Life Science

  - HPLC device
    Gilson, Detector 15X Series of UV/VIS

  - Software
    Trilution® LC

- **Anion-exchange chromatography**

  - Column:
    HiTrap Q Sepharose HP 5 ml, GE Healthcare Life Science

  - FPLC:
    ÄKTA FPLC UPC 900, Detector P-920, Amersham Pharmacia Biotech

  - Software:
    Unicorn Version 4

• Other equipment

- **Thermocyclers:**
  - GeneAmp PCR System 2700, Applied Biosystems
  - LightCycler, Roche, Basel, Switzerland
  - Thermal cycler C1000, BIO-RAD, Munich, Germany

- LightCycler® 480 II systems, ROCHE APPLIED SCIENCE, Mannheim, Germany

- **Agarose Gel Electrophoresis**
  Compact M, Biometra

- **Flow cytometer**
  Accuri C6, BD Biosciences
- **Centrifuges and rotors**
  - Sorvall RC6+ Centrifuge, Thermo Scientific
    Rotors: FiberLite® F14 – 6 x 250y
    FiberLite® F21 – 8 x 50y
  - Avanti J-26 x P Beckman Coulter
    Rotors: JLA 8.1000, model JLite
    JA 14, model J2-21
  - Sigma 1-14
  - Rotanta 460 R, Hettich Zentrifugen, Germany
    Rotor 4446

- **Spectrophotometers**
  - Nanoquant infinite M200 TECAN – plates spectrophotometer
  - Heλiosβ Thermo Electron Corporation – cuvette spectrophotometer
  - NanoDrop ND-1000 spectrometer, THERMO SCIENTIFIC, Rockford, IL

- **Cell homogenizers**:
  - B. Braun
  - Vibrogen – Zellmühle Edmunt Bühler GmbH

- **Lyophilisator**
  ALPHA 1-4 LOplus, Christ

- **Rotary evaporators**:
  - Hei – VAP Advantage, Heidolph
  - Büchi 461 Water Bath

- **Sonicator**

  Bandelin Sonorex

• Other materials

- **Glass**

  The glass materials, e.g. bottles, balloons, measuring cylinder etc. were prepared pyrogen-free by heating at 240°C for 4 h.

- **Dialysis membranes**
  - Spectra/Por® 3,500 u
  - Spectra/Por® 14-16 ku

- **Glass beads**

  0.1 mm, Roth, Karlsruhe

- **Well plates**
  - AB-Gene 96-well plate, non-skirted, Thermo Scientific, Certified DNase/RNase Free – for PCR reactions
  - Polystyren tissue™ 96-well plates, flat-bottomed, BRAND Scientific Inc. – for biofilm assay
  - 6-Well plates collagen coated, Serva, Heidelberg, Germany

- **Tips**
  - DNase/RNase Free Certified, sterile - for molecular biology
  - Sterile – for work with bacteria
  - Not sterile – for work with isolated polysaccharides

3.2. Methods

3.2.1. Preparation of bacterial and eukaryotic cells

3.2.1.1. Preparation of bacteria for the isolation of cell envelope components

Bacteria were cultivated on Brain Heart Infusion (BHI) 1.5% agar plates from frozen stocks in 20% glycerol, stored at -80°C. Fifty ml of BHI was then inoculated with one picked colony for 8-12 h as pre-culture. Pre-cultures were used for inoculation of 4 l of BHI in 5 l flasks, and bacteria were grown as standing cultures to the stationary phase (OD_{600} 0.5-0.8, depending on the strain) for 10-12 h. Then bacteria were harvested, (5524 *g*, 4°C, 20 min; rotor JLA8.1000) and washed with 0.1 M citrate buffer (for LTA, WTA, rhamnan and glycolipids) or PBS (for CPS). The bacterial pellet was used immediately or stored at -80°C.

0.1 M citrate buffer:	460 ml	0.1 M citric acid
	540 ml	0.1 M Sodium citrate dihydrate
		pH 4.7

3.2.1.2. Preparation of bacteria for the isolation of DNA and RNA

Bacteria were cultivated in 5 ml Todd Hewitt Broth or BHI for 12 h from frozen stocks in 20% glycerol, stored at -80°C. Three ml of bacterial culture was centrifuged [13000 *g* for 5 min at 22°C (room temperature – RT) in an MSE benchtop microfuge] and the supernatant was discard. Harvested bacteria were used immediately.

3.2.1.3. Preparation of bacteria for biofilm assay

Bacteria were cultivated on Brain Heart Infusion (BHI) 1.5% agar plates from frozen stocks in 20% glycerol, stored at -80°C. Five ml of BHI was then inoculated by one picked

colony for 8-12 h as a pre-culture. Polystyrene tissue culture plates were filled with 180 µl of BHI and 20 µl of pre-culture and were incubated for 18 h at 37°C.

3.2.1.4. Preparation of bacteria for stimulation of eukaryotic cells

Prior to the stimulation of pbMEC, RAW 264.7 and HEK293 cells, bacteria were cultivated on Todd Hewitt Broth (37°C, 16 h) to the logarithmic phase of growth (optical density at 600 nm (OD_{600}) of 0.5; 1 x 10^7 cells/ml). Plating of dilution series was used to calibrate cell counts from the OD readings. Then, cells were killed by incubation for 1 h at 80°C (*S. uberis*) or 1 h at 60°C (*E. coli*) which was verified by control plating. Finally, cells were spun down, washed twice and resuspended in RPMI 1640 medium at a density of 5 x 10^8 cells/ml. Aliquots were stored frozen at -20°C. The eukaryotic cells were challenged for different times with 10^7 particles/ml.

3.2.1.5. Disruption of bacterial cells

Disrupted cells were needed in order to isolate glycolipids, LTA, rhamnan and WTA. To 30 ml of bacterial cells resuspended in citrate buffer 0.1 M, 30 ml of glass beads were added, and cells together with glass beads were shaken for 5 min utilizing the cell homogenizer.

3.2.1.6. Preparation of pbMEC

The pbMEC were obtained as described previously (Yang et al., 2006). Briefly, an udder from a freshly slaughtered cow was rinsed with 70% ethanol and cubes containing secretory tissue (> 10 g) were immersed in HBSS (Hank's Balanced Salt Solution, buffered with HEPES, supplemented with APS solution; Sigma). Minced epithelial areas (~ 5 mm pieces) were immersed into 30 ml HBSS and rocked repeatedly for 5 min. Large clumps were allowed to settle, until the supernatant remained clear. The HBSS was replaced by 20 ml of HBSS supplemented with 200 U/ml collagenase Type IV, and the homogenate was shaken at 37°C. It was filtered every 30 min through a 60 mesh steel grid (Sigma) to collect the dispersed cells. This procedure was repeated for 4 h. Best results were obtained with cells after more than 30 min and less than 180 min of incubation. Cells from each aliquot

were collected (300 *g*, 5 min), washed twice in HBSS and finally plated on collagen-coated plates (Collagen R; Serva, Heidelberg, Germany). After ~ 6 days of unperturbed growth, fibroblasts were removed by repeated selective trypsinizations throughout the next weeks of continued propagation of the subcultures. Highly enriched pbMEC were maintained in RPMI medium and could eventually also be stored frozen.

3.2.1.7. Preparation of bovine MNC

Blood from healthy cattle was obtained by venipuncture of the vena jugularis externa into heparinized vacutainer tubes (Becton Dickinson, Heidelberg, Germany). The blood was layered on Ficoll-Isopaque (PAA, Pasching, Austria) and centrifuged at 4°C for 30 min at 1000 *g*. The interphase containing MNC was washed 3 times with PBS and finally resuspended in RPMI medium.

3.2.2. Isolation of the cell envelope components

3.2.2.1. Isolation of glycolipids

Glycolipids were isolated from disrupted cells of *S. uberis* 233, 0140J, T1-18 and mutant 0140J:ISS1P'(*sub0538&sub0539*).

3.2.2.1.1. Butanol-water extraction

Bacteria were prepared as described in 3.2.1.1, and disrupted with glass beads as written in 3.2.1.5. Supernatant was separated from the glass beads after centrifugation for 30 min, 5500 *g* in 4°C (rotor F-14). To the supernatant the same volume of *n*-butanol was added. The mixture was stirred for 1 h and then, for phases separation, centrifuged (5500 *g*, 4°C, 20 min; rotor F-14). The butanol phase was taken for further extraction of glycolipids.

3.2.2.1.2. Bligh and Dyer extraction

Butanol was evaporated on a rotary evaporator and the dry extract was resuspended in water and sonicated for 15 min. Chloroform and methanol were added to obtain the ratio $CHCl_3$/MeOH/water 1:2:0.8 (v/v). The mixture was vortexed for 20 min. For phase separation $CHCl_3$ was added in that way that the ratio was 2:2:0.8 (v/v) and the mixture was vortexed again for 30 s. Finally, water was added to reach the ratio $CHCl_3$/MeOH/ water 2:2:1.8 (v/v). The mixture was centrifuged (12 000 *g*, 15 min, 4°C, rotor F-21, Thermo Scientific), the organic phase was collected and dried with nitrogen. The obtained product was resuspended in 2 ml of $CHCl_3$/MeOH 8:2 and filtered through a 0.22 µm filter (13 mm Syringe Filter PTFE, GRACE). Sample was again dried under nitrogen, then placed in the vacuum desiccator and weighted.

3.2.2.1.3. TLC analysis

Glycolipids were analyzed by TLC. Prior to the separation the atmosphere in the chromatography chamber was equilibrated for 25-40 min with the running solution.

Eight µg (for Hanessian's stain) or 32 µg (for α-naphthol staining) of sample resuspended in chloroform/methanol 8:2 (v/v) was applied on the TLC plate using a 2 µl microsyringe. Then the plate was placed into a chamber and developed to 0.5 cm below the top of the plate. For visualising glycolipids and other components plates were observed under the UV (260 nm and 280 nm) light (bands were marked with a pencil), then plates were dipped into Hanessian's stain, dried and heated for 5 min at 150°C. For visualising glycolipids plates were dipped into α-naphthol staining, dried and heated for 5-10 min at 110°C.

Running solution:	65 ml	chloroform
	25 ml	methanol
	4 ml	water
α-Naphthol stain:	6 ml	H_2SO_4 (98%) added dropwise into
	50 ml	methanol (cooled on ice)
	4 ml	H_2O
	1.92 g	α-naphthol
Hanessian's stain:	471	ml H_2O
	29 ml	98% H_2SO_4
	0.5 g	$Ce(SO_4)_2$ x 4 H_2O
	25 g	$(NH_4)_6MO_7O_{24}$ x H_2O

3.2.2.1.4. Isolation of glycolipids from the crude lipid extract

The crude lipid extract was fractionated on a column (1 x 10 cm) of activated Silica Gel 60. Glycolipids were eluted successively with chloroform/methanol in the ratios of 9.7:0.3, 9.5:0.5, 9:1, 8.5:1.5 and 1:1. Fractions were monitored for glycolipids on TLC. Those fractions that contained the desired material were dried and further purified by preparative TLC.

3.2.2.1.5. Purification of glycolipids utilizing the preparative TLC

Prior to the separation Silica Gel Glass Plates (20 x 20 cm) were developed in the chromatography chamber over the top applying the washing solution. Then plates were dried, placed in an oven and heated at 120°C for 1 h. After that, the activated plates were either used immediately or stored in a desiccator. Before separation the atmosphere in the chromatography chamber was equilibrated with the appropriate solution for 25-40 min. Samples were applied on the TLC plate with a 2 µl microsyringe. Plates were placed into the chamber and developed to 0.5 cm below the top of the plate. Samples eluted in $CHCl_3$/MeOH 9.5:0.5 and 9:1 were developed in running solution 1, and the one eluted in $CHCl_3$/MeOH 1:1 in solution 2. For detection of the bands the margin of the plate was cut off and stained with a Hanessian's stain. The bands of interest were scraped off (region of scraping was determined by using the stained piece), and eluted with chloroform/methanol 1:1. Eluates were filtered with a 0.22 µm filter (13 mm Syringe Filter PTFE, GRACE) and dried with nitrogen, then in a vacuum desiccator and weighed.

Washing solution: chloroform / methanol 1:2

Running solution 1: chloroform/methanol/water 65:25:1

Running solution 2: chloroform/methanol/water 50:37.5:4

3.2.2.2. Isolation of LTA

Lipiteichoic acid was isolated from disrupted cells of *S. uberis* 233, 0140J, T1-18.

3.2.2.2.1. LTA extraction

After the disruption of the with glass beads and cell homogenizer (3.2.1.5), the supernatant was separated from the glass beads by centrifugation for 30 min, 5500 *g* at 4°C (rotor F-14). To the supernatant the same volume of *n*-butanol was added. The mixture was stirred for 1 h and then, for phase separation, centrifuged (5500 *g*, 4°C,

20 min; rotor F-14). The water phase was transferred into dialysis membrane (3.5 ku cut off), and dialysis was performed for 5-7 days at 4°C against 10 l of water changed 2-3 times per day. After dialysis the sample was freeze-dried.

3.2.2.2.2. HIC

Prior to separation on HPLC, the lyophilized sample was resuspended in buffer A (15% propan-1-ol/ 0.1 M ammonium acetate) and filtered (0.45 µm, PALL Life Sciences, HPLC certified). Then the sample was applied on the HiPrep column of octyl-sepharose and purified by HIC. The bound material was eluted applying a gradient from 100% buffer A to 100% buffer B (60% propan-1-ol/0.1 M ammonium acetate) over 60 min. Fractions 30-50 were checked for the presence of phosphate. Selection of these fractions for phosphate assay was done after initial experiments, in which all fractions were examined in regard of phosphate content. The desired product (LTA) was always present in fractions 36-45.

3.2.2.2.3. Purification of the LTA

Phosphate-containing fractions were combined after their characterization by a photometric phosphate assay. The purified LTA was washed repeatedly with water and freeze-dried to remove residual buffer.

3.2.2.3. Isolation and purification of WTA and rhamnan

The WTA and rhamnan were isolated from the disrupted cells of *S. uberis* 233.

3.2.2.3.1. Extraction of WTA and rhamnan

After the disruption of the bacteria with glass beads and cell homogenizer, supernatant was separated from the glass beads by centrifugation for 5 min, 1000 *g* at RT (rotor 4446). The glass beads were washed 3-5 x with citrate buffer. In order to release polysaccharides

bound to the PG, an enzymatic digestion was performed. First, 10 x buffer for enzymatic treatment was added to the resuspended cells particles, then lysozyme (0.2 mg/ml), DNase I and RNase (each 0.1 mg/ml) were added. The sample was shaken at 37°C for 24 h. The insoluble cell-wall fragments were removed by centrifugation (4°C, 30 min, 10 000 *g*, rotor F-14), and the supernatant was then treated with proteinase K (0.1 mg/ml) at 37°C for 24 h. After digestion, the solution was dialyzed (3.5 ku cut off) against water and lyophilized.

3.2.2.3.2. HIC

The sample was purified by HIC in order to remove the remaining LTA. The procedure was performed as described in 3.2.2.2.2. Fractions 4-14 were combined and the sample was lyophilized. These fractions, eluted with 100% buffer A contained material which, due to the lack of hydrophobic group, did not bind to the matrix of the column.

3.2.2.3.3. Anion-exchange chromatography

Prior to separation on FPLC, the lyophilized sample was resuspended in water and filtered (0.45 µm, PALL Life Sciences, HPLC certified). Then it was applied on HiTrep Q Sepharose column and purified by anion-exchange chromatography. The bound material was eluted with a gradient from 0 to 1 M of NaCl of 36 columns volume (1 column volume was 5 ml) with a flow rate 3 ml/min. Then the column was washed; first with 20 columns volume of 1 M NaCl, then with 5 columns volume of 2 M NaCl. Fractions 1-80 were examined in regard of phosphate content.

3.2.2.3.4. Purification of obtained polysaccharides

In order to desalt the obtained samples, separation on a column (2.5 x 100 cm) of Sephadex G-10 was performed. The eluation was carried out without a pump, with a buffer containing 4 ml pyridine and 10 ml glacial acetic acid in 1 l of water. The pyridine-acetate buffer was removed by repeated evaporation of the solvent on a rotary evaporator.

3.2.2.4. Isolation of the CPS

The CPS was isolated from cells of *S. uberis* 233, 0140J, T1-18 and *ΔHasA* mutant.

3.2.2.4.1. Extraction of the CPS

The bacterial pellet was prepared as described in 3.2.1.1. and the biomass was resuspended in 900 ml of sterile 0.9% NaCl solution in order to extract loosly bound CPS. After 6 h of stirring at RT, the cells were centrifuged (10000 *g*, 4°C, 45 min; rotor JA 14) and the supernatant was dialyzed (12-16 ku cut-off) against water and lyophilized (NaCl extract). The remaining sediment was further treated with 1% phenol at 4°C for 48 h in order to extract closer bound material. The cells were again sedimented (10000 *g*, 4°C, 45 min; rotor JA 14) and the supernatant was dialyzed against water and lyophilized (phenol extract).

3.2.2.4.2. Size exclusion chromatography

To further purify each of the exracts, both of them were applied on a column (2.5 x 80 cm) of Biogel P60. The eluation was carried out without a pump, with a buffer containing 4 ml pyridine and 10 ml glacial acetic acid in 1 l of water. The fractions were combined according to the obtained chromatogram. The purity of the isolated material was monitored by UV spectroscopy. When needed, treatment with DNase, RNase followed with proteinase K was performed. Samples were then further purified on a column (1.5 x 100 cm) of Bio-Gel P10. The pyridine-acetate buffer was removed by repeated evaporation of the solvent on a rotary evaporator.

3.2.2.5. Isolation of the EPS

The exopolysaccharide was isolated from culture filtrates after the cultivation of *S. uberis* 233, 0140J, T1-18 and EF20.

3.2.2.5.1. Acetone precipitation

Bacteria were grown in BHI culture medium at 37°C for 12 h. The biomass was centrifuged (8000 *g*, 4°C, 30 min; rotor JLA 8.1000) and the supernatant was filtered sterile through 0.22 µl filter (Milipore, USA). Three hundred ml of cold acetone was added to 100 ml of sterile culture supernatant and to 100 ml of sterile medium (blank), and samples were stirred at 4°C for ~ 16 h. Then, samples were transferred to -20°C and were incubated there without stirring for another 16 h.

3.2.2.5.2. Purification of EPS

The precipitants were separated from the supernatants, dissolved in water and treated with proteinase K at 37°C for 16 h. Next, dialysis (12-16 ku cut off) against 10 l of water was performed for 3 days. Each sample was then separated on a column (2.5 x 80 cm) of BioGel P60 and eluted without a pump with a buffer containing 4 ml pyridine and 10 ml glacial acetic acid in 1 l of water. The pyridine-acetate buffer was removed by repeated evaporation of the solvent on a rotary evaporator.

3.2.3. Analytical methods

3.2.3.1. Gas-chromatography

In order to identify and quantify the contents of neutral and amino sugars, fatty acids and uronic acids, gas-liquid chromatography (GLC) and GLC/mass spectrometry (GLC/MS) were applied. GLC was performed utilizing a gas chromatograph (HP 5890 series II) with FID and a column of Phenyl MathylSiloxane HP-5 (Agilent Technologies, 30 m x 0.25 mm x 0.25 µm film thickness). The temperature program was 150°C for 3 min, then 3°C min^{-1} to 320°C and hydrogen was used as a carrier gas (70 kPa). Fatty acids were detected using a gas chromatograph HP 6890N with FID and a column (Agilent Technologies, 30 m x 0.25 mm x 0.25 µm film thickness) of Phenyl MathylSiloxane HP-5 with the temperature program 120°C for 3 min, then 5°C min^{-1} to 320°C. The results of methanolysis were analysed after applying the sample on GLC-MS [Hewlett Packard HP 5890 (series II) gas chromatograph equipped with a fused-silica SPB-5 column (Supelco, 30 m x 0.25 mm x 0.25 µm film thickness), FID and MS 5989A mass spectrometer with vacuum gauge controller 59827A]. The temperature program was 150°C for 3 min, then 5°C min^{-1} to 330°C. Data were analyzed with GC ChemStation software (Agilent Technologies, USA).

3.2.3.1.1. Methanolysis

The methanolysis was performed either with 0.5 M HCl/MeOH for 45 min (weak methanolysis) or with 2 M HCl/MeOH for 4 h (strong methanolysis). First, 200 µl of methanolate was incubated at 85°C with 100 µg of analyzed sample. Then the reagent was evaporated with nitrogen and 30 µl of pyridine and 30 µl of Ac_2O were added for peracetylation at 85°C for 6 min. The samples were dried and dissolved in 50 µl of $CHCl_3$; 1 µl was injected into GLC/MS.

3.2.3.1.2. Neutral sugar analysis

To identify the neutral sugars present in analyzed samples as well as to determine their concentrations, a hydrolysis utilizing 200 µl of 2 M TFA for 2 h at 120°C was performed.

After hydrolysis, 3 µg of a xylose were added to each sample as the internal standard and then the samples were evaporated and rinsed three times, first with water then with 10% ether/hexane solution to remove fatty acids. Next, samples were dried under nitrogen, and 200 µl of water was added to each sample. The pH was monitored and set to 8 with 1 M NaOH when necessary. For reduction ~ 2 mg of $NaBH_4$ were added to the samples and the reaction proceeded in the dark for 16 h. The reduction was terminated with 2 M HCl. All samples were washed three times with 5% HOAc/MeOH solution and twice with methanol. For peracetylation, 50 µl of acetic anhydride (Ac_2O) and 50 µl of pyridine were added and samples were incubated at 85°C for 10 min. Then, the solvent was evaporated with nitrogen and transferred salt free with $CHCl_3$ to new 1.5 ml vials. One µl (from 100 µl) was injected in GLC. The concentration of neutral sugars was quantified relatively to the internal standard.

3.2.3.1.3. Amino sugars analysis

The aminosugars were determined in GLC only qualitatively. 250 µg of sample was hydrolyzed with 250 µl 4 M trifluoroacetic acid at 100°C for 4 h. Next samples were dried under nitrogen, washed three times with water, pre-acetylated with 60 µl of pyridine and 60 µl of Ac_2O for 10 min, dried and then reduced and peracetylated again as in neutral sugars protocol (3.2.3.1.2). Samples were dissolved in $CHCl_3$ and injected to GC (1 of 100 µl). The identification of aminosugars was based on comparison to the standard.

3.2.3.1.4. Fatty acid analysis

For determination of fatty acids to 200 µg of each sample 10 µg of 17:0 was added as an internal standard. After drying with nitrogen the hydrolysis utilizing 1 ml 0.5 M NaOH in H_2O:MeOH (1:1) at 85°C for 2 h was performed. Then, 4 ml of H_2O were added and the samples were neutralized with 200 µl of 4 M HCl, and fatty acids were extracted with 1 ml of $CHCl_3$ (3 x). The samples were strongly shaken for 1 min, and the extracted $CHCl_3$ phases were combined. Samples were placed at -20°C for ~ 16 h in order to freeze the remaining water. Next chloroform phase was quickly transferred to a fresh vial and the volume was reduced to about 100 µl. Then samples were treated twice with 5-6 drops of diazomethane; first for 1 min, then for 10 min, and evaporated with nitrogen until the yellow color (appearing after addition of diazomethane) was gone. One µl of sample was

injected into GLC. The concentration of the fatty acids was quantified relatively to the standard.

3.2.3.1.5. Uronic acid analysis

For uronic acid analysis 250 µg of sample was treated with 200 µl 0.5 M HCl/MeOH. The methanolysis was performed for 45 min in 85°C. The solvent was then evaporated with the nitrogen and the sample was then washed three times with methanol. The reduction was performed using $NaBD_4$ in 250 µl of H_2O/MeOH 4:1 (v/v) at RT for 16 h. After neutralization with 2 M HCl and washing three times with 5% HOAc/MeOH the procedure was performed like for neural sugars starting with hydrolysis. The uronic acids were identified by GLC compared to authentic standards.

3.2.3.1.6. Methylation analysis

Prior to the methylation analysis of EPS and CPS 0.5 mg of each of the samples were lyophilized after addition of 5 µl glycerol. In the analysis of linker of LTA (100 µg) this step was omitted. Then, the dry sample was dissolved in 1 ml DMSO and methylation was performed with 500 µl MeI for 1 h at RT under basic conditions (~ 300 µg of powdered NaOH was added just after addition of MeI). Then 7 ml of water and 2 ml of $CHCl_3$ were added, and the extraction was performed (3 x). The combined chloroform phases were washed with water to remove DMSO and the rest of MeI, evaporated to dryness under nitrogen and methylated again. Then, the sample was hydrolyzed with 4 M TFA at 100°C for 4 h, and reduced with $NaBD_4$ in H_2O:MeOH 1:1 (v/v) for 16 h. After terminating the reaction with 2 M HCl, evaporation with nitrogen was performed, and prior to peracetylation with 60 µl of pyridine and 60 µl of Ac_2O (10 min, 85°C) the samples were washed three times with 5% HOAc/MeOH and three times with MeOH. The obtained product was dissolved in 50 µl of $CHCl_3$, and the sample was analyzed by GLC-MS.

3.2.3.1.7. Absolute configuration

To determine the absolute configuration of sugars and alanine, 150 µg of sample was dissolved in 150 µl of 2 M HCl/MeOH and methanolysis was performed at 85°C for 2 h. Then samples were washed three times with MeOH.

In case of LTA and glycolipids, fatty acids were removed by rinsing 3 times with 10% ether/hexane.

When analyzing the CPS, reduction with $NaBD_4$ in H_2O/MeOH 4:1 (v/v) for 16 h at 4°C was performed. Then the sample was neutralized with 2 M HCl and washed with 5% HOAc/MeOH (3 x) and MeOH (3 x). This step was performed because of the presence of carboxygroup of glucuronic acid, which had to be protected from decarboxylation. Because of the presence of glucosamine in the sample peracetylation (30 µl pyridine and 30 µl Ac_2O; 10 min, 85°C) was carried out.

Then, butanolysis was performed (2 M HCl/S-BuOH, 65°C, 4 h) for all samples. The samples were then washed three times with MeOH and peracetylated (30 µl pyridine and 30 µl Ac_2O; 10 min, 85°C). The obtained products were dissolved in 50 µl of $CHCl_3$ and analyzed on GC. The determination was based on the respective D- and L-configured standards.

3.2.3.2. Photometric methods

3.2.3.2.1. Inorganic phosphate

To determine the content of inorganic phosphate 25, 50 and 75 µg of each sample and pairs of 2, 4, 6, 8, 10 µl of the standard (5 mg/ml in water; Na_2HPO_4) solution were placed into glass tubes and filled up to 100 µl of water. The blank (100 µl of water) was treated parallel to the samples and was used for calibration. All samples were incubated with 900 µl of the reagent at 37°C for 30 min. The extinction was measured at 820 nm.

Reagent:

0.4 M	H_2SO_4
0.16%	ammonium molybdate
3.30%	ascorbic acid

3.2.3.2.2. Organic phosphate

For the determination of the total content of phosphate 2, 5 and 10 µg of each sample and the doublets of 2, 4, 6, 8, 10 µl of the standard (5 mg/ml in water; Na_2HPO_4) were put into

glass tubes, washed from the tubes wall with 100 µl of water and dried in a vacuum desiccator for 18 h. The blank (100 µl of water) was treated parallel to the samples and was used for calibration. Then, all samples were incubated with 100 µl of the releasing reagent at 100°C for 1 h and then at 165°C for 2 h. After cooling on ice 1 ml of the color reagent was added to each tube and the solutions were incubated at 37°C for 90 min. The extinction was measured at 820 nm.

Releasing reagent:

30.6%	H_2SO_4
4.7%	$HClO_4$

Colour reagent:

0.1 M	sodium acetate
0.25%	ammonium molybdate
1%	ascorbic acid

3.2.3.3. Chemical and enzymatical degradation

3.2.3.3.1. Hydrofluoridc acid treatment

This treatment was applied in order to obatain the lipid anchor from LTA and dephosphorylated EPS. The molecules were treated with 50 µl 48% $HF_{aq.}$ at 4°C for 48 h, next the acid was evaporated under nitrogen and washed 3 x with water. For isolating the lipid anchor, the chloroform/water extraction (1:1 v/v) was performed and the desired product was recovered from the chloroform phase.

3.2.3.3.2. *O*-Deacetylation utilizing abs. hydrazine

Abs. (100%) hydrazine was used to obtain the deacylated lipid anchor (recovered after HF treatment) as well as *O*-deacylated LTA (without fatty acids and alanine). This treatment was performed also in order to eliminate the possibility of the OAc substitution at O-6 of

Glc in the EPS. Hydrazinolysis was performed as published (Holst, 2000). Briefly, to the dried LTA (6 mg), lipid anchor (900 µg) or EPS (1 mg), 1 ml/20 mg of abs. hydrazine was added. The mixture was incubated at 37°C for 1 h. Hydrazine was destroyed by adding to the cooled (on ice) sample 10 volumes of cold acetone. Sample was washed 2 x with acetone and the desired product was recovered from the water phase after chloroform-water extraction. For the EPS the extraction step was omitted and after drying, the sample was prepared for NMR measurement. *O*-Deacylated LTA was additionally dialyzed (3.5 ku cut off) against water in order to remove free Ala.

3.2.3.3.3. *O*-Deacetylation utilizing ammoniac solution

To remove the putative ester-bound acetyl group at O-6 of Glc of EPS (1 mg), the molecule was treated with 12% aqueous NH_3 solution at 37°C for 12 h. The NH_3 aq. was then evaporated with nitrogen, then sample was washed twice with water, and prepared for NMR spectroscopy.

3.2.3.3.4. Acetolysis of EPS

This degradation was performed on EPS. During acetolysis the (1→6)-linkage of the mannose residues were cleaved, while (1→3) and (1→2)-linkage remained intact. The procedure was performed as described previously (Kocourek and Ballou, 1969) with some modifications. To 5.5 mg of EPS 250 µl of pyridine and 250 µl of Ac_2O was added. The mixture was incubated at 100°C for 8 h, and then dried under nitrogen. Next, incubation at 40°C for 16 h with 250 µl Ac_2O, 250 µl HOAc and 25µl of 99.8% H_2SO_4 aq. took place. After that, in order to neutralize, 1 ml pyridine was added to the mixture and sample was dried with nitrogen. Three ml water and 3 ml chloroform were added to the sample and extraction was performed. After phase separation, the chloroform phase was washed with water, and the water phase was washed with chloroform. The organic phases were combined, and the sample was dried first with nitrogen, then additionally in a vacuum desiccator for 30 min. The product was dissolved in 0.5 ml MeOH exSch and 10 drops of 0.25 M methanolic sodium methoxide solution was added. After 20 min of incubation at RT 3 drops of 2 M HCl/MeOH was added. The solvent was evaporated, then the sample was washed with 0.5 ml water, dissolved in pyridinium-acetate buffer (4 ml of pyridine and 10 ml of acetic acid in 1 l of buffer) and separated on a column (1.5 x 100 cm) of Biogel P2

without a pump. The pyridinium-acetate buffer (used also as an eluent) was removed by repeated evaporation of the solvent on a rotary evaporator.

3.2.3.3.5. Degradation of EPS using the α-mannosidase

For enzymatic hydrolysis of the EPS, 4 mg of sample were dissolved in water and treated with α-mannosidase (100 μg) at 22°C for 19 days. Then the sample was treated with proteinase K at 56°C for 1 h and lyophilized. The dry sample was dissolved in 0.5 ml of pyridinium – acetate buffer (4 ml pyridine and 10 ml glacial acetic acid in 1 l of water), and fractionated through a column (1.5 x 100 cm) of BioGel P2. The elution of the sample was performed utilizing the same pyridinium – aceteate buffer as used for suspension of the sample, without a pump.

3.2.3.4. Nuclear magnetic resonance spectroscopy (NMR)

Isolated material and its components were analyzed by NMR spectroscopy. Prior the recording samples were dissolved in D_2O, or in case of glycolipids in the mixture of deutrized methanol and chloroform (1:2 v/v) and measured at 27°C or 42°C (LTA). All 1D and 2D NMR $^{1}H,^{1}H$ correlation spectroscopy (COSY), total correlation spectroscopy (TOCSY), rotating frame Overhauser effect spectroscopy (ROESY), as well as $^{1}H,^{13}C$ heteronuclear single quantum coherence (HSQC) and heteronuclear multiple bond correlation (HMBC) and $^{1}H,^{31}P$ heteronuclear multiple quantum coherence (HMQC) experiments were recorded by a Bruker DRX Avance III 700 MHz spectrometer (operating frequencies of 700.75 MHz for ^{1}H NMR, 176.2 MHz for ^{13}C NMR and 283.7 MHz for ^{31}P) and standard Bruker software. COSY, TOCSY, and ROESY experiments were recorded using data sets (t1 by t2) of 4096 by 512 points, with 16 scans for COSY, and 32 for TOCSY and ROESY. The TOCSY experiments were carried out in the phase-sensitive mode with mixing times of 60 ms, and in case of EPS and rhamnan additionally 120 and 180 ms, and ROESY of 300 ms. The ^{1}H, ^{13}C correlations measured in the ^{1}H-detected mode *via* HSQC-DEPT with proton decoupling in the ^{13}C domain and HMBC spectra were acquired using data sets of 4096 by 512 points and 80 scans for each t1 value. HMBC spectra were adjusted to J coupling constant value of 145 Hz and long range proton carbon coupling constant of

10 Hz. Chemical shifts were reported relative to external acetone (δ_H 2.225, δ_C 31.45) or for glycolipids internal TMS (δ_H 0.0, δ_C 0.0), and external phosphoric acid (δ_P 0.0).

3.2.3.5. Mass spectrometry

3.2.3.5.1. ESI FT-ICR MS

Lipoteichoic acid and Glycolipid 3 were analyzed by electrospray ionization Fourier-transformed ion cyclotron mass spectrometry (ESI FT-ICR MS) on an APEX Qe-Instrument (Bruker Daltonics, Billerica, MA, USA) equipped with a 7 Tesla magnet and a dual Apollo ion source. Mass spectra were recorded in the negative ion mode under standard instrumental parameters. Samples (~ 10 ng/µl) were dispersed in an ESI spray solution consisting of propan-2-ol, water, and triethylamine (50:50:0.001, by vol.) and were sprayed at a flow rate of 2 µl/min. Capillary entrance voltage was set to 3.8 kV, and drying gas temperature to 200°C. The mass spectra were charge deconvoluted and all masses given refer to the monoisotopic peaks of the neutral molecules.

3.2.3.5.2. MALDI FT ICR-MS

Glycolipids 1 and 2 were analyzed by matrix-assisted laser desorption ionization Fourier-transform ion cyclotron resonance mass spectrometry (MALDI FT ICR-MS) on APEX Qe-Instrument (Bruker Daltonics, Billerica, USA) equipped with a 7 Tesla actively shielded magnet and a dual Apollo ion source in positive ion mode. Mass spectra were recorded using standard experimental sequences as provided by the manufacturer. The samples (~ 1 µg/µl) were suspended in the mixture of methanol – water (1:1 v/v). Matrix solution was prepared from 2,5-dihydroxybenzoic acid (2,5-DHB) in 1% TFA at a concentration of 15 µg/µl. Three µl of matrix solution and 3 µl of sample solution were mixed and applied onto the stainless steel sample plate as 1.5 µl droplets. Samples were allowed to crystallize at 22°C. Laser irradiance was adjusted to reduce the formation of DHB-adduct ions.

3.2.4. Molecular biology methods

3.2.4.1. Isolation of the chromosomal DNA from *S. uberis*

Cells were prepared as described in 3.2.1.2. The cell pellet was washed once with TE buffer, resuspended in 375 µl of cell wall disruption buffer and incubated in 37°C for 30 min. Cells were lysed by addition of 20 µl lysis buffer and 3 µl of proteinase K. After 1 h of incubation in 37°C, 200 µl of saturated NaCl (approx. 6.0 M) was added in order to precipitate protein cell wall material. Sample was centrifuged (12500 *g*) for 10 min to obtain a firm pellet. The clear supernatant was carefully transferred to a fresh tube and an equal volume of Tris-equilibrated phenol/chloroform/isoamylalcohol (25:24:1 by vol.) was added. Sample was mixed and centrifuged (3 min, 13000 *g*, RT; MSE benchtop microfuge) in order to separate the phases. The aqueous (upper) phase was collected and nucleic acids were precipitated by adding 2 volumes of cold ethanol and incubation on ice for 1 h. The precipitant was spun down (13000 *g*, 5 min, RT), washed with 70% ethanol and air-dried. The obtained material was resuspended at 4°C in 50 µl of TE buffer containing 20 µg/ml of RNase A (made DNase-free by boiling for 5 min) and then was incubated at 37°C for 30 min. The DNA was stored in -20°C or used immediately.

TE buffer 10 ml:

0.1 ml	1 M Tris-HCl pH 7.5
0.1 ml	0.5 M EDTA pH 8.0 and
9.8 ml	sterile molecular biology grade water

Cell wall disruption buffer:

30 u/ml	mutanolysin
10 mg/ml	lysozyme
0.5 x	TE buffer (prepared as above)

Lysis buffer:

20% w/v	SDS
50 mM	Tris
20 mM	EDTA
	pH 7.8

Proteinase K:

20 mg/ml proteinase K
stored frozen at -20°C

3.2.4.2. Isolation of mRNA from *S. uberis*

Total RNA was isolated from an overnight (16 h) culture of *S. uberis* O140J and mutant 0140J::IS*S1*P'(*sub0538* & *sub0539*) using the Direct-Zol-RNA Miniprep Kit. Therefore, bacteria were lysed in Trizol and vortexed thoroughly for 10-15 min. Further RNA preparation and subsequent DNase I digestion were performed according to the manufacturer's instruction. Nucleic acid concentration and purity was determined with a NanoDrop ND-1000 spectrometer.

3.2.4.3. Isolation of mutants with IS*S1* insertion in *sub0538* gene from a mutant bank

The random mutant bank was generated as described by Ward at al. (Ward et al., 2001). Briefly, transformation of *S. uberis* 0140J with plasmid pGh9:IS*S1* was performed. Erythromycin resistant transformants were selected, and chromosomal insertion was achieved by temperature shift of grow condition from 28°C to 37°C. The glycerol stocks were stored in -70°C.

3.2.4.3.1. Primer design

The primers were designed in such way that the cross reactivity with other sequences of the *S. uberis* genome was limited. Primers p613 (sense) and p614 (antisense) were complementary to the inserted sequence IS*S1* while p800 (sense) and p801 (antisense) were complementary to the chromosomal DNA (Fig. 4).

Fig. 4. The sequence of the *sub0538* gene and the regions up- and downstream of the gene. Yellow – start and end of the *sub0538*; purple – the sequence of designed primers.

3.2.4.3.2. PCR-screening of the *S. uberis* 0140J pGh9:IS*S1* mutant bank – isolation of candidate plate

Bacteria were cultivated in sterile, flat-bottomed 96-well plates on Todd Hewitt broth containing erythromycin (1 μg/ml final concentration) at 37°C, overnight. Two and a half μl of grown bacteria from each well of a single plate (all together 90 plates) were combined into a 1.5 ml microtube (Fig. 5). Cells were sedimented and DNA was isolated as described in 3.2.4.1.

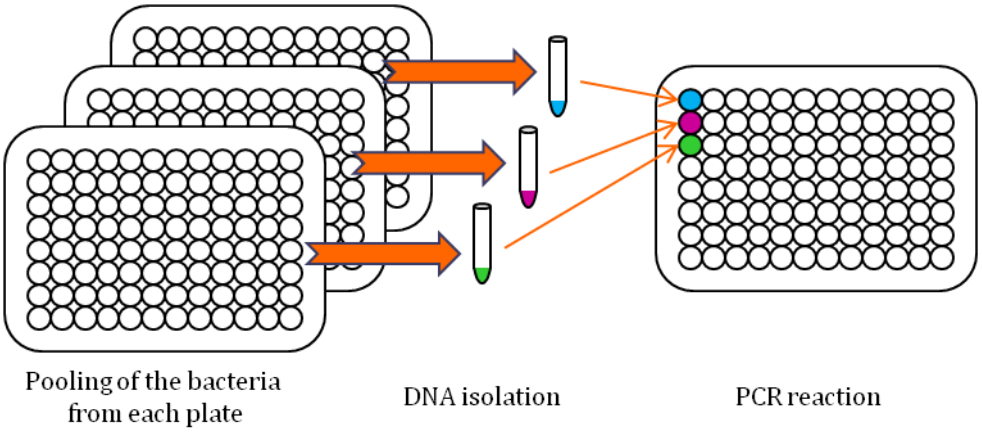

Fig. 5. The isolation of the candidate plate.

PCR reaction on the isolated DNA was performed using primers p614 and p801. The mastermix for the reactions was prepared as follow:

Mastermix:

100 µl	primer p614 (10 pmol/µl)
100 µl	primer p801 (10 pmol/µl)
400 µl	Phusion® HF Reaction Buffer (5 x)
200 µl	dNTPs (2 mM each)
40 µl	Phusion® High-Fidelity DNA Polymerase (2 units/µl)
900 µl	H_2O

For one reaction 16 µl of mastermix and 4 µl of 1:10 diluted pooled DNA from each bank plate were mixed. The DNA of the wild type *S. uberis* 0140J was used as a negative control. The PCR amplification reactions were run according to the following program:

98°C – 2 min
35 x { 98°C – 15 s; 63°C – 25 s; 72°C – 1 min }
72°C – 5 min
4°C – ∞

PCR products were loaded on 1% agarose gel after mixing with DNA gel-loading buffer (6 x). Gel was run for ~ 1 h at the voltage of 60-80 V, then stained in ethidium bromide for 10 min and visualized in UV light. The same procedure of the whole mutant bank

screening was performed utilizing the alternative pair of primers – p613 and p801 – to isolate candidates with the insert built in another orientation.

DNA gel-loading buffer (6x)

0.25%	bromophenol blue
40%	(w/v) sucrose
0.25%	xylene cyanol
0.25%	orange G

3.2.4.3.3. PCR-screening of the *S. uberis* 0140J pGh9:IS*S1* mutant bank – isolation of candidate transformant

Once candidate plates were isolated, the bacteria were cultivated in 300 µl of THB supplemented with erythromycin (1 mg/ml) per well. One hundred µl of bacteria from each row and each column were combined into 1.5 ml microtubes (20 for each plate). Bacterial cells were sedimented and resuspended in 240 µl for rows pellets and 160 µl for columns pellets of TE buffer. The tubes were placed in the heat block heated to 100°C for 8 min in order to release the DNA or the DNA isolation was performed. The PCR reaction was set in the same way as described above in 3.2.4.3.2. This PCR reaction identified coordinates of the candidate mutant (Fig. 6).

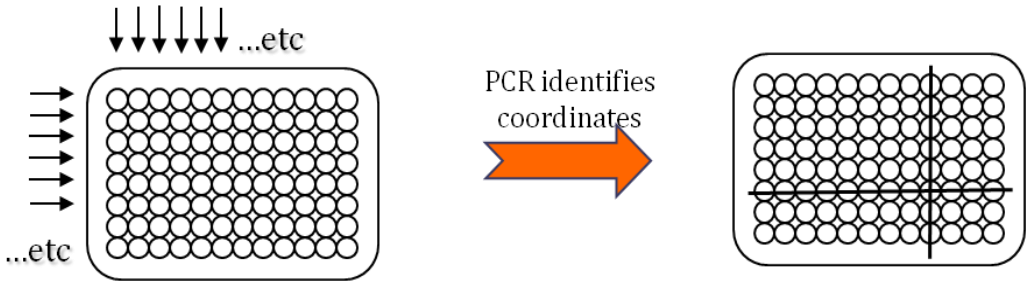

Fig. 6. The graphical outline of how to proceed with a candidate plate. After combining rows and columns and a PCR reaction, the candidate transformant could be found.

3.2.4.3.4. The control PCR reaction

Once the candidates were selected the DNAs were isolated and screened together with a DNA from a wild type *S. uberis* with three pairs of primers: p614 vs p801(A), p613 vs p800 (B) and p800 vs p801 (C). The expected product lengths for a positive mutant were ~ 1500 bp for pair A, ~ 200-300 bp for B and since the fragment for pair C would be too long to amplify no product was expected. For the wild type *S. uberis,* on the other hand, only ~ 1500 bp for pair C was supposed to be found. The reagents for 1 PCR reaction were as follow:

1 µl	Primer1 (10 pmol/µl)
1 µl	Primer2 (10 pmol/µl)
2 µl	dNTPs (2 mM each)
4 µl	Phusion® HF Reaction Buffer (5 x)
0.4 µl	Phusion® High-Fidelity DNA Polymerase (2 units/µl)
1 µl	1:10 diluted DNA
10.6 µl	H_2O

The PCR amplification reaction for pair A of primers was set as described in 3.2.4.3.2 and for pairs B and C were run according to the following program:

	98°C – 2 min
35 x	98°C – 15 s 59°C – 25 s 72°C – 1 min
	72°C – 5 min
	4°C – ∞

3.2.4.3.5. Excision of pG$^+$host vector to stabilize an IS*S1*-generated mutant

First, the pG$^+$host::IS*S1* transposant strain was grown in THB/Ery at 37°C for ~ 12-16 h. Then, the culture was diluted 10^6-fold in THB without addition of erythromycin and incubated in 28°C until saturated (18-24 h). This enables recombination by allowing plasmid replication in its permissive temperature. The culture was diluted in THB – without erythromycin (Ery) – to 10^{-5} and 10^{-6} and plated on Todd Hewitt agar (THA) plates with and without addition of erythromycin. They were incubated for 12-16 h at

37°C to promote the loss of excised plasmid. When the amount of colonies differed significantly on THA/Ery and THA, the bacteria from the plate without selective antibiotic were picked and plate on THA and THA/Ery. Colonies that grew only on non-selective plates lost the pG+host replicon and their mutations were stabilized.

3.2.4.3.6. Preparation of the DNA the sequencing

The DNA from cured mutant was isolated as described in 3.2.4.1. The PCR reaction utilizing primers p800 and p801 was performed. The reagents were as follow:

1 µl	p800 (10 pmol/µl)
1 µl	p801 (10 pmol/µl)
2 µl	dNTPs (2 mM each)
4 µl	Phusion® HF Reaction Buffer (5 x)
0.4 µl	Phusion® High-Fidelity DNA Polymerase (2 units/µl)
1 µl	1:10 diluted DNA
10.6 µl	H_2O

After the PCR reaction, the product was purified with QIAquick PCR Purification Kit and run on 1% agarose gel together with molecular mass marker. The estimation of the DNA concentration was based on the comparison of the intensity of the band corresponding to the amplified DNA to the intensity of the bands of marker. Ten µl of the product (50 ng/µl) was send for sequencing together with a primer p082 – complementary to the IS*S1* sequence.

3.2.4.4. Measurement of the genes expression in *S. uberis*

The mRNA was isolated as described in 3.2.4.1. For reverse transcription the Maxima® First Strand cDNA Synthesis Kit for RT-qPCR was used (7 µl isolated RNA, 2 µl master mix, 1 µl enzyme mix, 10 min RT, 30 min 55°C, 5 min 85°C in a thermal cycler). cDNA concentrations were typically between 1000-2000 ng/µl and the absorbance ratio of 260/280 nm was usually around 1.8. Gene-specific primer pairs and TaqMan® probes were designed with the UPL assay design center (ProbeFinder Version 2.45). Primer sequences and probes are given in Table 7. Real-time RT-qPCR was performed using the

Probe Master Kit (5 µl master mix, 0.8 µl per primer (6.25 µM), 0.1 µl UPL probe, 2.3 µl dH_2O, 1 µl cDNA sample) and the LightCycler® 480 II systems according to following lines:

95°C – 10 min
55x { 60°C – 5 s
95°C – 5 s
40°C – 30 s

Crossing points (Cp values) of target genes and the reference gene were determined by the second derivative maximum algorithm. The relative gene expression was calculated considering the individual efficiency of each PCR reaction setup determined by a standard curve. The expression of *sub0538* gene was normalized to the expression of the house keeping gene *sub0888.*

3.2.4.5. Isolation of mRNA from eukaryotic cells

Tissue cubes were snap frozen in liquid nitrogen immediately after slaughter and stored at -80°C. TRIzol was used to prepare total RNA hereof after a storage time of no longer than 3-4 weeks. The purified RNA was stored frozen (-80°C).

3.2.4.6. Measurement of gene expression in eukaryotic cells

cDNA was synthetized from isolated mRNA using the Superscript II Reverse Transcriptase. The product was purified with the High Pure purification kit and served as a template RT-PCR. The PCR products were resolved on 2% agarose gel. The specific bands were retrieved and cloned into the pGEM T-easy vector (Promega, Madison, WI) for sequencing. Abundances of *ACCA* transcripts derived from the respective promoters were measured with the FastStart Sybr-Green I reaction kit and the LightCycler instrument essentially as described (Molenaar et al., 2003). Briefly, a cDNA equivalent to an input of 75 ng of total RNA and a mixture of all amplification primers (25 pg each). The PCR cycle program was as follows:

95°C 5 min
40x { 60°C 10 s
72°C 20 s
83°C 30 s
95°C 15 s

Authenticity of the amplicons was validated by their homogenous melting profile, but also by determining the size of the products on ethidium bromide stained agarose gels. Assays for all different transcripts had initially been validated by sub-cloning and sequencing of the respective amplicons retrieved from Light Cycler runs. Relative mRNA copy numbers were titrated against external standards consisting of serial dilutions (10^6 – 10 copies) of plasmid clones harboring the respective amplicons of the diagnostic exons. The measured gene expression was normalized to the expression of *CLIC1*.

3.2.5. *In vitro* methods

3.2.5.1. Stimulation experiments

3.2.5.1.1. Transfection and lucifarase assay for measurement of NF-κB activation

The reconstitution of the TLR-signalling cascade in HEK293 cells and the assay of luciferase activity performed HEK293, RAW 264.7 and pbMEC were described (Yang et al., 2006; 2008). All plasmid DNAs used for transfection of mammalian cells were prepared free of endotoxins. Plasmid DNAs were transiently transfected into tissue culture cells using Lipofectamin 2000 (Invitrogen, Karlsruhe, Germany). For luciferase assay, cells were transfected with 100 ng of an expression vector of the Renilla luciferase driven by an artificial promoter featuring five NF-κB attachment sites [ELAM-promoter; recloned from the pNiFty vector (Invitrogen)]. HEK293 cells were additionally transfected with bovine TLR2 cloned into pFLAG-CMV-1 expression vector (Yang et al., 2006). To transfect a single well of a six well plate, two different premixes were prepared. Premix one consisted of up to 3 µg of DNA dissolved in 100 µl of the salt base from the DMEM medium, without any additives. The second premix consisted of 6 µl of Lipofectamin 2000, suspended in the same medium. Each premix was incubated for 5 min, before both were combined and incubated for another 20 min. Meanwhile, the cells (80% confluent) were washed twice with PBS and covered with 800 µl of DMEM salt base medium. The 200 µl of the premix were added and incubated. After 3 h, 1 ml of DMEM medium, supplemented with twice the complement of all usual additives (including 20% foetal calf serum) were added and the cells were allowed to recover overnight. Next, they were split and distributed to a 24 well plate for stimulation experiments. To this end, the stimulating agents (either inactivated

bacteria or LTA or glycolipids) were added immediately and left together with the cells for the duration of the experiment.

3.2.5.1.2. Stimulation experiment for measurment of gene expression

Prior to the challenge, pbMEC and RAW 264.7 were inoculated into a 9 cm dish, coated with collagen R. Then, the cells were lifted off with trypsin and washed twice in RPMI growth medium. The entire suspension was distributed into 6 wells of a collagen coated 6-well plate. This ensured that the cells were plated at high densities to deliberately avoid cell proliferation. The cells were allowed to attach for 24 h.
Subsequently, some wells were challenged with 10^7 heat killed *E. coli* 1303/ml, 10^7 *S. uberis*, LTA or glycolipids (5 µg/ml or 10 µg/ml). Other cells were kept as unchallenged controls. The cells were collected after different times (3 h, 6 h and 24 h), washed three times with phosphate buffered saline (PBS) to remove the bacteria. Total RNA was prepared.

3.2.5.1.3. Preparation of LTA for stimulation experiments

In order to inactivate any residual contamination with lipoproteins, the LTA was treated with 1% H_2O_2 at 37°C for 24 h (Zähringer et al., 2008).

3.2.5.2. Biofilm assay

The ability to form a biofilm was examined among various *S. uberis* strains in polystyrene microtiter plates following the protocol described by Baldassarri et al. (Baldassarri et al., 2001). Bacteria were prepared as described in 3.2.1.3. In order to confirm equivalent growth rates, the plates were read in a microtiter plate reader at OD_{630}. The culture medium was then discarded and the wells were washed with 150 µl of PBS. Special care was taken not to disturb the biofilm on the bottom of the wells. The plates were dried at 37°C for 1.5 h and then stained with 150 µl of Hucker´s crystal violet for 3 min. The stain

was then removed by rinsing the plates thoroughly under tap water. The plates were again dried for 30 min at 37°C. OD was determined at 630 nm.

Hucker´s crystal violet: A: 0.5 g of crystal violet in 5 ml of 95% EtOH
B: 0.2 g of ammonium oxalate in 20 ml H2O
5 ml A mixed with 20 ml B and sterile filtered

3.2.5.3. Phagocytosis/adherence assay

Heat killed *Staphylococcus aureus, E. coli* (Institute of Veterinary Microbiology, Hannover, Germany) and *S. uberis* EF 20 and O140J were labeled with fluoresceinisothiocyanate (FITC, Sigma-Aldrich, St. Louis, Missouri, USA). Bacteria were centrifuged at 14000 *g* for 5 min and peleted bacteria were resuspended in RPMI medium (PAA, Pasching, Austria) and adjusted to 2 x 10^8 particles/ml. Peripheral blood mononuclear cells (2 x 10^6/ml) were labeled with PE-Cy5-conjugated antibody to CD172a (AbD Serotec, Oxford, UK) to identify monocytes. Labeled MNC were plated in 96 well plates (2 x 10^5 monocytes / well) and incubated with bacteria at a ratio of 50 bacteria to one monocyte for 60 min (37°C, 5% CO_2). Control samples were incubated without bacteria. In order to assess bacterial adherence to monocytes, NaN_3 (0.01%) was added to parallel set ups. Other set ups contained EPS (1 µg/ml and 5 µg/ml). After incubation, cells were washed 2 x with PBS and suspended in 100 µl ToPro-3 (Invitrogen, Germany) to stain dead cells. Cells and phagocytosis/bacterial adherence were assessed by flow cytometry.

3.2.5.4. Statistical analyses

All data obtained are shown as means ± SEM. The statistical significance of differing mean values were assessed with unpaired Student's *t*-test, as provided with the Excel-software package. Significant differences were considered at * $p < 0.05$, ** $p < 0.01$, *** $p < 0.001$.

4. Results

4.1. Induction of immune functions by heat-inactivated *S. uberis* strains

First stimulation experiments were carried out on heat-inactivated *S. uberis* 0140J, 233 and T1-18. The inactivation of bacteria was performed as described in 3.2.1.4 and visualized (Fig. 7) in the optical microscopy (magnification x 100).

Fig. 7. Optical micrograph (100 x magnified) of heat-inactivated *S. uberis* 0140J. The cells are not disrupted by heat treating.

Such prepared bacteria were used for the stimulation experiments of HEK293, RAW 264.7 and pbMEC cells. In an experiment using HEK293 cells transfected with bovine TLR2 receptor it was shown that neither *S. uberis* strain 233 nor O140J can effectively activate NF-κB, while other mastitis causative bacteria do so (Fig. 8). Observed activation of NF-κB in HEK293 cells by *S. uberis* O140J was only 0.1 fold (*e.g*. 10%) higher than the control (culture medium). In comparison the other strains induced NF-κB up to 5-14 fold. The very slight activation of HEK293 after challenging with O140J strain can be explained through irritation of cells by bacteria, what was supported by the fact that the induction was not dose-dependent. In contrast, activation of NF-κB by other mastitis strains was clearly dose-dependent.

In order to examine if NF-κB could be induced in pbMEC and macrophages, another stimulation experiment utilizing heat-inactivated cells was performed. The activation of

NF-κB in pbMEC cells was very slight but significant (*t*-test, unpaired, *<0.05), while macrophages were activated by *S. uberis* cells on the same or higher level than by *E. coli* (Fig. 9).

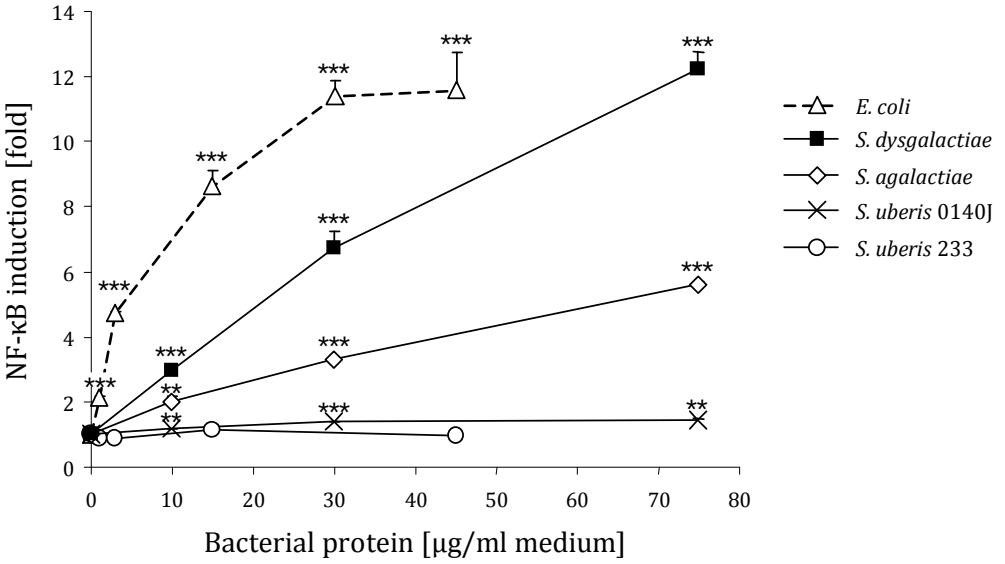

Fig. 8. NF-κB induction by different mastitis causative bacteria in HEK cells transfected with TLR2 receptor. The stars above the errors bars refer to the significance, when compared to the control – culture medium (*t*-test, unpaired, * $p < 0.05$, ** $p < 0.01$, *** $p < 0.001$).

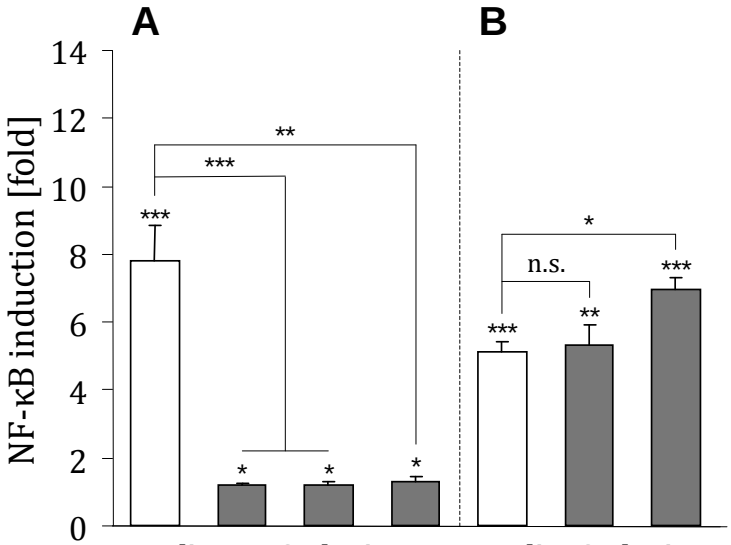

	E. coli	*S. uberis*			*E. coli*	*S. uberis*	
	1303	**0140J**	**233**	**T1-18**	**1303**	**0140J**	**233**
mean	**7.8**	**1.2**	**1.2**	**1.3**	**5.1**	**5.3**	**6.9**
SEM	1.02	0.05	0.08	0.17	0.34	0.58	0.33

Fig. 9. The NF-κB induction in (A) pbMEC cells and (B) RAW 264.7 cells (macrophages) by *S. uberis* 0140J, 233 and T1.18. *E. coli* heat-inactivated cells were used as a positive control. The stars above the errors bars, refer to the significance, when compared to the control – culture medium; the stars above the line indicating two columns refer to the significance calculated for these two biological replica (*t*-test, unpaired, * $p < 0.05$, ** $p < 0.01$, *** $p < 0.001$).

Also mRNA expression of the genes encoding for the main immune factors was measured in challenged pbMEC and RAW 264.7 cells.

In pbMEC, the expression of the genes encoding for the major pro-inflammatory cytokines (TNF-α, IL-1A, IL-6 and IL-8), after stimulating with heat-inactivated *S. uberis* cells, was only slightly higher than in the untreated control (as an example IL-6 shown in a Fig. 10). The similar activation pattern was observed for *LAP*, *iNOS* and *SAA3*.

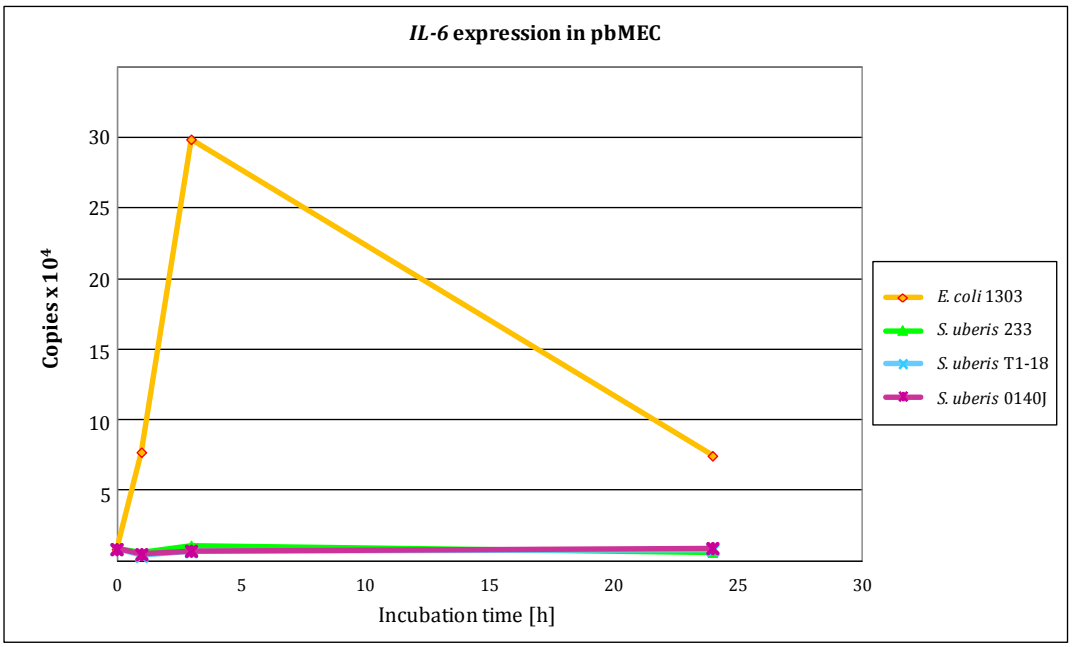

Fig. 10. mRNA expression of the gene encoding for IL-6 – one of the major pro-inflammatory cytokine – in pbMEC after challenging with different strains of *S. uberis*. *E. coli* was used as a positive control for the experiment.

Heat-inactivated *S. uberis* could not induce the expression neither of the investigated pro-inflammatory cytokines nor of antimicrobial factors in pbMEC. It was however noticed, that the gene involved in detoxification of xenobiotics substances (*CYP1A1*) was highly induced. After only 1 h postinduction the expression of this gene was 130 times higher, and a maximum induction was observed after 3 h and amounted 550 fold in *S. uberis* 233 and 450 fold in case of the 2 other strains. After 24 h from challenging, the expression of that gene returned to the basic level (Fig. 11).

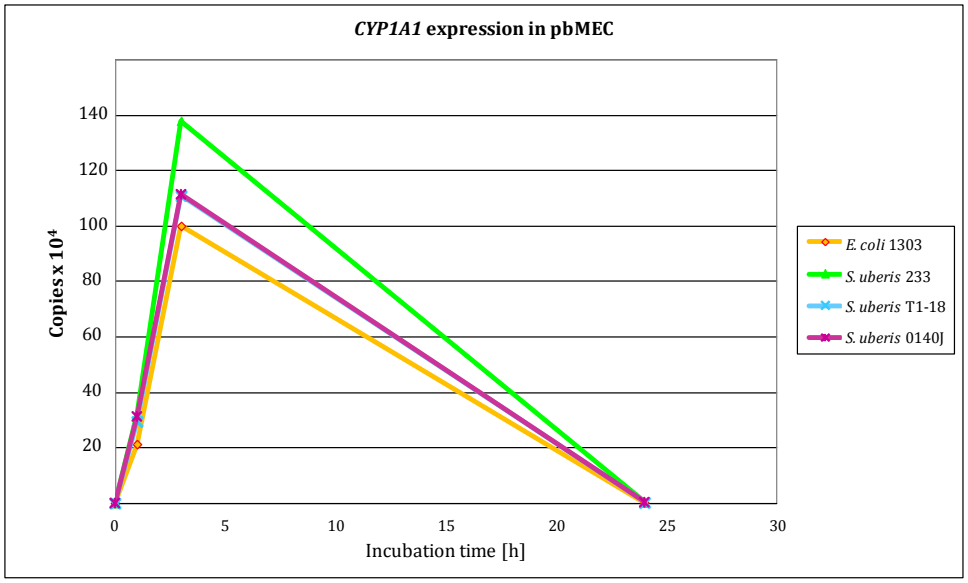

Fig. 11. mRNA expression of the gene *CYP1A1* – involved in detoxification of xenobiotic substances – in pbMEC after challenging with *S. uberis* strains. *E. coli* was used as a positive control for the experiment.

In murine macrophages (RAW 264.7), the expression of major cytokines (TNF-α, IL1A, IL6 and CXCL2) after challenging with *S. uberis* was on a much higher level than before stimulation. While the stimulation with *S. uberis* cells was not as effective as with *E. coli*, it was strong and always highly significant for all genes. As examples, expressions of *TNF-α* and *IL6* are shown on Fig. 12 and Fig. 13. The alteration of mRNA levels of cytokine-encoding genes after stimulation with *E. coli* and different strains of *S. uberis* is presented in Table 10.

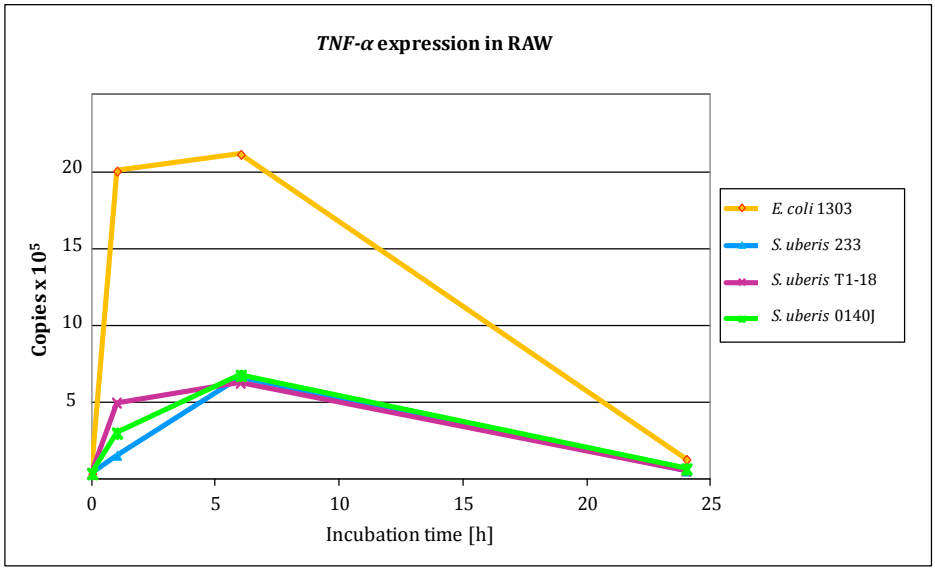

Fig. 12. mRNA expression of the gene encoding for TNF-α in RAW 264.7 cells after challenging with *S. uberis* strains. *E. coli* was used as a positive control for the experiment.

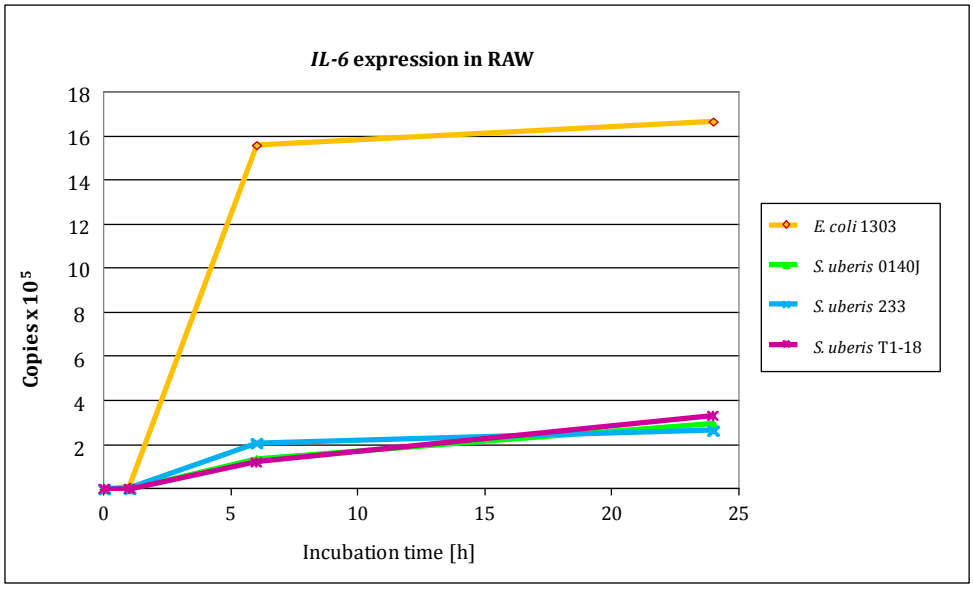

Fig. 13. mRNA expression of the gene encoding for IL6 in RAW 264.7 after challenging with *S. uberis* cells. *E. coli* was used as a positive control for the experiment.

Table 10. The alteration of mRNA levels of cytokine-encoding genes in RAW 264.7 cells, 1, 6 and 24 h after stimulation with *E. coli* or *S. uberis.*

Fold change												
Cytokine	***E. coli***			***S. uberis* 0140J**			***S. uberis* 233**			***S. uberis* T1-18**		
	1 h	**6 h**	**24 h**	**1 h**	**6 h**	**24 h**	**1 h**	**6 h**	**24 h**	**1 h**	**6 h**	**24 h**
IL-1A	5.6	333.1	565.3	1.1	70.4	34.9	1.2	82.5	37.7	1.1	55.1	38.1
IL-6	21.5	2888.1	3085.5	0.7	253.4	549.2	2.0	386.9	490.8	1.3	223.4	614.6
CXCL2	65.8	110.9	71.7	5.1	159.5	43.9	18.6	222.1	41.1	10.7	183.3	52.9
TNF-α	50.6	53.4	3.3	4.0	16.8	1.4	12.5	15.8	1.4	7.6	17.1	1.8

4.2. Glycolipids

4.2.1. Isolation and purification of glycolipids

Glycolipids were obtained from disrupted *S. uberis* 233, 0140J and T1-18 cells as described in 3.2.2.1. All three extracts were monitored on TLC plates stained with Hanessian's stain (universal) and α-naphthol stain (specific for sugars). Extracts were run together with the standard of glycolipids (Glc+Gro+2FA, GlcN+Gro+2FA, Qui6S+Gro+2FA). Further purification and analyses were performed on the extract of 233, since one band more (NG) was observed after staining with an α-naphthol compare to the two other extracts (where three glycolipids G1, G2 and G3 were present) (Fig. 14).

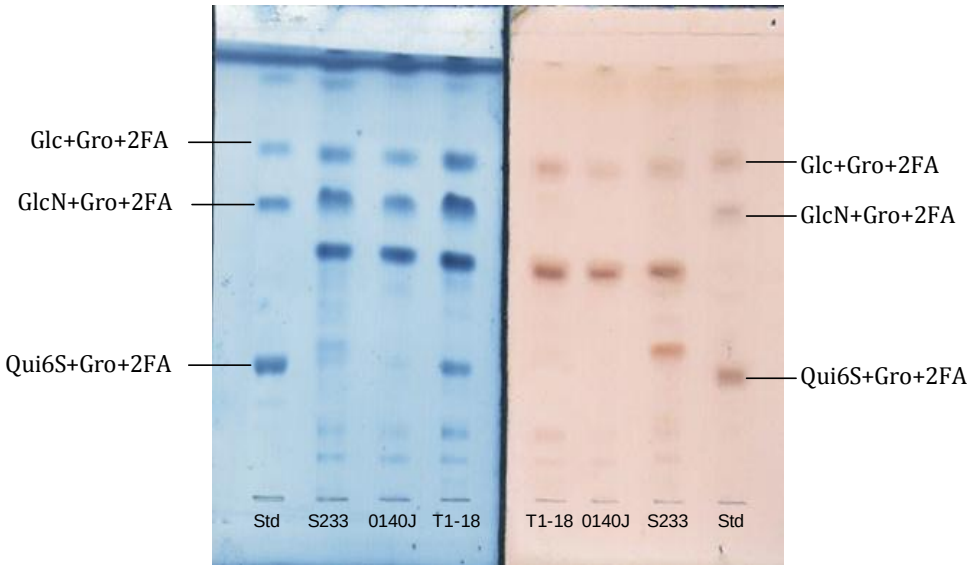

Fig. 14. TLC of total lipid extracts of *S. uberis* 233, 0140J and T1-18 and a standard (Glc+Gro+2FA, GlcN+Gro+2FA, Qui6S+Gro+2FA). Samples were developed using a mixture of $CHCl_3$/MeOH/H_2O (65/25/4, v/v/v) and visualised with Hanessian's stain (blue – left side) and α-naphtol stain (pink – right side).

Glycolipids were eluted successively from crude lipid extract (35 mg) with chloroform/methanol in the ratios of 9.7:0.3, 9.5:0.5, 9:1, 8.5:1.5 and 1:1 as described in 3.2.2.1.4. G1 was eluted with $CHCl_3$/MeOH in ratio 9.5:0.5, G2 with $CHCl_3$/MeOH 9:1, G3 with $CHCl_3$/MeOH 1:1 and NG was in both 9.5:0.5 and 8.5:1.5 fractions. Then, the eluants were purified by preparative TLC as described in 3.2.2.1.5. The isolated glycolipids were

pure, as was visualised by TLC (Fig. 15) and yielded: 2.0 mg (G1), 3.5 mg (G2), 1.2 mg (G3) and 300 μg (NG).

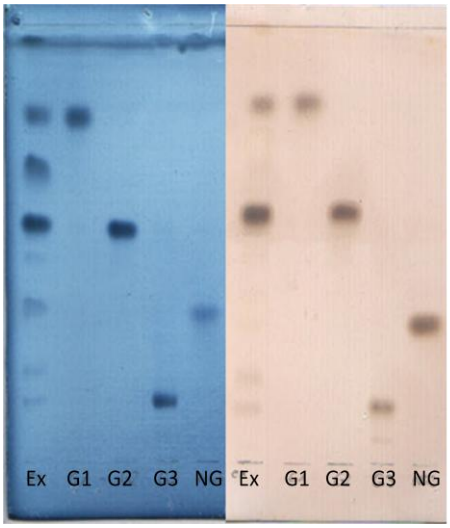

Fig. 15. TLC of total lipid extract (Ex), purified glycolipids (G1, G2, G3) and additional substance (NG) isolated from *S. uberis* 233. Samples were developed using a mixture of $CHCl_3$/MeOH/H_2O (65/25/4, v/v/v) and visualised with Hanessian's stain (blue – left side) and α-naphtol stain (pink – right side).

4.2.2. Compositional analysis

Methanolysis of G1, G2 and G3 showed the presence of hexose and fatty acids, while in NG pentose and adenine was observed. Further analyses of sugar components as alditol acetate revealed the presence of the glucose in G1, G2 and G3 and ribose in NG. The fatty acids were identified by GLC as 14:0, 16:1, 16:0, 18:1 and 18:0 in the approx. molecular ratio of 1.0:7.6:16.9:29.3:7.0 in G1; 1.0:7.2:16.9:19.2: 8.2 in G2 and 1:6.3:11.1:9.7:4.8 in G3.

4.2.3. NMR analyses of glycolipids

The ^{1}H NMR spectrum of NG showed high similarity to that of adenosine published in the literature (Ciuffreda et al., 2007). The absence of fatty acids excluded the possibility that the isolated molecule was a glycolipid (NG not glycolipid) and was not further investigated.

The ^{1}H NMR spectrum of isolated G1 showed one anomeric proton at δ 4.83. In case of G2 and G3 two anomeric signals (δ 4.96 and δ 5.00, δ 4.93 and δ 4.99 respectively) of the same intensity could be observed. In all glycolipids the signals corresponding to the fatty acids were identified in the region 2.36 – 0.89 (Fig. 16).

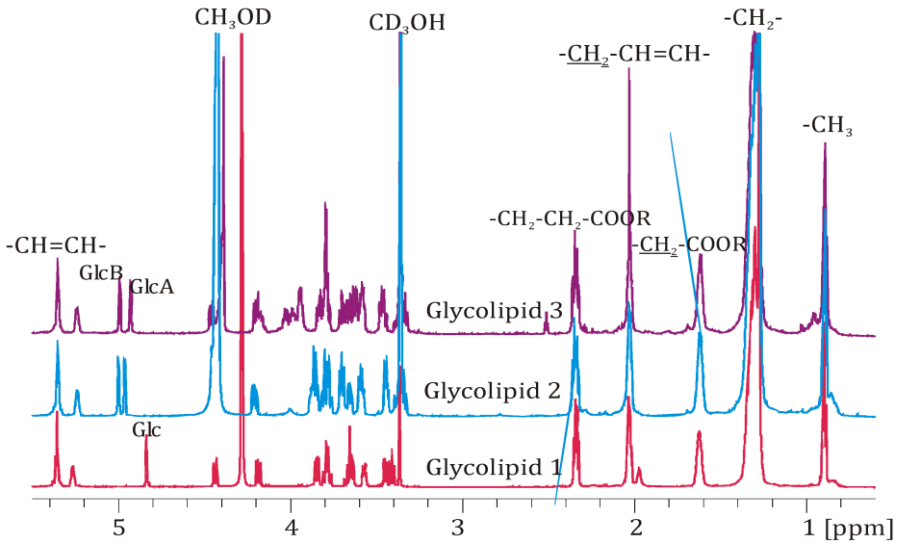

Fig. 16. ^{1}H NMR spectrum (700 MHz) of glycolipids isolated from *S.uberis* 233 recorded in $CHCl_3$/MeOH 2:1 at 27°C relative to internal TMS (δ_H 0.00; δ_C 0.00).

The analyses of the 2D homonuclear ^{1}H, ^{1}H COSY and TOCSY, and heteronuclear ^{1}H, ^{13}C HSQC-dept spectra allowed the assignment of proton and carbon chemical shifts of the hexoses and Gro of G1 (Fig. 17, Table 11), G2 (Fig. 18, Table 12) and G3 (Fig. 19, Table 13). Additionally, the ^{31}P NMR spectrum identified a phosphodiester group (δ +2.78) in G3.

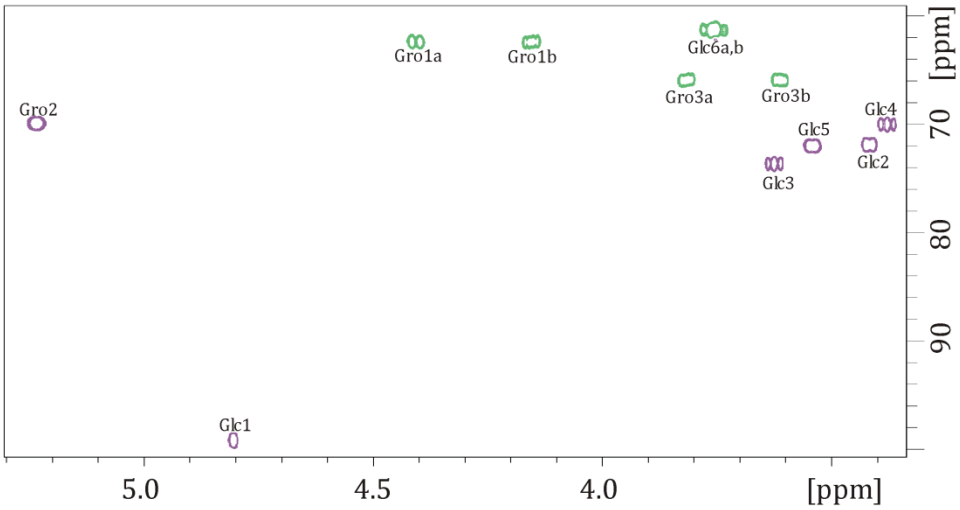

Fig. 17. Part of the ^{1}H,^{13}C HSQC-DEPT spectrum (700 MHz) of G1 isolated from *S. uberis* 233, recorded in $CDCl_3/CD_3OD$, 2:1 (v/v) at 27°C relative to internal TMS (δ_H 0.00; δ_C 0.00).

Table 11. ^{1}H and ^{13}C NMR data of G1 isolated from *S. uberis* 233. Spectra were recorded in $CDCl_3/CD_3OD$, 2:1 (v/v) at 27°C relative to internal TMS (δ_H 0.00; δ_C 0.00).

		1a	1b	2	3a	3b	4	5	6a	6b
Glc	^{1}H	4.83		3.43	3.64		3.40	3.56	3.78	3.78
	^{13}C	99.5		70.4	74.0		70.2	72.6	61.6	
Gro	^{1}H	4.43	4.18	5.25	3.85	3.63				
	^{13}C	62.7		70.2	66.2					

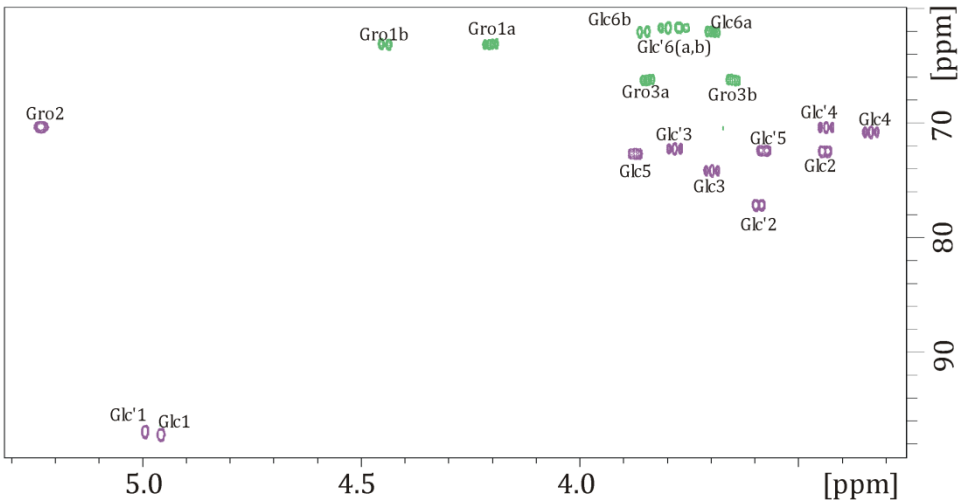

Fig. 18. Part of $^{1}H,^{13}C$ HSQC-DEPT spectrum (700 MHz) of G2 isolated from *S. uberis* 233 recorded in $CDCl_3/CD_3OD$, 2:1 (v/v) at 27°C relative to internal TMS (δ_H 0.00; δ_C 0.00).

Table 12. ^{1}H and ^{13}C NMR data of G2 isolated from *S. uberis* 233. Spectra were recorded in $CDCl_3/CD_3OD$, 2:1 (v/v) at 27°C relative to internal TMS (δ_H 0.00; δ_C 0.00).

		1a	1b	2	3a	3b	4	5	6a	6b
Glc	^{1}H	4.96		3.44	3.70		3.33	3.87	3.69	3.85
	^{13}C	97.2		70.4	74.2		70.7	72.6	62.0	
Glc'	^{1}H	5.00		3.59	3.77		3.44	3.58	3.78	3.78
	^{13}C	97.0		77.1	72.2		72.5	72.4	61.7	
Gro	^{1}H	4.45	4.20	5.23	3.83	3.64				
	^{13}C	63.2		70.4	66.2					

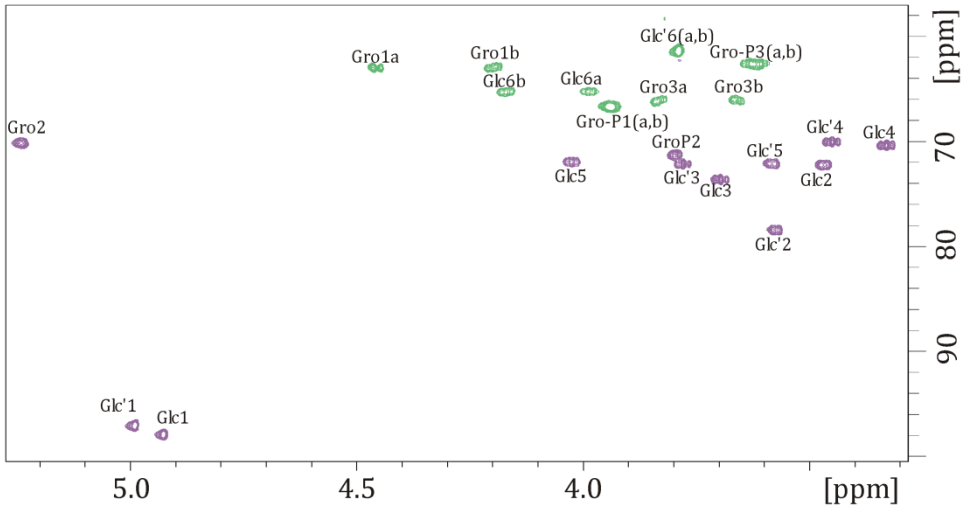

Fig. 19. Part of $^{1}H,^{13}C$ HSQC-DEPT spectrum (700 MHz) of G3 isolated from *S. uberis* 233 recorded in $CDCl_3/CD_3OD$, 2:1 (v/v) at 27°C relative to internal TMS (δ_H 0.00; δ_C 0.00).

Table 13. ^{1}H and ^{13}C NMR data of G3 isolated from *S. uberis* 233. Spectra were recorded in $CDCl_3/CD_3OD$, 2:1 (v/v) at 27°C relative to internal TMS (δ_H 0.00; δ_C 0.00).

		1a	1b	2	3a	3b	4	5	6a	6b
Glc	^{1}H	4.93		3.47	3.69		3.32	4.02	3.99	4.17
	^{13}C	97.9		72.3	73.6		70.4	71.9	65.2	
Glc'	^{1}H	4.99		3.57	3.78		3.45	3.58	3.78	3.78
	^{13}C	97.0		78.5	72.2		70.0	72.1	61.4	
Gro-P	^{1}H	3.94	3.94	3.79	3.62	3.62				
	^{13}C	66.9		71.4	62.8					
Gro	^{1}H	4.45	4.18	5.24	3.82	3.64				
	^{13}C	63.0		70.2	66.0					

In ROESY experiments, *intra*-residual nOe contacts of the Glc residues between H-1 and H-2 were found, which characterized Glc as α-pyranoses. The α-configuration of Glc residues was also confirmed by $J_{1,2}$ value taken from the ^{1}H NMR spectrum (G1 -$J_{1,2}$ 3.88 Hz; G2 –Glc $J_{1,2}$ 3.84 Hz, Glc' $J_{1,2}$ 3.50 Hz; G3 – Glc $J_{1,2}$ 3.61 Hz, Glc' $J_{1,2}$ 3.43 Hz). The *gluco* configuration, was confirmed by an *intra*-residual H-2/H-4 nOe connectivity. In the ROESY spectrum of G1 nOe contacts between H-1 Glc/H-3a,b Gro suggested the linkage between Glc 1 and Gro

3, which was proved by the HMBC spectrum, in which a cross peak H-3a,b Gro/C-1 Glc was observed. In summary the NMR data of G1 indicated the structure: α-D-Glc*p*(1→3)-Gro-1,2-diacyl.

The ROESY spectrum of G2 identified the nOe contacts H-1 Glc/H-2 Glc' and H-1 Glc'/H-3a,b Gro, and HMBC spectrum showed the contacts H-2 Glc'/C-1 Glc and H-1 Glc'/C-3 Gro thus, the structure was α-D-Glc*p*-(1→2)-α-D-Glc*p*(1→3)-Gro-1,2-diacyl.

Also for G3 2D NMR spectroscopy was applied in order to analyze the linkage between the components. The *inter*-residual nOe connectivity between H-1 of Glc and H-2 of Glc' as well as that between H-1 of Glc' and H-3a,b of Gro were observed in the ROESY spectrum. The linkages of Glc1 to Glc'2 and Glc'1 to Gro3 were confirmed by a HMBC experiment, in which the cross-peaks H-1 Glc/C-2 Glc' and H-1 Glc'/C-3Gro were found. Furthermore, a $^{1}H,^{31}P$ HMQC spectrum was analyzed, and correlations of the phosphodiester group at δ +2.78 and protons H-6a,b of Glc and H-1a,b of Gro-P were observed. In summary the structure of glycolipid 3 was: Gro-3-phosphoryl-6-O-α-D-Glc*p*-(1→2)-α-D-Glc*p*(1→3)-Gro-1,2-diacyl.

4.2.4. Mass spectrometry of glycolipids

ESI FT-ICR MS in the negative ion mode of glycolipids worked only in case of G3. The spectrum revealed the presence of the most prominent molecular mass at 1072.62 u corresponding to the molecule composed of 2 hexoses, 2 Gro, phosphate, 1 16:0, and 1 18:1 or 1 16:1 and 1 18:0 (calculated mass 1072.6311 u). The mass spectrum additionally possessed groups of molecules representing heterogeneity in the fatty acids substitution pattern, i.e. 16:1 + 16:0, 18:1 + 18:1, 18:0 + 18:1 and 14:0 + 16:1. For the other 2 glycolipids MALDI FT ICR-MS in the positive ion mode was used. The obtained spectra showed main peaks at 778.1 u for G1 and 939.7 u for G2 that corresponded to 1 hexose for G1 and 2 hexoses for G2, 1 Gro, 1 16:0 and 1 18:1 or 1 16:1 and 1 18:0, and 1 Na^{+} (calculated mass 778.6 u and 940.6 respectively). Additionally, like in case of G3, diverse fatty acids (16:1 + 16:0, 18:1 + 18:1, 18:0 + 18:1 and 14:0 + 16:1) contributed in heterogenous make up. Taken together the data obtained from chemical analyses, NMR and MS spectroscopy revealed the structure of glycolipids as shown in a Fig. 20.

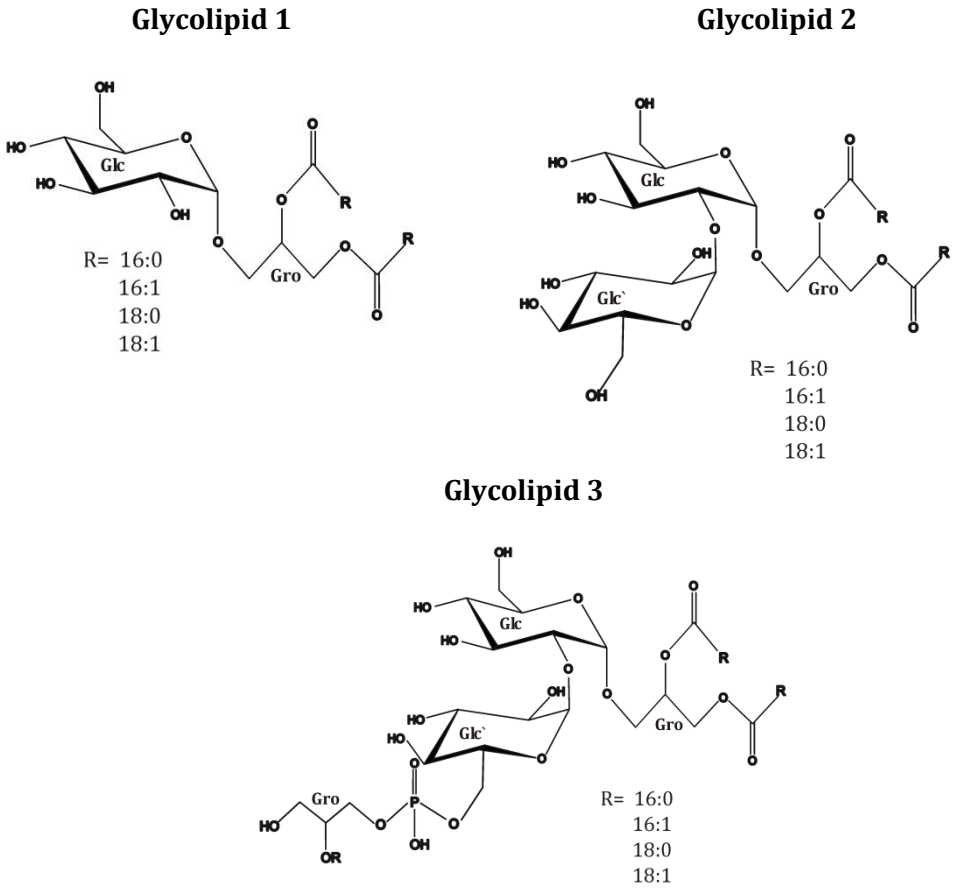

Fig. 20. The structures of G1-G3 isolated from S. uberis 222, 0140J and T1-18.

4.2.5. Inactivation of *sub0538* encoding for the glycosyltransferase required for the synthesis of G2 and G3 from G1.

The gene *sub0538* – identified with the basic local alignment tool (BLASTP) - shares high similarity with *iagA* from *S. agalactiae* and *bgsA* from *E. faecalis*, genes encoding for diglucosyldiacylglycerol synthetase. Since this enzyme plays an important role in adhesion to epithelial cells and biofilm formation in above mentioned bacteria, an attempt of isolating a mutant with inactivated *sub0538* was made.

The mutant bank consisting of about 9000 transformants was screened using a PCR method with primers p614 and p801 as described in 3.2.4.3.2. The desired product size was ~ 1500 bp. Screening (Fig. 21) revealed 5 potential candidate plates (32, 47, 48, 53 and 83). Rows and columns from selected plates were combined and PCR reaction with primers p614 and p801 was performed (3.2.4.3.3). This experiment gave 6 potential candidates (47F5, 49B4, 49F5, 53G2, 53H8 and 83A7; Fig. 22).

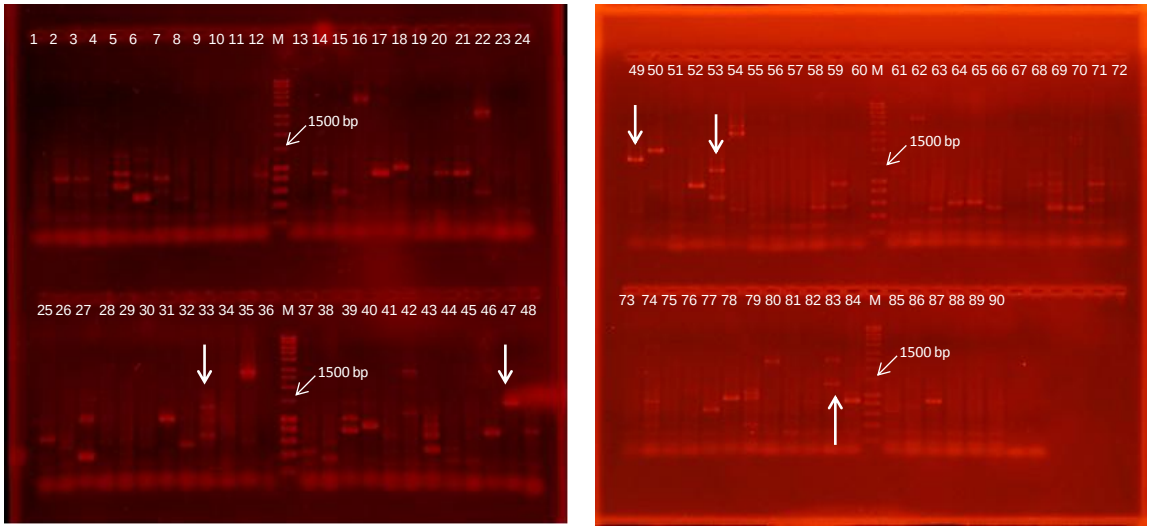

Fig. 21. Electrophoretic separation (1% agarose gel) of PCR reaction products (p614 and p801). The template used in the reaction was DNA isolated from combined mutants growing on the same 96-well plate. Numbers 1-90 – numbers the plates, M – marker, arrows indicate the PCR products of the desired size.

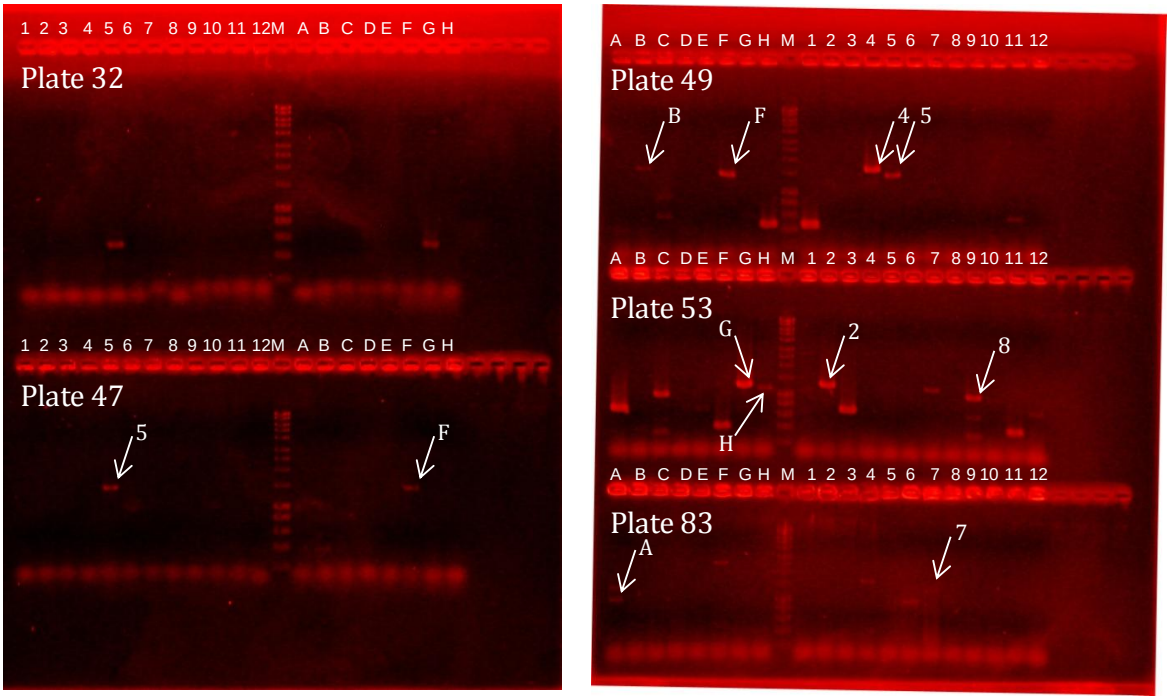

Fig. 22. Electrophoretic separation (1% agarose gel) of PCR reaction products (p614 and p801). The template used in the reaction was DNA isolated from combined rows and columns of the analyzed plate. Letters A-H – combined rows; numbers 1-12 –combined columns, M – marker, arrows indicate the PCR products of the desired size.

The DNAs from selected candidates were isolated and screened together with wild type *S. uberis* with three pairs of primers: p614 vs p801(A), p613 vs p800 (B) and p800 vs p801

(C). The expected product lengths for a positive mutant were ~ 1500 bp for pair A, ~ 200-300 bp for B and since the fragment for pair C would be too long to amplify no product was expected. For the wild type *S. uberis,* on the other hand only ~ 1500 bp for pair C was supposed to be found (Fig. 23). The experiment revealed only one positive transformant – 49B4; the other 5 candidates were considered 'false positive'.

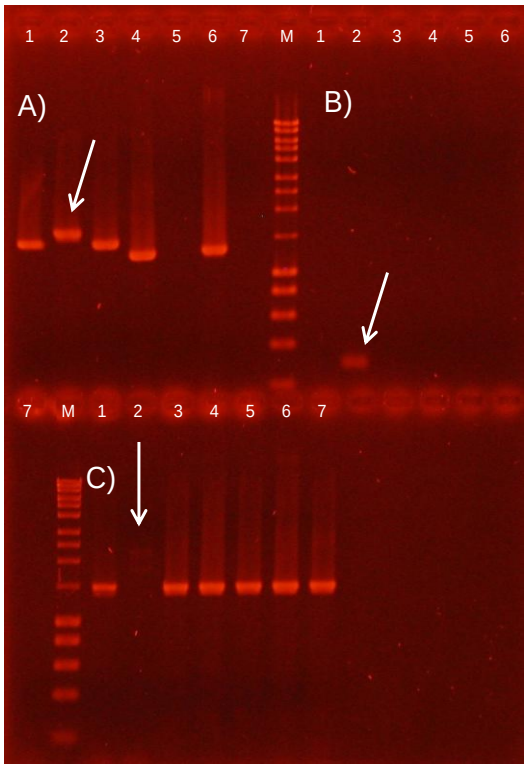

candidate	Nr
47F5	1
49B4	2
49F5	3
53G2	4
53H8	5
83A7	6
WT	7

Primers:
A) P614 vs p801 – expected product ≤1500 bp
B) P613 vs p800 – expected product ~ 200-300 bp
C) P800 vs p801 – in wild type ~1500; in mutant no product (too big fragment to amplify)

Fig. 23. Electrophoretic separation (1% agarose gel) of PCR reaction products. Pairs of primers: p614 vs p801 (A), p613 vs p800 (B) and p800 vs p801 (C). The templates used in the reaction were DNAs isolated from selected candidates. Numbers 1-7 – assign candidates specified in the table, M – marker, arrows indicate the PCR products of the desired sizes.

Mutant 49B4 was cured from a plasmid pG+ host (3.2.4.3.5) and the mutation was stabilized. In order to check where exactly the insertion occurred, the DNA of the mutant was isolated and sequencing was performed (3.2.4.3.6). The control PCR reaction of the DNA isolated from the cured mutant as well as wild type (WT) *S. uberis* was carried out with primers p800 and p801 (both complementary to the genomic DNA). The expected products sizes were ~ 1500 bp for WT and ~ 2000 bp for the mutant. The result of the experiment was as expected (Fig. 24).

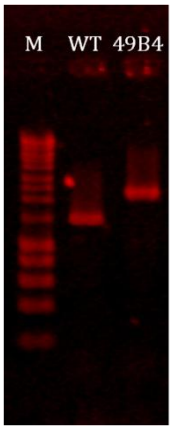

Fig. 24. Electrophoretic separation (1% agarose gel) of PCR reaction product (p800 vs p800). The templates used in the reaction were DNAs isolated from wild type (WT) *S. uberis* 0140J and cured mutant 49B4, M – marker.

The analyses of the DNA sequence of the mutant 49B4 showed that the insert was built 34 bp upstream the start codon of the gene of interest (Fig. 25). The attempt of isolating mutants with another pairs of primers p613 and p801 was performed. However, this did not succeed either.

NNNNNNNNNNNNNTTAATAGTTCNTTGATATATCCTCGCTGTCATTTTTATTCATTTTACACTAAAATA
GACTTATCAGAAAACTTTGCAACAGAACCGAAAATTCCTTGGAAATAAGCTATAATAGATTCTATGAAAG
TCTTACTATACTTAGAAGCTGAAAATTTCTTACGAAAATCTGGGATAGGTCGTGCCATTAAACATCAAGT
AAAAGCCTTGACGTCTGTTGGACAAGCCTTTACGACAAATCCTAAAGATGACTATGACCTTGTTCATGTT
AACACTTATGGCATTGCTAGCTGGTTGTTAATGACAAAAGCTAAAAAAGCTGGCAAAAAAGTGATCATGC
ATGGTCATTCTACAGAAGAGGATTTTAGAAATTCCTTTATTCTTTCTAATCAATTATCCCCTATGTTTAA
AAAATACCTTTGTCTTTTTTACAAGAAAGCAGATGCCATCATCACGCCAACTCTCTATTCAAAATCTCTGA
TTGAAAACTATGGGATAAACAAGCCAGTTTTTGCCATTTCAAATGGGATTGATCTGAAACAATATGGTCC
AAATCCTCAAAAAGAGGAAGCTTTCCGACGTTATTTTAATGTAAAAGATGGCGAAAAAGTTGTCATGGGT
GCAGGGCTTTTCTTCAAACGAAAAGGCATTGATGATTTTGTAAAAGTTGCTGAAAAAATGCCAGATGTCA
CATTTATTTGGTTTGGAGAAATGAATAAATGGATGATTCCAGCTGAAATAAGAAAGATTGTTAATGGCAA
TCATCCTGAAAATGTTATTTTTCCAGGATACATTAAAGGTGACGTTTATGAAGGCGCAATGACAGGGGCT
GATGCTTTCTTTTTCCCAAGTCGTGAAGAAACAGAAGGCATTGTAGTACTGGAAGCCTTAGCAAGTAAAC
AGCATGTCCTTGTCAGAGATATCCCTGTTTATTCTGGTTGGGTAAATCAAGATAGCGCGGANATGGCTTC
AGATATAGATGGATTTGTTAAGGCATTACGGAAAATCTTAAATGGTCAAAGTCAGAAAACCATGGNAGGT
TATCAGGTTGCAGAAAGCAGAAGTATTGAAAAAANTAGCTTTGGANTTAGTAGACNCTTATCAAAAAGT
AATGGNNTNNNNNATGCGAGTTGGTCTATTTACAGANNCTTACTTTNCNNAAGTTTCNGNNGNNGCAA
CCNGTATTCNANNTTGAAAGAAGANCTAGNAAAAAGAANNCATNANNCTANNTCTTTACCACNANNNN
NAAAACNTNNNNNCNNNNANNATCNNNNNNNNNNGANTNNNNNNCCNNNNNNNNCTTTACNGATC
NNNNNNNNNNNNNNNNNTNNTNNNNTNNNAANNGCNNANCNNNTNNNATNNNNNNANNNNNN
NANNNNNNCNNNNAN

Start of the *sub0538* gene
P082 primer sequence

Fig. 25. Sequencing data of IS*S1* antisense strand reading out through terminal repeat into positive strand of *S. uberis* 0140J at *sub0538* locus for mutant 49B4.

4.2.6. PCR screening of the DNA of various *S. uberis* strains for the presence of the *sub0538*

The DNA of various *S. uberis* strains was isolated and a PCR reaction using primers p800 and p801 was performed in order to check if *sub0538* was present in all mastitis strains, and if the length of this gene was the same. The result of the experiment showed that all mastitis causing strains as well as avirulent EF20 strain possess the gene and the length of it remained unchanged Fig. 26.

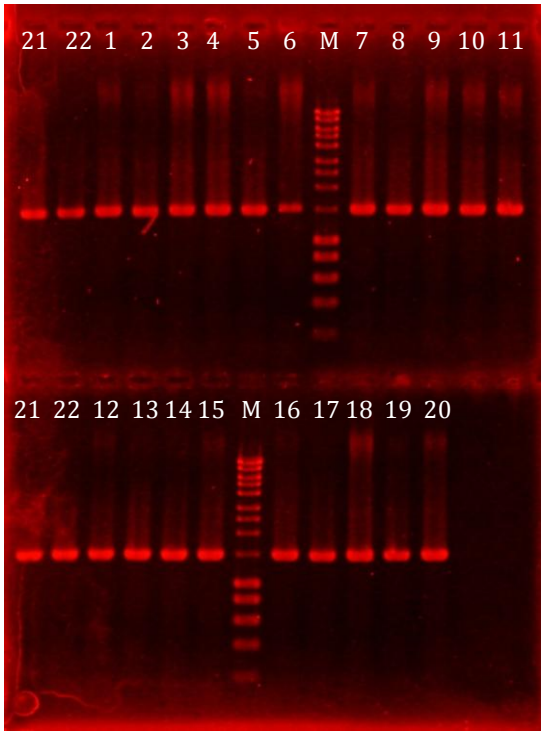

nr	strain	disease
1	C6344	Mastitis (clinical)
2	C5072	Mastitis (clinical)
3	S6261	Mastitis (clinical)
4	C9359	Mastitis (clinical)
5	Ab71	Mastitis (clinical)
6	4428	Mastitis (clinical)
7	5291	Mastitis (clinical)
8	5130	Mastitis (clinical)
9	6780	Mastitis (clinical)
10	Ab1947	Mastitis (clinical)
11	C8329	Mastitis (subclinical)
12	C5388	Mastitis (subclinical)
13	B190	Mastitis (subclinical)
14	6736	Mastitis (subclinical)
15	C7131	Mastitis (subclinical)
16	S7010	Mastitis (subclinical)
17	B362	Mastitis (subclinical)
18	6707	Mastitis (subclinical)
19	4244	Mastitis (subclinical)
20	3448	Mastitis (subclinical)
21	0140J	Virulent strain
22	EF20	Avirulent strain

Fig. 26. Electrophoretic separation (1% agarose gel) of PCR product (p800 vs p801). The templates used in the reaction were DNAs isolated from various *S. uberis* strains. Numbers 1-22 – assign *S. uberis* strains specified in the table together with the caused disease, M – marker.

4.2.7. Mutant 0140J::IS*S1* P'(*sub0538* & *sub0539*)

Detailed analyses of the noncoding sequence upstream the *sub0538* gene as well as the sequencing result of mutant 49B4 revealed that the insert was in the promoter region, namely in the -35 element (Fig. 27).

AACAGAATCAGCCTAAGGGCTGATTTTTTTGCCTATTAinsertGTGAAAATTCCTTGGAAATAAGCTATAA
TAGATTCTATG

-35 element insert -10 element start of the *sub0538*

Fig. 27. Noncoding sequence upstream the *sub0538* gene; the important parts of the promoter, locus of the insert and start codon are marked with different colors.

The element -35 occurs in strong promoters which promote the gene expression on a high level. Mutations in the -35 region result in lower expression of genes regulated by them (Cooper, 2000). Additionally, it was shown that the promoter is not only regulating the expression of *sub0538*, but also of *sub0539* (Fig. 28). The mutant 49B4 was therefore renamed into 0140J::IS*S1* P'(*sub0538* & *sub0539*).

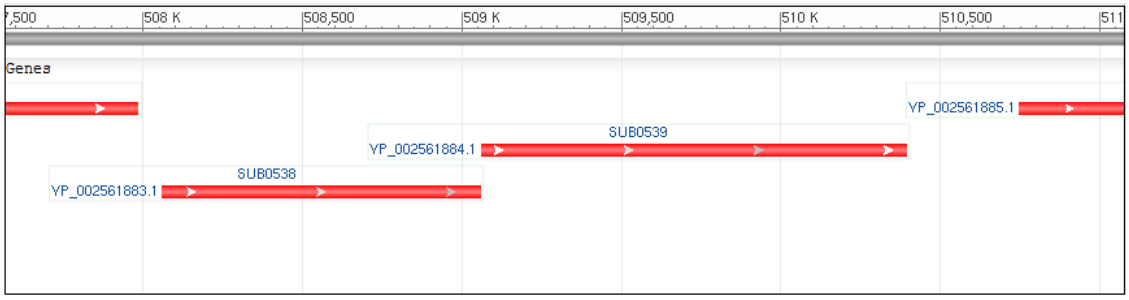

Fig. 28. Genomic region of *sub0538* showing that this gene is located in a cluster, together with *sub0539*. The picture is a snip shot taken from ncbi database: http://www.ncbi.nlm.nih.gov/gene/?term=SUB0538.

In the ncbi database it was found that *sub0539* is a gene encoding for another glycosyltransferase. The description of that gene states:

'GT1_UGDG_like. This family is most closely related to the GT1 family of glycosyltransferases. UDP-glucose-diacylglycerol glucosyltransferase (UGDG; also known as 1,2-diacylglycerol 3-glucosyltransferase) catalyzes the transfer of glucose from UDP-glucose to 1,2-diacylglycerol forming 3-D-glucosyl-1,2-diacylglycerol' (http://www.ncbi.nlm.nih.gov/Structure/cdd/cddsrv.cgi?uid=99987).

The colony morphology did not differ from the wild type. We noticed, however, that the mutant grew only to OD_{600} 0.5, which was lower compared to that of strain O140J (OD_{600} of the stationary phase 0.8).

4.2.8. The expression of *sub0538* in mutant 0140J::IS*S1*P' (sub0538 & sub0539)

The expression of the gene *sub0538* was determined in *S. uberis* O140J and its mutant O140J::ISS1P'(*sub0538* & *sub0539*), and was normalized to the expression of the house keeping gene *sub0888*. The expression of *sub0538* was 5.77 fold lower in the mutant than in the wild type. The eventual contamination of RNA samples with DNA was excluded.

4.2.9. Synthesis of glycolipids by the mutant O140J::IS*S1*P' (*sub0538* & *sub0539*)

Glycolipids were extracted from the mutant. The extract was analyzed by TLC (Hanessian's as well as α-naphthol stain). The intensities of the bands corresponding to G1, G2 and G3 were lower when compared to the wild type (0140J), or another *S. uberis* 233 and T1-18 (Fig. 29).

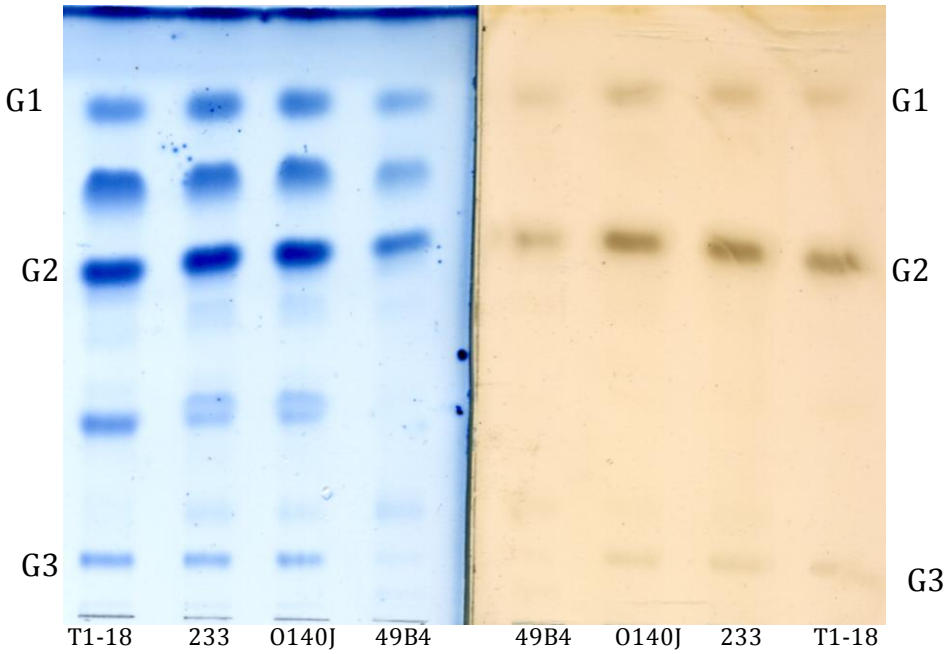

Fig. 29. TLC of total lipid extracts of *S. uberis* T1-18, 233, 0140J and a mutant 49B4 [O140J::ISS1P'(*sub0538* & *sub0539*)]. Samples were developed using a mixture of $CHCl_3$/MeOH/H_2O (65/25/4, v/v/v) and visualised with Hanessian's stain (blue – left side) and α-naphtol stain (pink – right side).

4.2.10. Biofilm formation by different *S. uberis* strains and the mutant 0140J::IS*S1*P'(*sub0538* & *sub0539*)

Since it was reported that glycolipids play an important role in biofilm formation (Theilacker et al., 2009), the biofilm assay was carried out for various *S. uberis* strains. The mutation in the promoter of the *sub0538* and *sub0539* (49B4) significantly reduced the ability to form the biofilm when compared to the wild type (0140J). Strains T1-18 and 233 were strong by produced biofilm, while the avirulent strain EF20 seemed to produce biofilm on a similar level as O140J (Fig. 30).

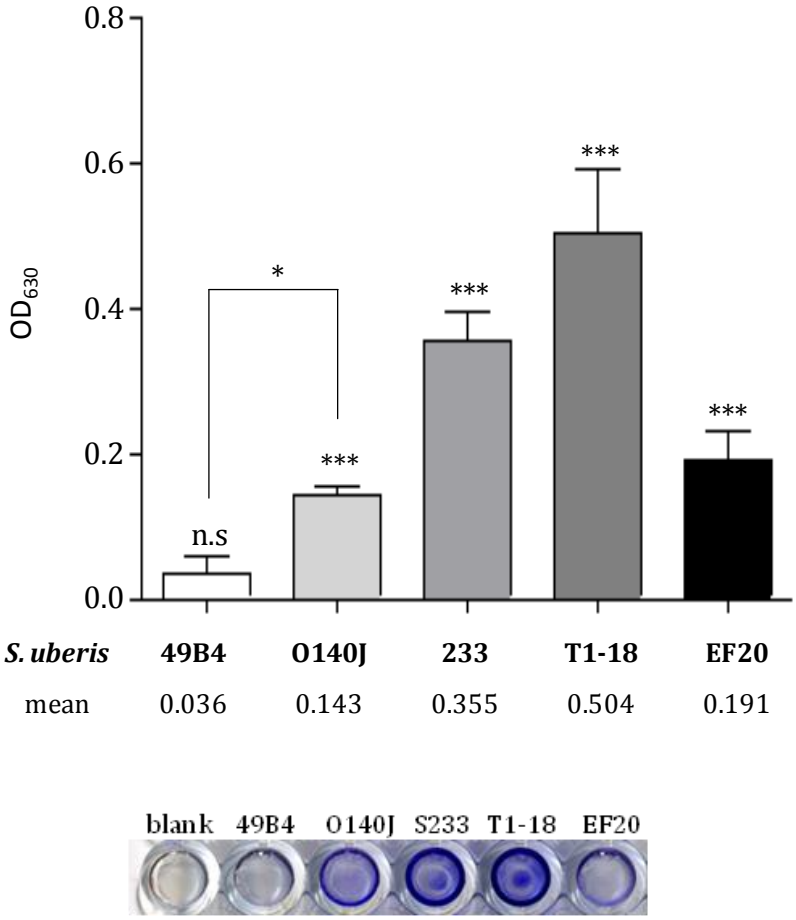

Fig. 30. Biofilm assay. *S. uberis* 0140J, 233, T1-18, EF20 strains and mutant with an insert in promoter region of *sub0538* and *sub0539* (49B4) were investigated in regard to biofilm production on plastic surfaces. The amount of biofilm is expressed as OD_{630}. The mutant strain forms significantly less biofilm compared with the wild type strain. The stars above the errors bars refer to the significance, when compared to the control (blank, BHI culture medium). The star above the line indicating two columns refers to the significance calculated for these two biological replica (*t*-test, unpaired, * $p < 0.05$, ** $p < 0.01$, *** $p < 0.001$). The picture below the graph is a photograph taken from the representative wells.

4.2.11. Biological activity of glycolipids

The activity of the isolated glycolipids was examined in pbMEC. Despite the fact that NF-κB was not induced in challenged cells, the expression of the genes encoding for cytokines, chemokines, and antimicrobial factors was investigated after stimulation with G1. The expression of genes involved in primary response (*IL-1, IL-6, IL-8, TNF-α, iNOS*) was not increased after challenging with G1 similar as the expression of those genes involved in secondary response (*LAP, SAA3* and *CCL5*). Only the expression of the gene encoding CYP1A1 was strongly increased after the stimulation with G1. CYP1A1 is involved in detoxification of xenobiotic substances (Fig. 31). This gene was also the only one found to be upregulated in pbMEC after challenging with heat-inactivated *S. uberis* cells.

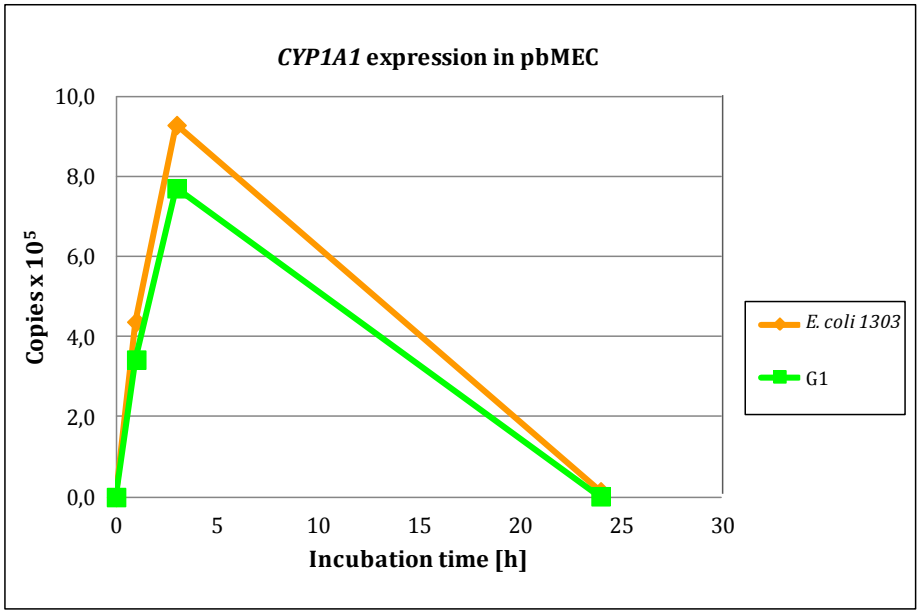

Fig. 31. mRNA expression of *CYP1A1* – involved in detoxification of xenobiotic substances – in pbMEC after challenging with G1. *E. coli* was used as a positive control for the experiment.

4.3. LTA

4.3.1. Isolation of LTA

The LTAs were extracted from ~ 26 g of wet mass of disrupted bacterial cells of *S. uberis* 233, 0140J and T1-18 as described in 3.2.2.2. The yield of obtained LTA was on average 2.5 mg (0.01%).

4.3.2. Chemical analysis of the LTA

Compositional analysis of LTAs of *S. uberis* identified Glc and Rha (in an approx. molecular ratio of 12:1), phosphate, alanine (Ala), glycerol (Gro) and 16:1, 16:0, 18:1, and 18:0, in the approx. molecular ratio 1:3:2:1.3. Further analyses by NMR spectroscopy showed no signals of Rha, therefore this hexose was considered as a contamination. The absolute configurations of Ala and Glc were determined as D. Methylation analysis of the isolated lipid anchor (3.2.3.1.6) revealed the presence of one terminal and one 2-substituted glucose by identifying 1,5-di-*O*-acetyl-2,3,4-tri-*O*-methyl-[1-^{2}H]glucitol and 1,2,5-tri-*O*-acetyl-3,4-di-*O*-methyl-[1-^{2}H]glucitol.

4.3.3. NMR spectroscopy

1D NMR experiments showed no differences between the LTAs isolated from different *S. uberis* strans (Fig. 32). The data and further experiments discussed below refer to the LTA isolated from *S. uberis* 233. On 1D ^{1}H NMR spectrum the characteristic signal for Gro substituted by Ala at *O*-2 (H-2, δ 5.38), Ala (H-2, δ 4.29; H-3, δ 1.63), H-3 of free Ala (δ 1.53), other signals of Gro (δ 4.11 – 3.62), and of fatty acids (δ 2.33 – 0.86) were observed. Additionally, two anomeric signals at low intensity, belonging to two Glc residues (at δ 5.15 and δ 5.06) were present.

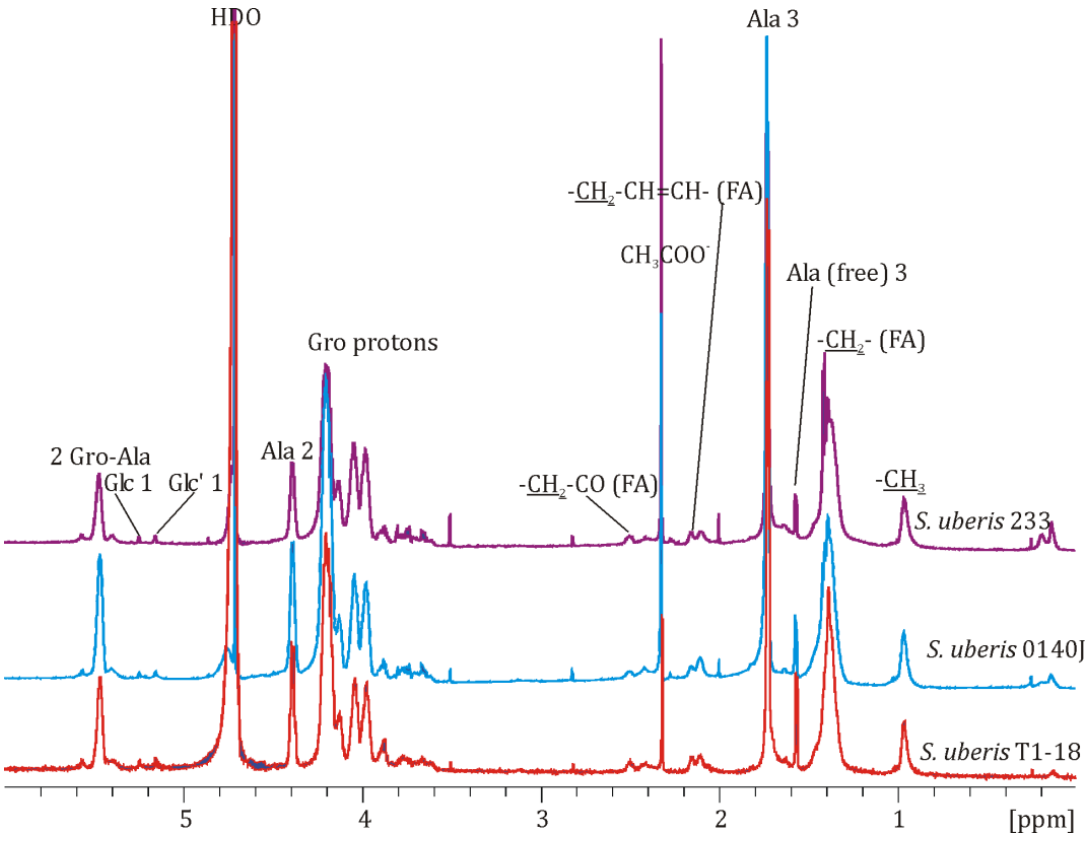

Fig. 32. ^{1}H NMR spectra of native LTAs (700 MHz) recorded in D_2O at 42°C for *S. uberis* 233, 0140J and T1-18.

Detailed analyses of COSY, TOCSY, ROESY, HSQC and HMBC spectra assigned all chemical shifts (Table 14, Fig. 33). Furthermore, a ^{31}P NMR spectrum identified a phosphodiester group (δ +0.42). The HMBC spectrum confirmed the substitution of Gro by Ala at *O*-2 due to the cross peak Gro-Ala H-2/Ala C-1.

Table 14. ^{1}H and ^{13}C NMR data of the native LTA isolated from *S. uberis* 233. Spectra were recorded in D_2O at 42°C relative to external acetone (δ_H 2.225; δ_C 31.45).

Residue		1a	1b	2	3(a)	3b
P-**Gro**-P	^{1}H	3.90	3.97	4.04	3.90	3.97
	^{13}C	67.3		70.3	67.3	
P-**Gro**(-P)-Ala	^{1}H	4.11	4.11	5.38	4.11	4.11
	^{13}C	64.6		75.1	64.6	
Ala-(P-)Gro-P	^{1}H	-	-	4.29	1.63	
	^{13}C	170.8		49.9	16.2	
Ala free	^{1}H	-	-	3.98	1.53	
	^{13}C	174.9		50.5	16.64	

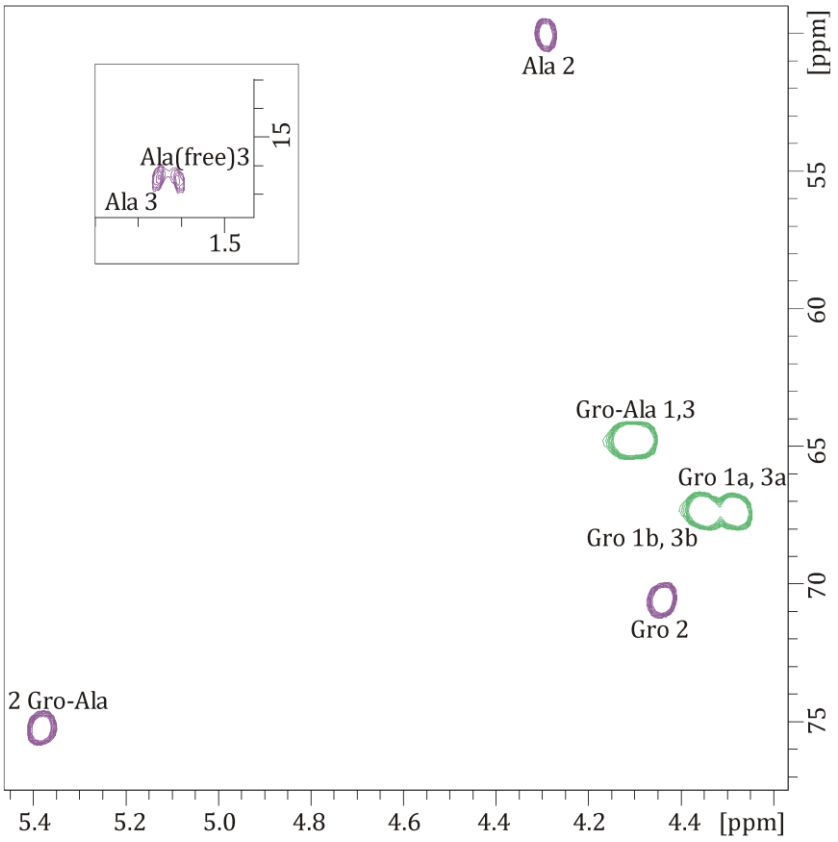

Fig. 33. Part of the $^{1}H,^{13}C$ HSQC-DEPT spectrum (700 MHz) of LTA isolated from *S. uberis* 233 recorded in D_2O at 42°C relative to external acetone (δ_H 2.225; δ_C 31.45).

In order to isolate and determine the structure of the lipid anchor, depolymerization utilizing 48% aq. HF (on 6 mg of LTA) was performed. The product recovered from chloroform phase after water/chloroform extraction was treated with abs. hydrazine (as described in 3.2.3.3.1, 3.2.3.3.2) and the lipid anchor (300 µg, 6%) could be isolated and investigated by 1D and 2D NMR spectroscopy. The ^{1}H NMR spectrum confirmed the presence of both Glc residues [signals at δ_H 5.16 (Glc 1) and δ_H 5.09 (Glc' 1)]. COSY, TOCSY and HSQC experiments were applied for the assignment of the proton and carbon chemical shifts of the two hexoses and of one Gro (Table 15, Fig. 34), representing the linker backbone. The *intra*-residual nOe contacts between H-1 and H-2 of the Glc residues observed in ROESY spectrum and chemical shifts of the anomeric protons (5.16 and 5.09) proved both sugars to be α-pyranoses. The *gluco* configuration was confirmed by an *intra*-residual H-2/H-4 nOe connectivity. NOe contacts observed in the ROESY spectrum between Glc' H-1/Glc H-2 and Glc H-1/Gro H-3 identified the structure α-D-Glc*p*-(1→2)-α-D-Glc*p*-(1→3)-Gro.

Table 15. ^{1}H and ^{13}C NMR data of the deacylated lipid anchor isolated from LTA of *S. uberis* 233. Spectra were recorded in D_2O at 42°C relative to external acetone (δ_H 2.225; δ_C 31.45).

Residue		1(a)	1b	2	3(a)	3b	4	5	6a	6b
α-D-Glc*p*	^{1}H	5.16		3.67	3.84		3.45	3.69	3.77	3.87
	^{13}C	96.66		76.13	72.15		70.29	72.50	61.81	
α-D-Glc*p*'	^{1}H	5.09		3.56	3.77		3.44	3.91	3.77	3.85
	^{13}C	96.75		72.05	73.50		70.23	72.66	61. 31	
Gro	^{1}H	3.82	3.52	3.95	3.67	3.60				
	^{13}C	69.65		71.41	63.21					

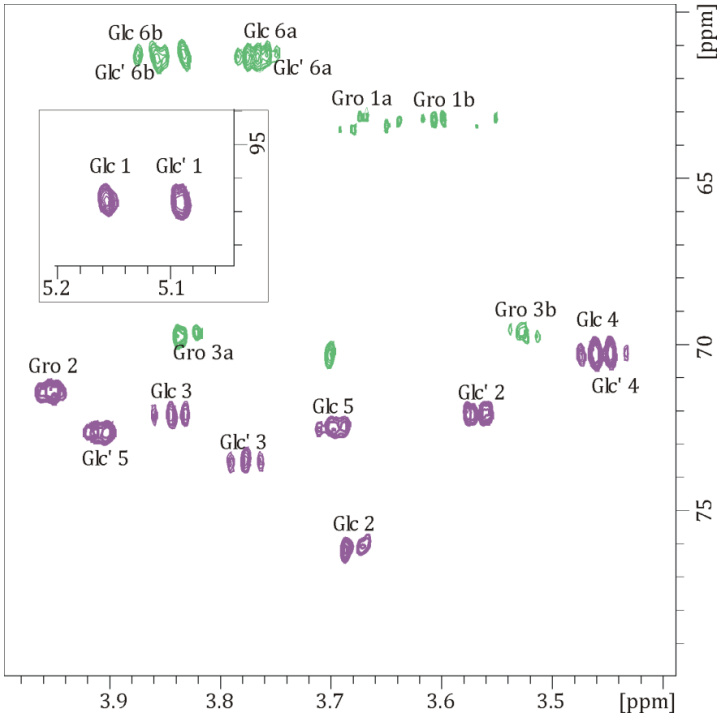

Fig. 34. Part of ^{1}H,^{13}C HSQC-DEPT spectrum (700 MHz) of the *O*-deacylated lipid anchor isolated from the LTA of *S. uberis* 233. The spectrum was recorded in D_2O at 42°C relative to external acetone (δ_H 2.225; δ_C 31.45).

Furthermore, the analysis of the aqueous phase obtained after HF treatment of the native LTA was performed. ^{1}H, COSY, TOCSY and HSQC experiments confirmed D-Ala as the only substituent of Gro at *O*-2 (H-1a,3a δ 3.76; H-1b,3b, δ 3.81; H-2, δ 5.12, Table 16, Fig. 35). Also prominent signals belonging to a Gro'-Ala residue originating from migration of Ala to *O*-1 of Gro due to the cleavage of the phosphodiester bonds were observed (H-1a, δ 4.28; H-1b, δ 4.36; H-2, δ 4.01; H-3a, δ 3.62; H-3b, δ 3.66). Additionally, signals corresponding to unsubstituted Gro, bound and free Ala were assigned (Table 16).

Table 16. ^{1}H and ^{13}C NMR data of the aqueous phase components obtained after HF treatment of LTA isolated from *S. uberis* 233. Spectra were recorded in D_2O at 42°C relative to external acetone (δ_H 2.225; δ_C 31.45).

Residue		1(a)	1b	2	3(a)	3b
Gro	^{1}H	3.55	3.63	3.77	3.55	3.63
	^{13}C	63.42		72.92	63.42	
Gro-Ala (Ala in pos. 2)	^{1}H	3.76	3.81	5.12	3.76	3.81
	^{13}C	60.83		78.43	60.83	
Gro'-Ala (Ala in pos. 1)	^{1}H	4.28	4.36	4.01	3.62	3.66
	^{13}C	67.84		70.06	62.90	
Ala-Gro	^{1}H	-	-	4.26	1.59	
	^{13}C	171.44		49.50	15.96	
Ala (free)	^{1}H	-	-	3.96	1.52	
	^{13}C	174.9		50.50	16.52	

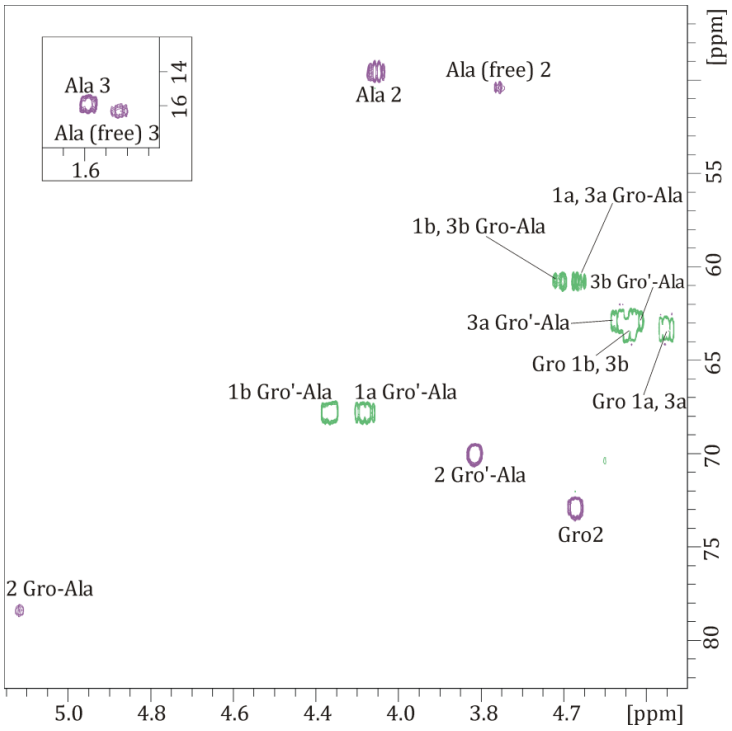

Fig. 35. Part of the ^{1}H,^{13}C HSQC-DEPT spectrum (700 MHz) of the aqueous phase obtained after HF treatment of LTA isolated from *S. uberis* 233. Spectrum was recorded in D_2O at 42°C relative to external acetone (δ_H 2.225; δ_C 31.45).

In order to prove the linkage of the poly(phospho-Gro) chain to Glc‘ of the lipid anchor, the LTA (6 mg) was *O*-deacylated with abs. hydrazine (3.2.3.3.2) and dialyzed (yield 1 mg, 17%). The ^{1}H NMR spectrum of the product lacked signals corresponding to fatty acids, Gro-Ala, and Ala when compared to native LTA (Fig. 36). Signals of H-1 of Glc and Glc’ were more pronounced, and the correlation Gro C-1/Glc’ H-6 was observed on the HMBC spectrum (not shown), identifying the linkage of the hydrophilic backbone of LTA to *O*-6 of Glc’.

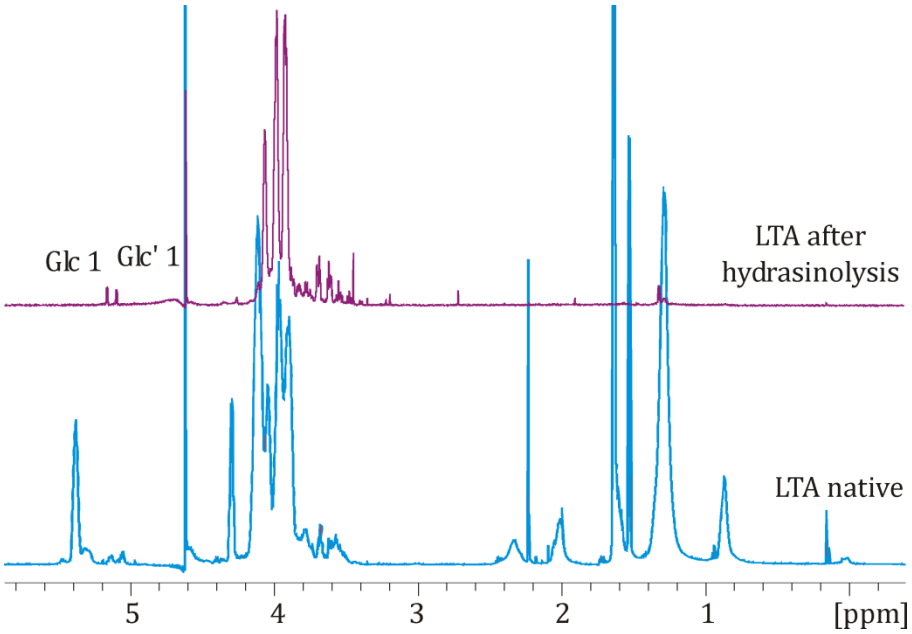

Fig. 36. ^{1}H NMR spectra of *O*-deacetylated LTA and native LTA (700 MHz) recorded for *S. uberis* 233 in D_2O at 42°C relative to external acetone (δ_H 2.225; δ_C 31.45).

The degree of LTA substitution by Ala was quantified as 44% calculating from the ^{1}H NMR spectrum of native LTA the integral ratio of total Gro signals (δ 4.11 – 3.62 and δ 5.35) and the signal at δ 1.64, corresponding to the CH_3 group of bound Ala. The integral ratio of the anomeric proton of Glc (δ 5.16) in the ^{1}H NMR spectrum of deacylated LTA and the region of Gro signals (δ 4.05 – 3.87) identified an average chain length of 25 phospho-Gro units.

4.3.4. Mass spectrometry of the LTA

ESI FT-ICR MS in the negative ion mode of LTA revealed the presence of the most prominent molecular mass at 918.6 u that corresponded to the lipid anchor composed of 2 hexoses, 1 Gro, 1 16:1, and 1 18:0 (calculated mass 918.6280 u). The mass spectrum additionally identified groups of molecules due to heterogeneity in the fatty acid

substitution pattern i.e. 16:1 + 16:0, 16:1 + 18:1, 16:1 + 18:0, 18:1 + 18:1, 18:0 + 18:1, as well as in the length of the poly(phospho-Gro) chain /Δm = 154 u).

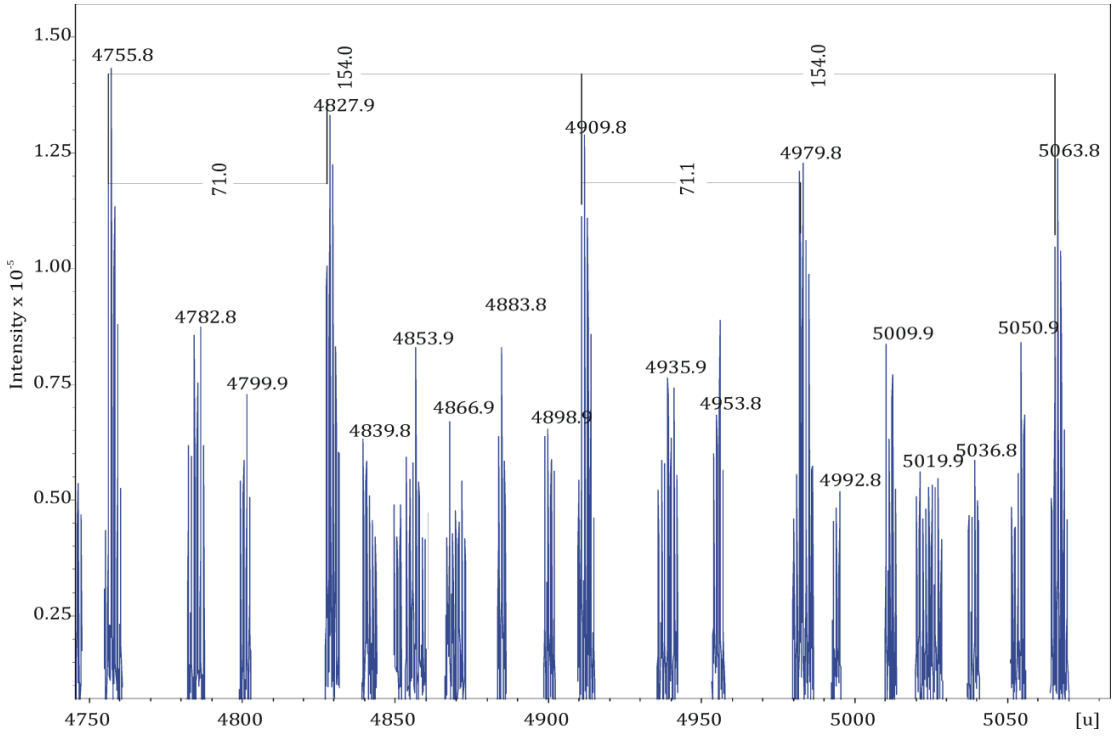

Fig. 37. Excerpt of the ESI-MS spectrum of the native LTA isolated from *S. uberis* 233. The mass 4755.8 u corresponded to 1 18:0, 1 18:1, 2 Hex, 1 Gro, 22 P-Gro; 154.0 – mass of phospho-Gro unit, 71.0 – mass of alanine.

Taken together, the obtained data elucidated the structure of the LTA strains as depicted in Fig. 38.

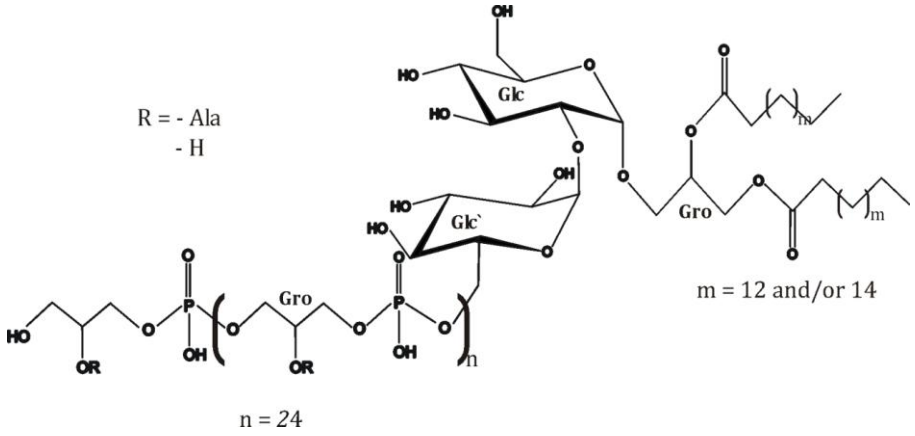

Fig. 38. The structure of LTA isolated from *S. uberis* 233.

4.3.5. Biological activity of the LTA

In order to examine whether the isolated LTA was biologically active, HEK293 cells transfected with TLR2 and pbMEC were stimulated, and the induction of NF-κB was measured. The activation of TLR2 was very slight but significant (*t*-test, unpaired, p * < 0.05, p ** < 0.01, p *** < 0.001), while NF-κB in pbMEC was well activated.

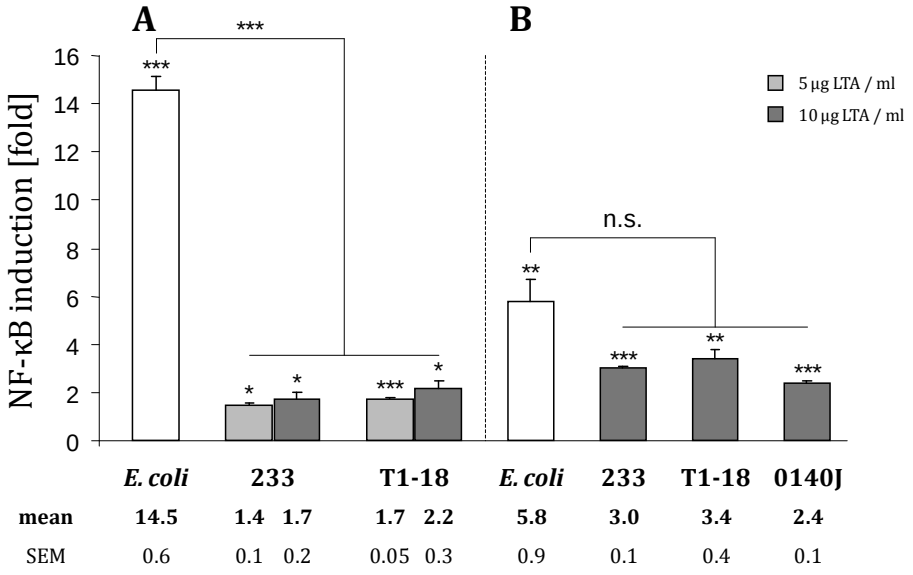

Fig. 39. NF-κB induction in (A) HEK293 cells transfected with boTLR2 and (B) pbMEC by LTA isolated from various *S. uberis* strains. *E. coli* heat-inactivated cells were used as a positive control. The stars above the errors bars refer to the significance, when compared to the control; the stars above the line indicating two columns refer to the significance of differences calculated between these samples assayed in duplicate (*t*-test, unpaired, * p < 0.05, ** p < 0.01, *** p < 0.001).

Despite the fact that TLR2 activity was very low, inactivation of the lipoproteins which could eventually contaminate the samples was performed (3.2.5.1.3). After the treatment, the NF-κB induction decreased and it was not significant anymore in HEK293 cells, whereas in pbMEC this activation was still significant (Fig. 40). In order to investigate whether the expression of pro-inflammatory and antimicrobial genes in pbMEC changed after the challenge, cells were challenged with LTA. The LTAs used for this experiment originated from *S. uberis* 233 and T1-18 and were applied in the concentrations of 1 µg/ml and 10 µg/ml. All genes encoding for the master cytokines (*IL-1A, IL-6, CXCL2* and *TNF-α*) and *iNOS2* achieved a maximum level of mRNA concentrations after 3 h from stimulation. After 24 h the transcription of these genes returned to the baseline level (as an example, *IL-6* expression is shown in Fig. 41). An alteration of expression of genes involved in

secondary response (*SAA3, LAP, CCL5*) was also observed after LTA challenge. The highest concentration of the mRNA from those genes was identified after 24 h poststimulation (as an example, *LAP* expression is shown in Fig. 42). The change of mRNA concentrations of all analyzed genes after LTAs stimulation is presented in Table 17.

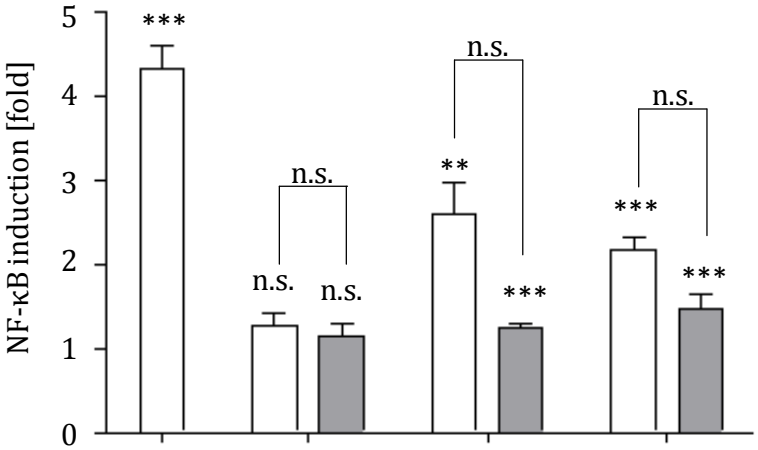

		native	H_2O_2	native	H_2O_2	native	H_2O_2
mean	**4.3**	**1.3**	**1.1**	**2.5**	**1.2**	**2.2**	**1.5**
SEM	0.21	0.17	0.15	0.97	0.03	0.13	0.19

Fig. 40. NF-κB induction in pbMEC by LTAs 'native' and peroxide-treated, from *S. uberis* O140J, 233 and T1-18. *E. coli* heat-inactivated cells were used as a positive control. The stars above the errors bars refer to the significance, when compared to the control (culture medium); the stars above the line indicating two columns refer to the significance calculated for these two biological replica (*t*-test, unpaired, * $p < 0.05$, ** $p < 0.01$, *** $p < 0.001$ n.s. – not significant).

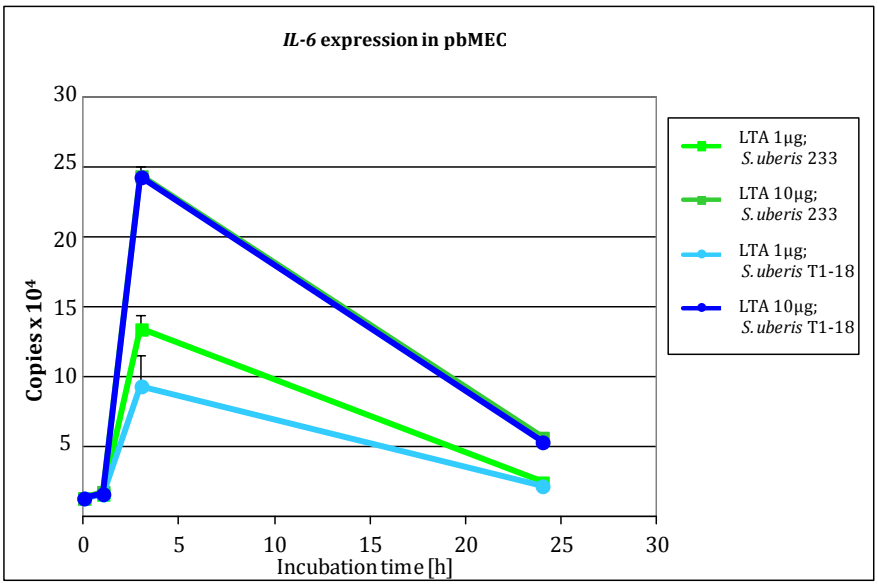

Fig. 41. mRNA expression of the gene *IL-6* in pbMEC after challenging with LTA from *S. uberis* 233 and T1-18.

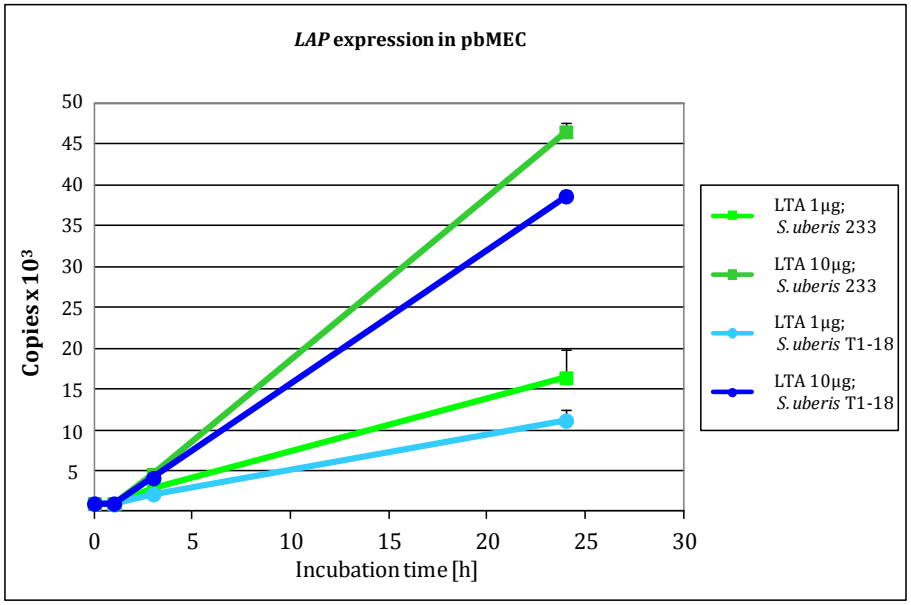

Fig. 42. mRNA expression of the gene *LAP* in pbMEC after challenging with LTA from *S. uberis* 233 and T1-18.

Table 17. The alteration of mRNA levels of investigated genes 1, 3 and 24 h after stimulation with LTA from *S. uberis* 233 and T1-18.

Fold change												
Cytokine	**LTA 1 µg *S. uberis* 233**			**LTA 10 µg *S. uberis* 233**			**LTA 1 µg *S. uberis* T1-18**			**LTA 10 µg *S. uberis* T1-18**		
	1 h	**3 h**	**24 h**	**1 h**	**3 h**	**24 h**	**1 h**	**3 h**	**24 h**	**1 h**	**3 h**	**24 h**
IL-1A	1.2	6.2	0.8	1.4	13.7	1.8	1.1	3.7	0.9	1.3	14.4	2.0
IL-6	1.2	10.1	1.7	1.4	17.5	4.0	1.3	6.5	1.5	1.3	17.5	3.8
CXCL2	3.0	37.8	2.9	3.3	65.3	9.6	2.3	22.9	2.3	3.4	69.8	8.7
TNF-α	4.7	67.9	2.9	5.8	103.7	13.2	3.9	40.6	2.5	6.3	108.1	12.6
iNOS	1.0	54.5	1.9	1.1	112.3	6.9	1.0	28.8	1.5	1.0	105.2	5.7
LAP	1.0	2.9	15.4	1.0	4.4	44.3	0.5	2.0	10.2	1.0	3.9	36.8
SAA3	1.1	33.7	28.3	1.1	47.0	116.4	1.2	20.9	40.7	1.2	47.5	111.5
CCL5	1.0	6.6	5.5	1.1	13.8	25.9	1.0	3.4	4.5	1.1	12.6	31.1
CYP1A1	1.0	1.7	0.9	2.1	23.2	1.4	1.1	1.3	1.2	1.8	18.7	1.7

4.4. WTA and rhamnan

4.4.1. Isolation of the polysaccharides

The polysaccharides were isolated from ~ 13 g of wet mass of disrupted bacterial cells of *S. uberis* 233. In order to release the polysaccharides from the cell wall, samples were treated with lysozyme and purified by dialysis, followed by HIC. This step was applied in order to remove eventual remains of LTA. Since the obtained product was heterogenic (data not shown), separation utilizing anion-exchange chromatography was performed. Obtained fractions were combined according to the phosphate content (3 pools), and yielded: 1 mg (0.008%) – pool 1, 3.4 mg (0.026%) – pool 2 and 3.3 mg (0.025%) –pool 3.

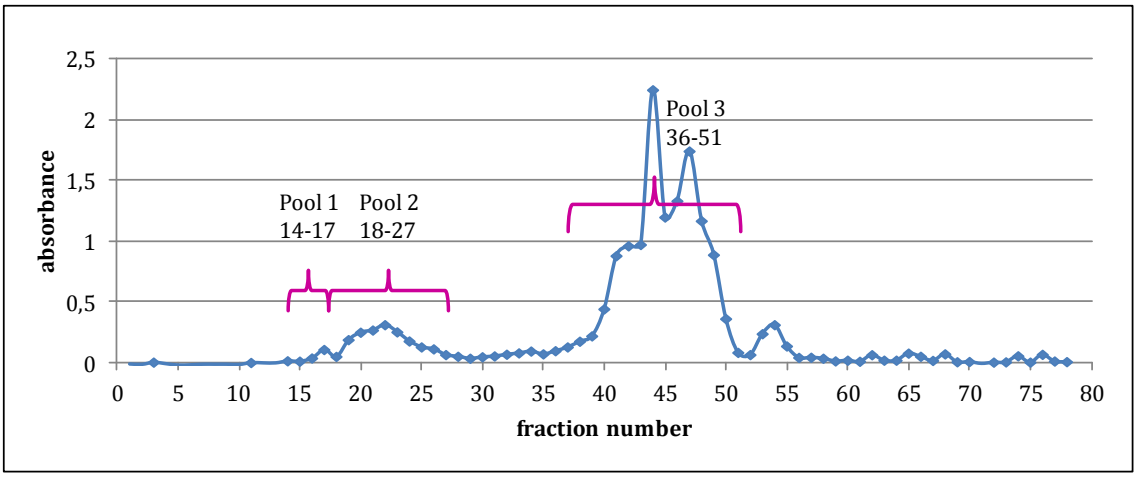

Fig. 43. Phosphate content determination of the samples obtained from anion-exchange chromatography. Based on the phosphate content fractions were combined to three pools, as indicated.

4.4.2. Chemical analysis

Compositional analysis of each from the obtained pools identified Glc and Rha [(in an approx. molecular ratio of 1:4 for pool 1, 1:5 (pool 2) and 10:1 (pool 3)], phosphate, GlcN and MurNAc. In pool 2 and 3, additionally Gro was identified. Further analyses by NMR spectroscopy showed that in pool 3 Gro was linked to the phosphate, thus identifying this molecule as WTA. Analyses of the ^{1}H NMR spectra revealed no significant differences between pools 1 and 2, and based on the high content of rhamnose, this molecule was

identified as rhamnan. The absolute configurations of Rha and Glc were determined as L and D respectively.

4.4.3. NMR spectroscopy of the rhamnan

The 1D ^{1}H NMR spectra of pool 1 and 2 showed no significant differences in the anomeric region. Since the quality of the 2D spectra recorded for pool 1 was not sufficient for a successful assignment of the signals, further analyses were performed on pool 2. The ^{1}H NMR revealed 5 major signals in anomeric region (4 originating from Rha and 1 from Glc residues), several characteristic signals δ 1.28-1.24 for the methyl group at of 6-deoxyhexoses, and 2 signals at δ 2.06 and δ 2.02 originated from *N*-acetyl group. Anomeric configurations were assigned on the basis of the chemical shifts of $^{1}J_{C\text{-}1,\,H\text{-}1}$ values derived from a coupled $^{1}H,^{13}C$-HSQC as α for Rha and Glc.

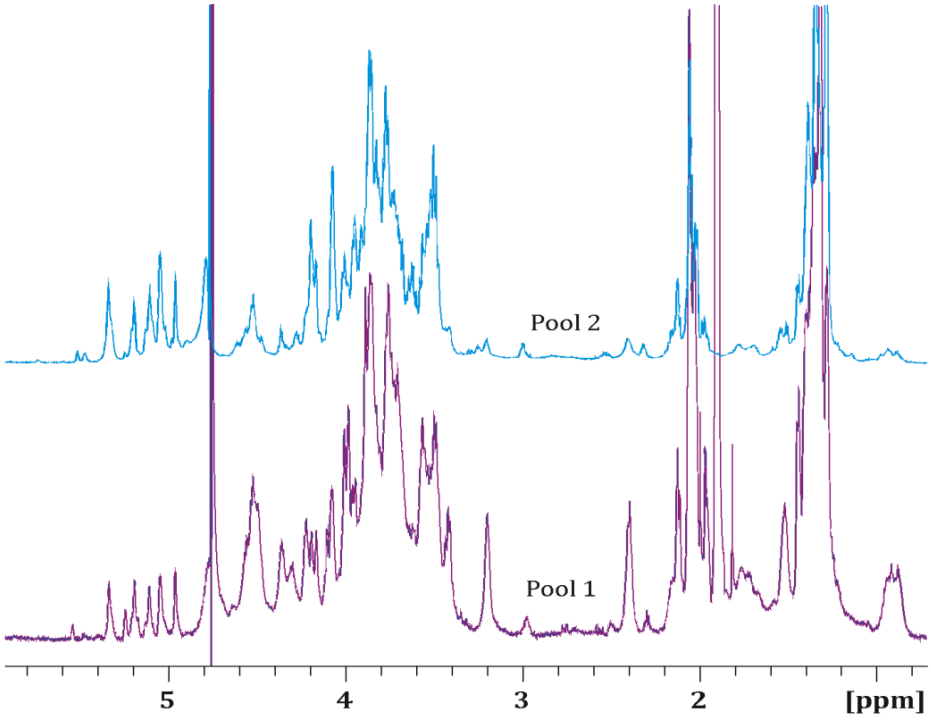

Fig. 44. ^{1}H NMR spectra (700 MHz) of polysaccharides from *S. uberis* 233 revealed from pool 1 and pool 2 after anion-exchange chromatography. Spectra were recorded in D_2O at 27°C relative to external acetone (δ_H 2.225; δ_C 31.45).

The HSQC spectrum showed many signals in the anomeric region, which were low in the 1D ^{1}H NMR spectrum. The intensity of the signals in Fig. 45 was lowered so that only strongly pronounced ones were visible.

Detailed analyses of COSY, TOCSY, ROESY, HSQC and HMBC spectra allowed the complete assignment of ^{1}H and ^{13}C chemical shifts of the most pronounced signals (Fig. 45, Table 18).

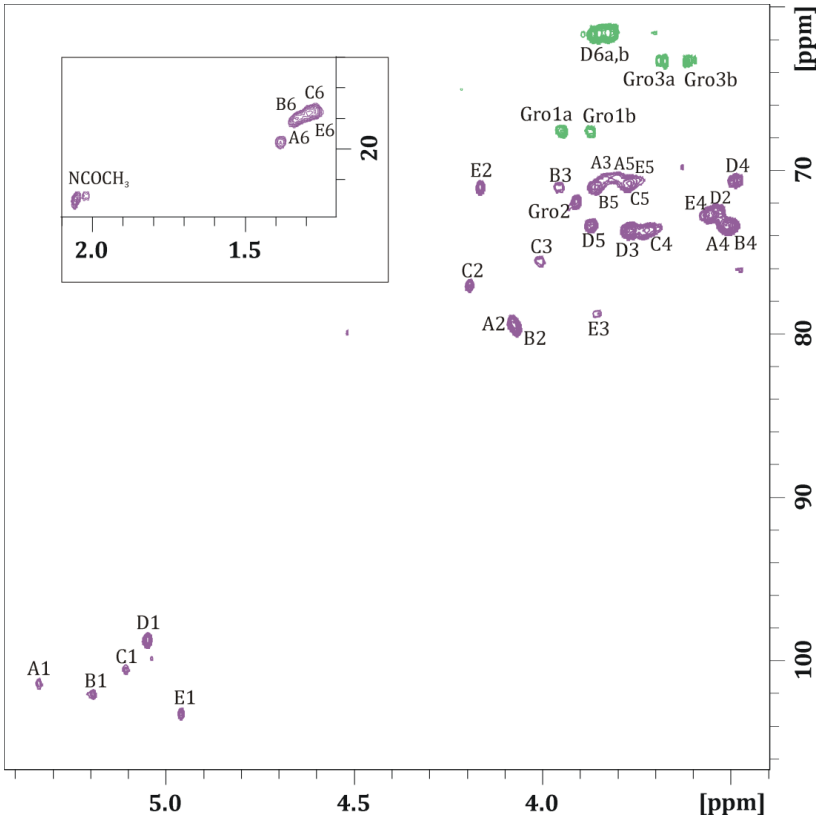

Fig. 45. Part of $^{1}H,^{13}C$ HSQC-DEPT spectrum (700 MHz) of the rhamnan isolated from *S. uberis* 233. The spectrum was recorded in D_2O at 27°C relative to external acetone (δ_H 2.225; δ_C 31.45).

Table 18. ^{1}H and ^{13}C NMR data of the rhamnan isolated from *S. uberis* 233. Spectra were recorded in D_2O at 27°C relative to external acetone (δ_H 2.225; δ_C 31.45).

		1	2	3	4	5	6a	6b
A	**^{1}H**	5.34	4.07	3.84	3.49	3.80	1.34	
2-Rha	**^{13}C**	101.4	79.2	70.6	73.4	70.4	18.1	
B	**^{1}H**	5.19	4.08	3.96	3.51	3.84	1.32	
2-Rha	**^{13}C**	102.1	79.2	71.1	73.4	70.4	17.9	
C	**^{1}H**	5.11	4.19	4.00	3.71	3.76	1.28	
2,3-Rha	**^{13}C**	100.5	77.0	75.6	73.7	70.6	17.7	
D	**^{1}H**	5.05	3.54	3.76	3.48	3.87	3.83	3.85
t-Glc	**^{13}C**	98.7	72.5	73.7	70.6	73.4	61.7	
E	**^{1}H**	4.96	4.16	3.86	3.56	3.74	1.28	
3-Rha	**^{13}C**	103.2	71.1	78.8	72.8	70.5	17.7	

The HMBC experiment was applied in order to investigate the linkages between the residues. The resonances **A**, H-1/**C**, C-3; **B**, H-1/**E**, C-3; **C**, H1/**A**, C-2 or/and **B**, C-2; **E**, H-1/**B**, C-2 and **C**, H-2/**D**, C-1 were observed (for A-E, see Table 18). The correlations were further confirmed by a ROESY experiment, which revealed *inter*-residual nOe contacts between **A**-1/**C**-3, **B**-1/**E**-3, **C**-1/**A**-2 or/and **B**-2, **D**-1/**C**-2 and **E**-1/**B**-2. Based on these data, it was assumed that there were two different rhamnans in the sample, the first one, a simple chain composed of 2- and 3- substituted Rha with structure: →2)-**B**-(1→3)-**E**-(1→, and a second one, of the same main chain, with a Glc residue substituting position 2 of **C** {structure: →2)-**A**-(1→3)-[**D**-(1→2)-]**C**-(1→}. Since there was no indication that both partial structures were linked (no cross connectivity between **E-**1 and **A-**2 was observed, and the nOe contacts between 3-**A**/4-**D** and 6-**A**/2-**D** were found in the ROESY spectrum, whereas no similar crosspeaks could be observed between **B** and **D**) it was thought that two different rhamnans were present in the sample. The proposed structures of the rhamnans are depicted in Fig. 46.

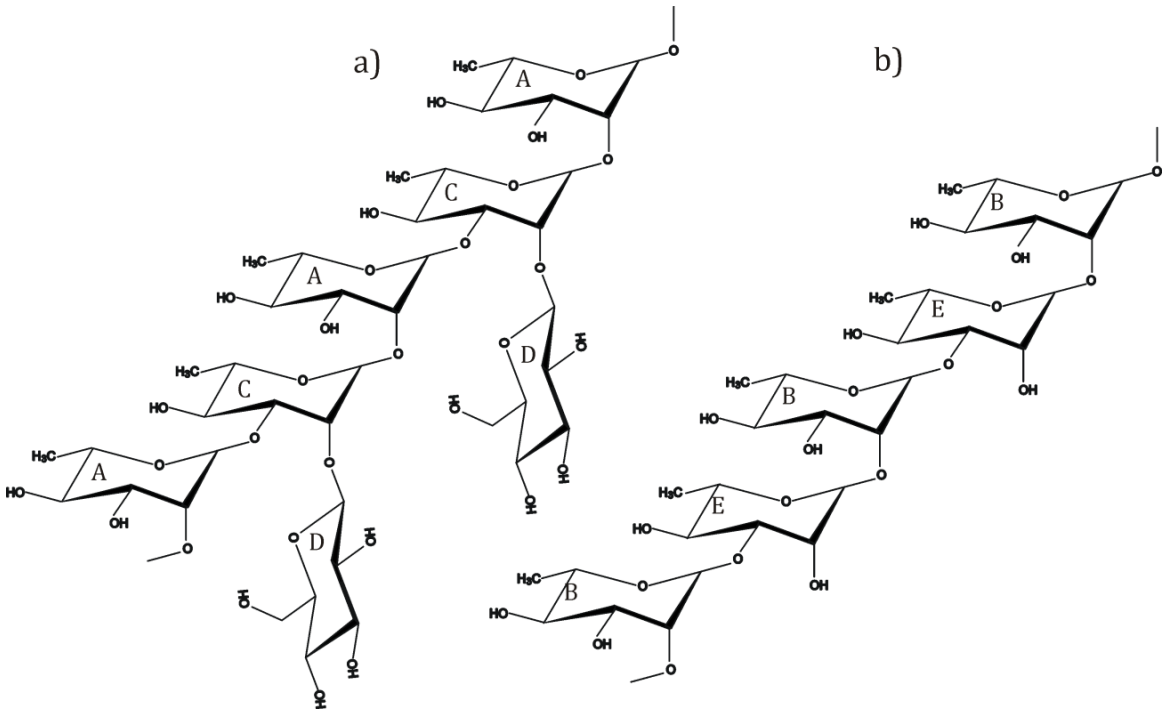

Fig. 46. Proposed structures of the rhamnans of *S. uberis* 233 a) branched rhamnan substituted with Glc residues, b) unbranched rhamnan. The capital letters refer to the residues defined in Table 18.

Moreover, the ^{31}P NMR spectrum showed several signals. In ^{1}H,^{31}P HMQC experiment, the most prominent crosspeaks were detected between a phosphoester signal at δ +1.78 with protons at δ 3.91 and δ 3.95, δ 4.05 and δ 4.25. The spin system of this molecule was solved and suggested the presence of phosphoglycerol (H-1a δ 3.87, H-1b δ 3.95, C-1 δ 67.6, H-2 δ 3.91, C-2 δ 71.8, H-3a δ 3.61, H-3b δ 3.68, C-3 δ 63.24). No connectivities

between signals originating from this molecule and any other could be found either in the HMBC or in the ROESY spectra, indicating phosphoglycerol to be a contamination. Furthermore, since the analysed sample was the one eluting between rhamnan and WTA (fraction 2, Fig. 43), the contamination with short chains of phospholgycerol is likely.
Less pronounced crosspeaks between ^{31}P at δ -12.5 and ^{1}H at δ 5.47 and between ^{31}P at δ -10.7 and ^{1}H at δ 4.19 and 4.23 were observed. The intensities of the phosphate peaks were similar and their chemical shifts identified a pyrophosphate group. It was attempted to assign the chemical shifts of molecules, bound to this group, but this was, however, not possible.

4.4.4. NMR spectroscopy of WTA

The 1D ^{1}H-NMR spectrum of WTA showed in the anomeric region two signals A and B (δ 5.16 and δ 5.09, respectively) of similar, low intensity and one more intense signal at δ 4.64 (C), all originating from Glc residues. Additionally, several signals of ring protons and Gro at δ 4.22 – 3.31 and some characteristic for *N*-acetyl groups at δ 2.08-2.02 were observed.

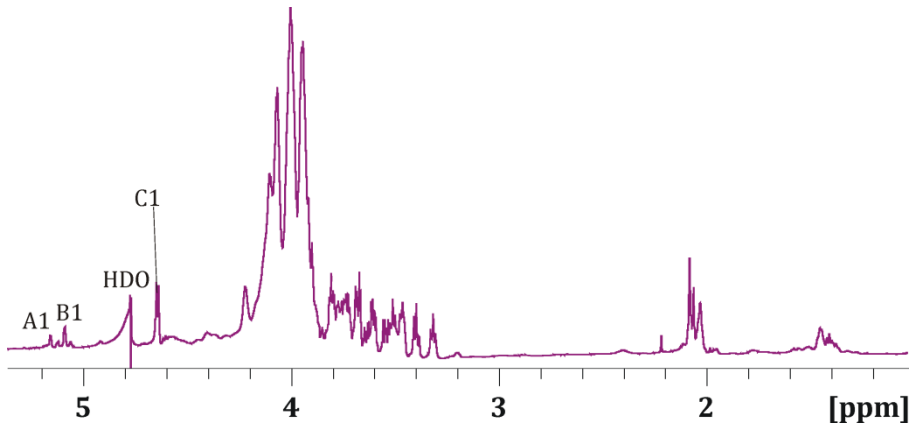

Fig. 47. ^{1}H NMR spectrum of the WTA isolated from *S. uberis* 233 (700 MHz) recorded in D_2O at 27°C relative to external acetone (δ_H 2.225; δ_C 31.45).

2D NMR experiments allowed the assignment of all chemical shifts (Table 19). The *intra*-residual nOe contacts between H-1 and H-2 of **A** and **B** (observed in the ROESY spectrum) and the chemical shifts of anomeric protons (5.16 and 5.09) proved both sugars to be α-pyranoses. Their *gluco* configuration was confirmed by an *intra*-residual H-2/H-4 nOe

connectivity. Additionally, nOe contacts between **B** H-1/**A** H-2 and **A** H-1/**D** H-3 indicated the structure α-D-Glc*p*-(1→2)-α-D-Glc*p*-(1→3)-Gro. Any other connectivities were not found indicating no linkages with WTAs chains. The β-configuration of **C** was confirmed by $J_{1,2}$ 7.9 Hz and its *gluco* configuration was proven by an *intra*-residual H-2/H-4 nOe connectivity.

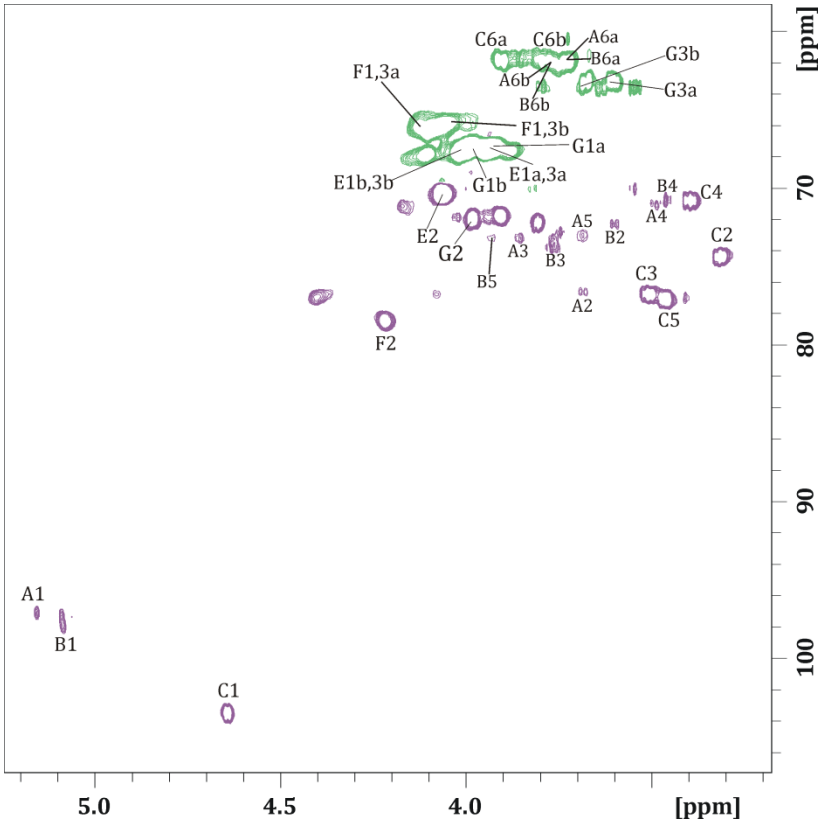

Fig. 48. Excerpt of $^{1}H,^{13}C$ HSQC-DEPT spectrum (700 MHz) of the WTA isolated from *S. uberis* 233. The spectrum was recorded in D_2O at 27°C relative to external acetone (δ_H 2.225; δ_C 31.45).

Furthermore, the ^{31}P NMR spectrum showed a signal at δ +1.2 revealing the presence of the phosphodiester linkage. The $^{1}H,^{31}P$ experiment showed the correlation to the region δ 4.16-3.85.

Inter-residual resonances between **C**-1 and **F**-2, observed in both, ROESY and HMBC spectra proved the substitution at position 2 of glycerol by **C**, but also signals characteristic for an unsubstituted phosphoglycerol were observed (**E**). Additionally, the signals of a glycerol residue which *O*-1 is bound to the phosphate, whereas its *O*-3 is free (**G**) were found. The fact that signals of **G** were detected indicated that the WTAs chains were rather short. The proposed structure of the WTA was shown on Fig. 49.

Table 19. ^{1}H and ^{13}C NMR data of the WTA isolated from *S. uberis* 233. Spectra were recorded in D_2O at 27°C relative to external acetone (δ_H 2.225; δ_C 31.45).

Residue		1(a)	1b	2	3(a)	3b	4	5	6a	6b
A	^{1}H	5.16		3.68	3.86		3.49	3.69	3.71	3.81
α-D -Glc*p*	^{13}C	97.1		76.6	73.1		71.0	73.0	61.8	
B	^{1}H	5.09		3.60	3.77		3.46	3.93	3.71	3.81
α-D-Glc*p*	^{13}C	97.3		72.3	73.9		70.7	73.1	61. 8	
C	^{1}H	4.47		3.31	3.51		3.40	3.46	3.90	3.77
β-D-Glc	^{13}C	103.3		74.4	76.7		70.8	76.9	61.9	
D	^{1}H	3.83	3.51		3.67	3.60				
Gro-αGlc	^{13}C	70.0			63.1					
E	^{1}H	3.93	4.02	4.06	3.93	4.02				
-P-Gro-P-	^{13}C	67.5		70.3	67.5					
F	^{1}H	4.11	4.03	4.22	4.11	4.03				
-P-Gro-(βGlc)P-	^{13}C	66.1		78.5	66.1					
G	^{1}H	3.90	3.96	3.91	3.60	3.68				
-P-Gro	^{13}C	67.8		71.6	63.2					

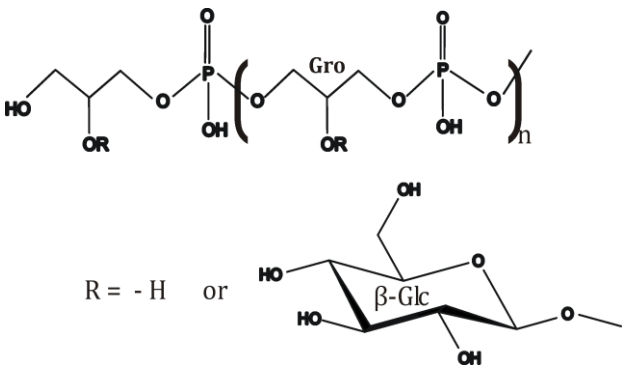

Fig. 49. Proposed structure of WTA of *S. uberis* 233.

Due to the fact that the isolation was performed utilizing lysozyme in order to release the WTA from the cell wall it was expected to find signals characteristic for MurNAc and GlcNAc, originating from PG. However, only signals characteristic for *N*-acetyl groups were found. Therefore, the information on its linking to PG is still missing.

4.5. CPS

4.5.1. Isolation of CPS

The capsular polysaccharide was extracted from ~ 13 g of wet mass of *S. uberis* 233, 0140J and T1-18 with 0.9% NaCl, followed by 1% phenol extraction as described in 3.2.2.4. Prior to the size exclusion chromatography on Bio-Gel 60, samples were centrifuged [16162 *g* (Sigma 1-14) 10 min, RT] in order to obtain a clear supenatant. Both phenol and NaCl extracts gave only one main fraction. The purity of the isolated material was monitored by UV spectroscopy, and revealed a high contamination with nucleic acids. Treatments with DNase I, and RNase followed by proteinase K was performed. Samples were then fractionated on Bio-Gel P10 and gave two pools the first of which eluted in the void volume, and the second at the end of the elution. The purity of the sample was satisfying and both extracts were used in chemical as well as NMR analyses.

4.5.2. Chemical analysis of CPS

First, weak methanolysis (2M HCl/MeOH, 45 min, 85°C) followed by acetylation of both phenol and NaCl extracts was performed. The GLC-MS spectra of both samples were similar and revealed the presence of hexuronic acid, hexosamine, and a dimer composed of both of them. Further analyses for uronic acids (3.2.3.1.5) and amino sugars (3.2.3.1.3) identified GlcN and GlcA acid as the only components of the CPS. The absolute configuration of GlcA and GlcN was determined as D. Methylation analysis revealed the presence of 3-substituted GlcN and 4-substituted Glc by identifying 1,3,5-tri-*O*-acetyl-2,4,6-tri-*O*-methyl-[1-^{2}H]glucitol and 2-acetamido-1,4,5-tri-*O*-acetyl-4,6-di-*O*-methyl-[1-^{2}H]glucitol. The Glc residue appeared, due to reduction of –COOH group of GlcA.

4.5.3. NMR analysis of CPS

Both phenol and NaCl isolated CPS were used for ^{1}H NMR experiment. Proton spectra of both samples were highly similar (Fig. 50), therefore 2D NMR experiments were performed only on the NaCl extract isolate.

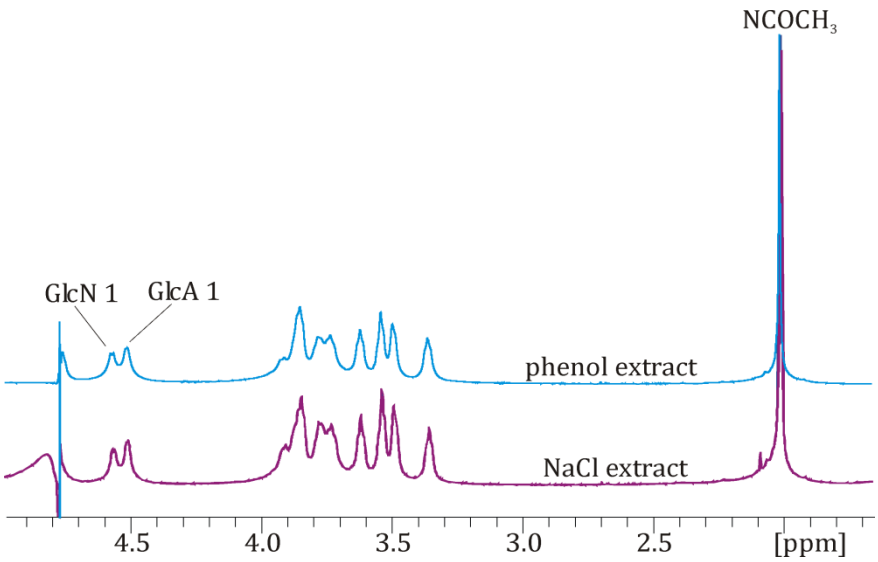

Fig. 50. ^{1}H NMR spectra of the CPS obtained from both phenol and NaCl extractions (700 MHz) recorded for *S. uberis* 233 in D_2O at 27°C relative to external acetone (δ_H 2.225; δ_C 31.45).

The 1D ^{1}H-NMR spectrum showed two signals in the anomeric region (δ 4.55 and δ 4.50) of the same intensity, several signals of ring protons at δ 3.91 – 3.35, and one characteristic signal of a *N*-acetyl group at δ 2.0. Detailed analyses applying COSY, TOCSY, ROESY and HSQC experiments assigned all chemical shifts (Table 20, Fig. 51).

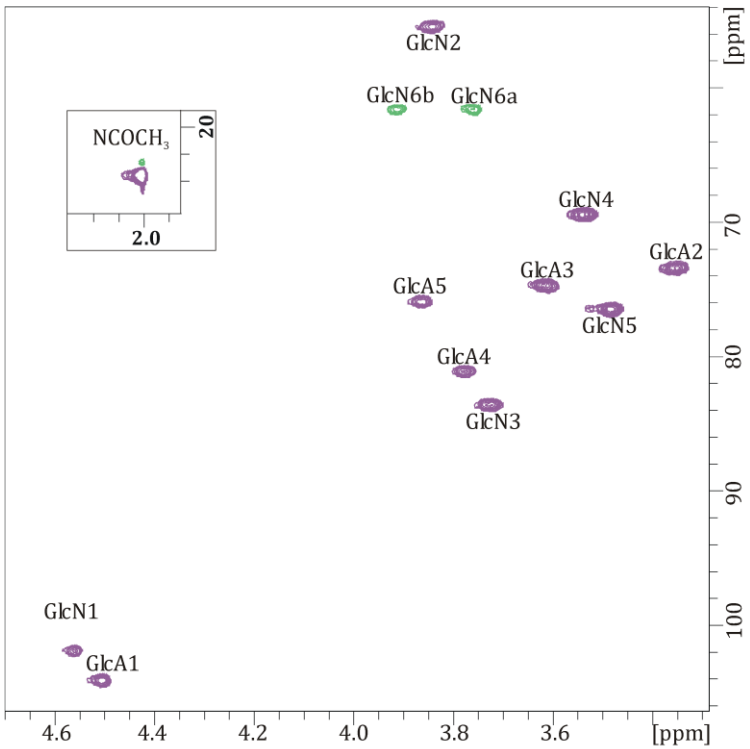

Fig. 51. Excerpt of ^{1}H,^{13}C HSQC-DEPT spectrum (700 MHz) of the CPS isolated from *S. uberis* 233. Spectrum was recorded in D_2O at 27°C relative to external acetone (δ_H 2.225; δ_C 31.45).

Table 20. ^{1}H and ^{13}C NMR data of the CPS isolated from *S. uberis* 233. Spectra were recorded in D_2O at 27°C relative to external acetone (δ_H 2.225; δ_C 31.45).

		1	2	3	4	5	6a	6b	$NCOCH_3$	$NCOCH_3$
GlcN	^{1}H	4.55	3.84	3.72	3.53	3.48	3.76	3.91	2.0	-
	^{13}C	102.0	55.5	83.6	69.5	76.6	61.7		23.7	176.0
GlcA	^{1}H	4.50	3.35	3.61	3.77	3.85	-	-		
	^{13}C	104.3	73.5	74.8	81.2	76.0	173.7			

The β-configurations of both, GlcN and GlcA were confirmed by $J_{1,2}$ 7.5 Hz (GlcN) and $J_{1,2}$ 6.5 Hz (GlcA). In a ROESY experiment, the *gluco* configuration of GlcN and GlcA was proved by an *intra*-residual H-2/H-4 nOe connectivity. *Inter*-residual nOe contacts between protons 1 GlcN/4 GlcA and 1 GlcA/3 GlcN were observed.

Taken together, the data of the compositional analysis and NMR experiments identified the structure →4)-β-D-Glc*p*A-(1→3)-β-D-Glc*p*NAc-(1→ (Fig. 52, hyaluronic acid).

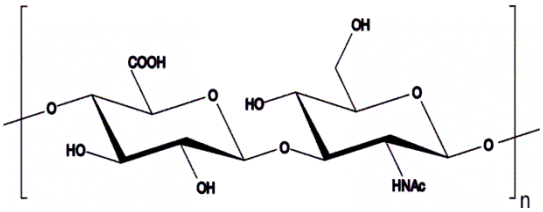

Fig. 52. Structure of the CPS of *S. uberis* 233, 0140J and T1-18.

4.5.4. The activation of pbMEC by a decapsulated mutant (*ΔHasA* mutant)

The Δ *Has A* mutant of *S. uberis* which is impaired in capsule production was investigated in regard of stimulation NF-κB and the *IL-1A, IL-6, IL-8, TNF-α* in pbMEC. The experiment showed that there were no differences in activation of pbMEC between the wild type and decapsulated mutant. The activation of the immune genes did not occur either (data not shown), as in case of encapsulated strains. In order to investigate, whether the *ΔHasA* mutant indeed did not produce a capsule, it was attempted to isolate the CPS, but none could be obtained.

4.6. EPS

4.6.1. Isolation of EPS

The EPS was isolated from the sterile culture medium after the cultivation of *S. uberis* 233, 0140J, T1-18 and EF20 as described in 3.2.2.5. From 100 ml of the culture medium, about 5 mg (in average) of EPS was obtained.

4.6.2. Chemical analysis

Methanolysis (2M HCl/MeOH, 4 h, 85°C) followed with acetylation of EPS was performed. The GC-MS spectra revealed the presence of hexoses, hexosamines and 6-deoxyhexose. Further analyses for neutral sugars (3.2.3.1.2) and amino sugars (3.2.3.1.3) identified a large amount (over 80%) of Man, and small amount of Glc (5.2%), Gal (5.3%), GlcN (5.2 %) and traces of Fuc (2.4 %) and GalN (1.8 %). The absolute configuration of Man and Glc was determined as D. Methylation analysis revealed the presence of 2-substituted, 3-substituted, 6-substituted, 2, 6-disubstituted hexoses and terminal hexoses.

4.6.3. NMR analyses of EPS

The ^{1}H-NMR spectra of the EPSs isolated from different strains of *S. uberis* showed no differences and appeared rather complex. In the low field anomeric region 11 signals were present, 10 identifiable as Man spin systems with a different magnetic environment, and 1 identified as a Glc. Anomeric configurations were assigned on the basis of the chemical shifts of $^{1}J_{C\text{-}1,\,H\text{-}1}$ values derived from a coupled ^{1}H,^{13}C-HSQC as α for Man and β for Glc. On the HSQC-DEPT spectrum 4 signals of $-CH_2$ groups were at low field. This observation along with reported data (Sandal et al., 2011), let us assume that the EPS was a (1→6)-linked, highly branched mannopolysaccharide. In order to determine the length and substitution of the branches, acetolysis reaction (3.2.3.3.4) was performed. This reaction cleaves less stable (1→6)-glycosidic linkages, leaving stronger linkages intact. The reaction mixture was fractionated on Bio-Gel P2 column, and yielded 3 sugar-containing pools that were analyzed by NMR spectroscopy (Fig. 53).

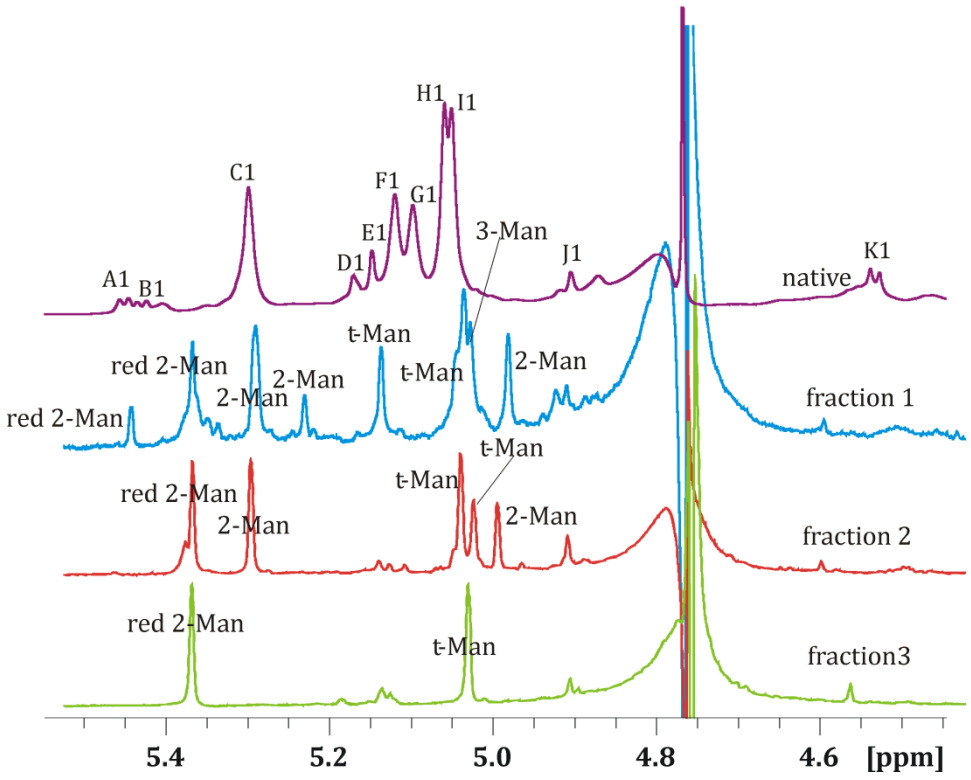

Fig. 53. The anomeric region of ^{1}H NMR spectra (700 MHz) recorded in D_2O at 27°C relative to external acetone (δ_H 2.225; δ_C 31.45). Investigated were the native EPS (for capital letters see and the Table 21.) and products obtained from acetolysis and fractionation on BioGel P2 (fractions 1-3).

In the spectra of all fractions signals at δ 5.37 were present and in that of fraction 1 additionally at δ 5.45, which indicated the product, rose by acetolysis. Those signals appeared probably due to the modification of the original protocol (Kocourek and Ballou, 1969) where 2M HCl instead of dry ice was used for neutralization. This could lead to the interaction of free reducing end of Man residues with an *O*-methyl group at δ 3.40, and thus to the lowfield shift of the signals. In further analyses no cross peaks between *O*-methyl signal at δ 3.40 and protons at δ 5.45 and δ 5.37 were found. Furthermore the chemical shifts of ^{13}C (HSQC) at δ 93.26 and δ 93.56, respectively, suggested no substitution. These Man residues were originating from the main chain. In fraction 1, the ^{1}H NMR spectrum possessed 8 signals in the anomeric region. 1D and 2D experiments allowed to assign all signals. ROESY and HMBC experiments were used, in order to identify the linkages between the Man residues. It was established that there were two tetrasaccharides present in the sample with the structure:

α-D-Man*p*(1→2)α-D-Man*p*(1→2)α-D-Man*p*(1→2)α-D-Man*p* red

and

α-D-Man*p*-(1→3)α-D-Manp(1→2)α-D-Man*p*(1→2)α-D-Man*p* red

Fraction 2 also consisted of two chains. The chains were structurally the same but experienced a different environment, their structure was:

α-D-Man*p*(1→2)α-D-Man*p*(1→2)α-D-Man*p* red

A disaccharide with the structure red α-D-Man*p*(1→2)α-D-Man*p* red was found to be a component of fraction 3.

Thus, the acetolysis revealed only four kinds of oligosaccharides to be present in branches, attached to the main polymer backbone. Furthermore, due to the fact that no fraction containing monosaccharides was found, it was assumed that the amount of unbranched (1→6) Man was very low.

All signals originating from 2- and 3- substituted Man residues were then found and proven on the NMR spectra of native EPS. Additionally, the ^{1}H and ^{13}C chemical shifts of **A**, **B**, **F**, **G**, **J** and **K** were assigned (Fig. 54,Table 21). Due to the absence of these signals in the samples obtained after acetolysis, it was assumed that these residues were in the main chain. Indeed **A**, **F**, **G** and **J** were substituted in position 6, **F** and **G** additionally at position 2. The intensity of signals originating from the spin system of **J** proved the observation that very low amounts of unbranched residues were present in the main chain.

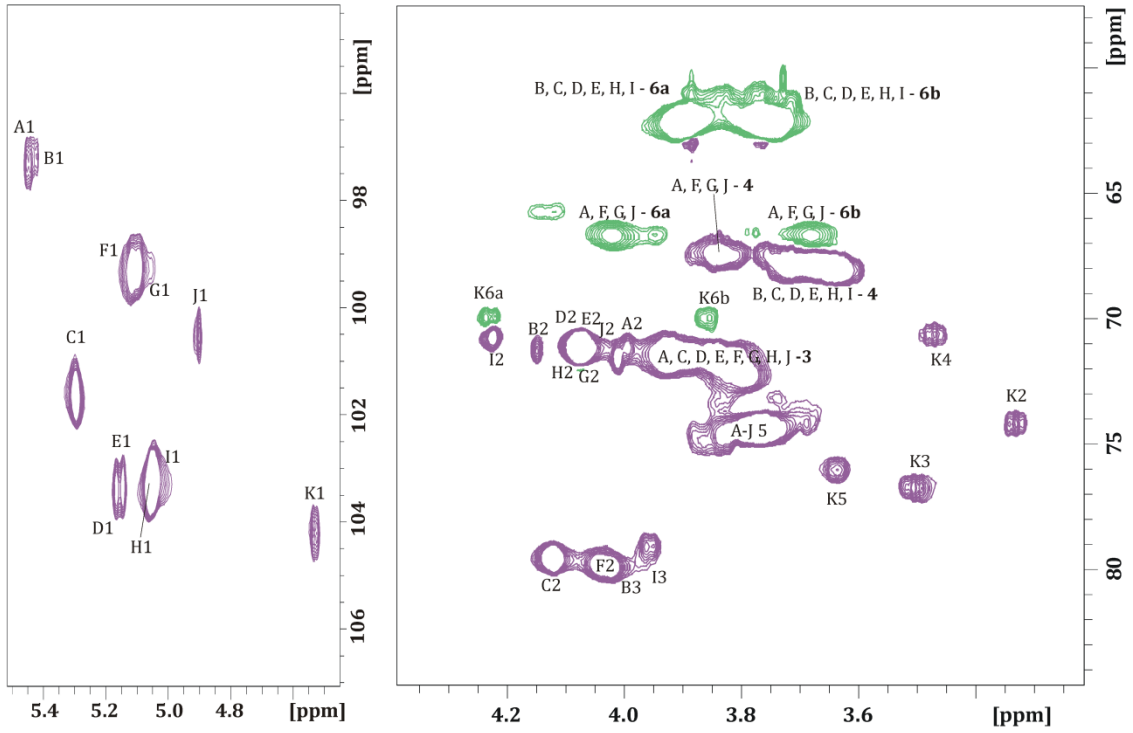

Fig. 54. Excerpt of the ^{1}H,^{13}C HSQC-DEPT spectrum (700 MHz) of the EPS isolated from *S. uberis* strains. On the left side the anomeric region of the spectrum is shown, the right side shows that of the ring protons. Capital letters are explained in Table 21. The spectrum was recorded in D_2O at 27°C relative to external acetone (δ_H 2.225; δ_C 31.45).

Table 21. ^{1}H and ^{13}C NMR data of the EPS isolated from *S. uberis* EF20. Spectra were recorded in D_2O at 27°C relative to external acetone (δ_H 2.225; δ_C 31.45).

		1	2	3	4	5	6a	6b
A **1-P,6-Man**	^{1}H	5.45	4.01	3.92	3.70	3.81	3.66	4.01
	^{13}C	97.4	71.6	71.4	67.9	74.5	66.7	
B **1-P,3-Man**	^{1}H	5.43	4.14	4.02	3.66	3.84	3.89	3.71
	^{13}C	97.4	71.3	78.6	67.9	74.5	62.1	
C **2-Man**	^{1}H	5.30	4.12	3.91	3.72	3.78	3.89	3.71
	^{13}C	101.6	79.5	71.4	67.9	74.4	62.1	
D **t-Man**	^{1}H	5.17	4.08	3.89	3.64	3.78	3.89	3.75
	^{13}C	103.3	71.2	71.5	68.0	74.4	62.1	
E **t-Man**	^{1}H	5.15	4.07	3.89	3.64	3.78	3.89	3.76
	^{13}C	103.3	71.2	71.5	68.0	74.4	62.1	
F **2,6-Man**	^{1}H	5.12	4.04	3.92	3.84	3.77	3.66	4.01
	^{13}C	99.3	79.8	71.5	67.5	74.4	66.7	
G **2,6-Man**	^{1}H	5.10	4.01	3.91	3.84	3.77	3.66	4.01
	^{13}C	99.3	79.8	71.5	67.5	74.4	66.7	
H **t-Man**	^{1}H	5.06	4.07	3.84	3.63	3.76	3.89	3.75
	^{13}C	103.3	71.2	71.5	68.0	74.4	62.1	
I **3-Man**	^{1}H	5.05	4.22	3.95	3.66	3.77	3.89	3.75
	^{13}C	103.3	70.8	79.1	67.9	74.4	62.1	
J **6-Man**	^{1}H	4.90	3.99	3.83	3.84	3.77	3.98	3.72
	^{13}C	100.6	71.2	71.7	67.6	74.4	66.6	
K **t-Glc**	^{1}H	4.53	3.32	3.49	3.47	3.64	4.22	3.85
	^{13}C	104.2	74.2	76.7	70.6	76.0	70.0	

A and **B** gave a cross peak between their anomeric protons at δ 5.45 and δ 5.43, and ^{31}P at δ -1.11, **B** was suggested to be terminal. In order to prove this claim, the cleavage of the phosphodiester utilizing 48% HF followed by a separation on Bio-Gel P2 was performed. The ^{1}H NMR spectrum (Fig. 55) of the pool collected from the void volume of the column lacked signals **A**, **B** and **D**. ROESY and HMBC spectra of native EPS proved the linkage between **B** and **D** by showing the crosspeak 1**D**/3**B**. Based on these observations it was concluded that on the reducing end of the (1→6)-linked α-Man*p* main chain linked there was the cap α-D-Man*p*-(1→3)-α-D-Man*p*-1→P←1-α-D-Man*p*-(6←.

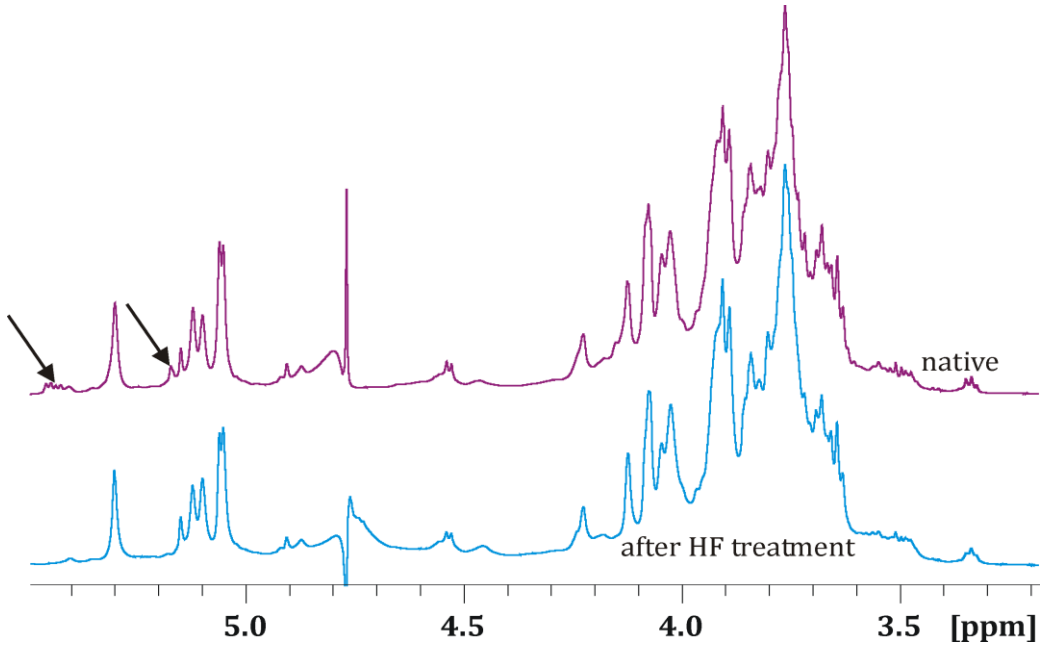

Fig. 55. ^{1}H NMR spectra (700 MHz) recorded in D_2O at 27°C relative to external acetone (δ_H 2.225; δ_C 31.45) of the native and HF-treated EPS fractionated on BioGel P2. The black arrows on the spectrum of native EPS show the signals missing on the spectrum after dephosphorylation.

ROESY and HMBC spectra of the native EPS confirmed most of the linkages. The cross peaks **H**1/**F**2, **C**1/**G**2, **I**1/**C**2, **E**1/**I**3, **H**1/**C**2 were observed.

The big challenge in establishing the structure turned out to be the Glc residue. Despite the fact that the spin system was solved, no cross peaks between Glc and Man residues were found. Since no signals originating from Glc were observed in the acetolysis products, it was assumed that Glc was a substituent of the main chain. Furthermore, C-6 of the Glc was strongly shifted downfield, suggesting a strong electronegative substitution. The presence of an acetyl group at C-6 was excluded by deacetylation reactions performed on the sample (3.2.3.3.2, 3.2.3.3.3). Neither hydrazine nor ammonia solution treatment resulted in changes of chemical shifts of **K** C-6. Another strong electronegative substituent, present in few published polysaccharides, could be sulfate group (Nazarenko et al., 2003). This was, however not proven. The proposed structure of EPS is depicted in Fig. 56.

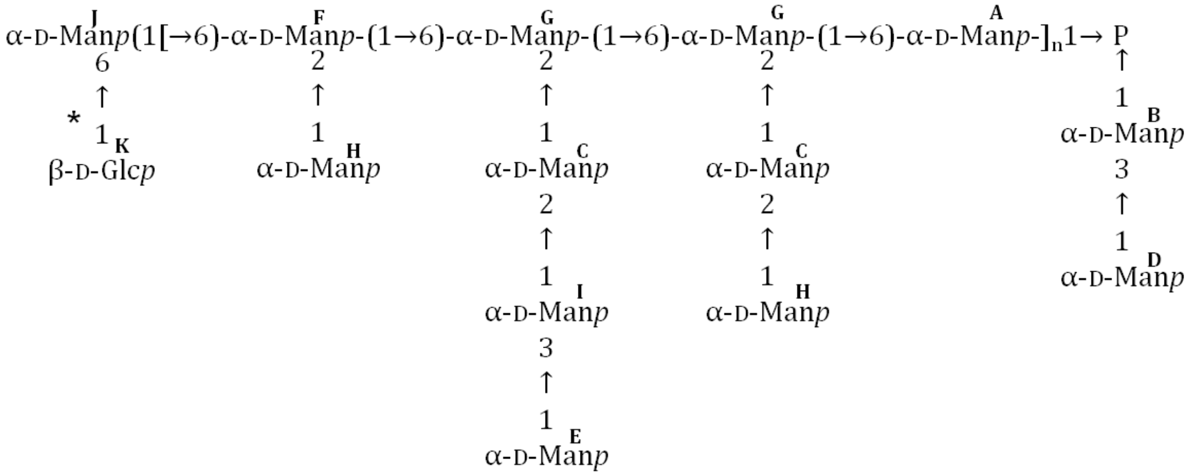

Fig. 56. The proposed structure of the isolated EPS. The capital letters are as in Table 21. * - The linkage between **J** and **K** was not proven, furthermore the position 6 of **K** was substituted with some unidentified, strongly electronegative, hydrogen-free group.

4.6.4. The role of EPS in phagocytosis and adherence to bovine monocytes

Due to the fact that the CPS isolated from *Streptococcus suis* had an antiphagocytic effect on macrophages (Houde et al., 2011), it was interesting to examine the effect of the isolated from *S. uberis* EPS on phagocytosis and adherence to monocytes. The experiment was performed as described in 3.2.5.3.

First, *S. uberis* EF 20 and *S. uberis* O140J were used for challenging monocytes. The uptake of bacteria by monocytes as well as the ability of *S. uberis* to adhere to the cells was investigated. The result (Fig. 57) showed that *S. uberis* EF20 adhered to a higher percentage of monocytes and was phagocytosed more readily compared to *S. uberis* O140J.

The next experiments were performed with addition of EPS in the concentration 1 µg/ml and 5 µg/ml. *E. coli* and *S. aureus,* causative agents of mastitis as well, were used in the experiment in order to investigate if the eventual antiphagocytic effect was species-dependent. The experiment showed that EPS has no effect on adherence to monocytes for any of used heat-inactivated bacteria (Fig. 58).
The addition of EPS (1 or 5 µg/ml) to the culture seemed to have as well no inhibiting effect on the phagocytosis rates of *S. uberis* O140J, *E. coli* or *S. aureus* by bovine monocytes,

but EPS present at 5 μg/ml significantly enhanced the phagocytosis of *S. uberis* EF20 (Fig. 59).

It was also noticed that, although *S. uberis* could adhere to monocytes and be phagocytosed, this did not occur at the same high level as in case of *E. coli* and *S. aureus*.

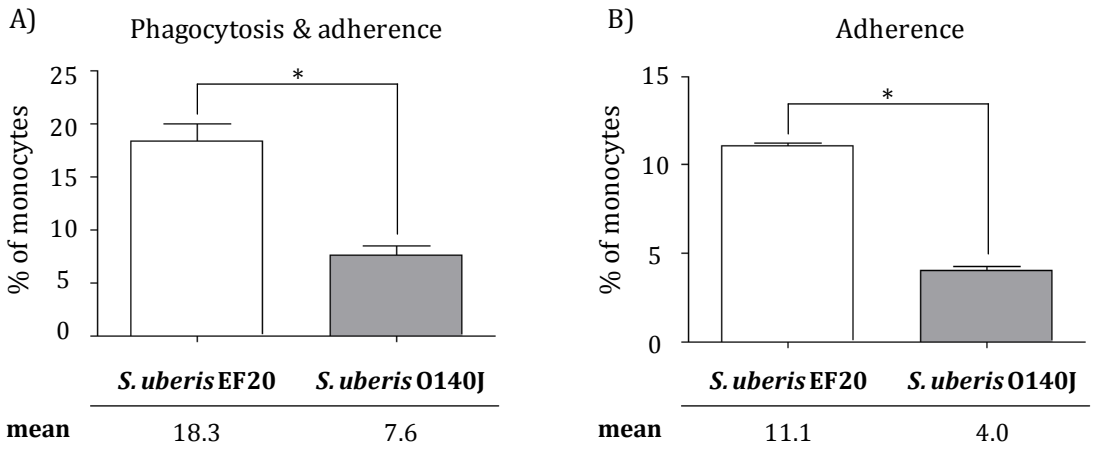

Fig. 57. The phagocytosis/adherence assay; A) The percentage of monocytes with attached or phagocytosed *S. uberis* EF20 and *S. uberis* O140J; B) The percentage of monocytes with attached *S. uberis* EF20 and *S. uberis* O140J. The star above the line indicating two columns refers to the significance calculated for these two biological replica (*t*-test, unpaired, $p^* < 0.05$).

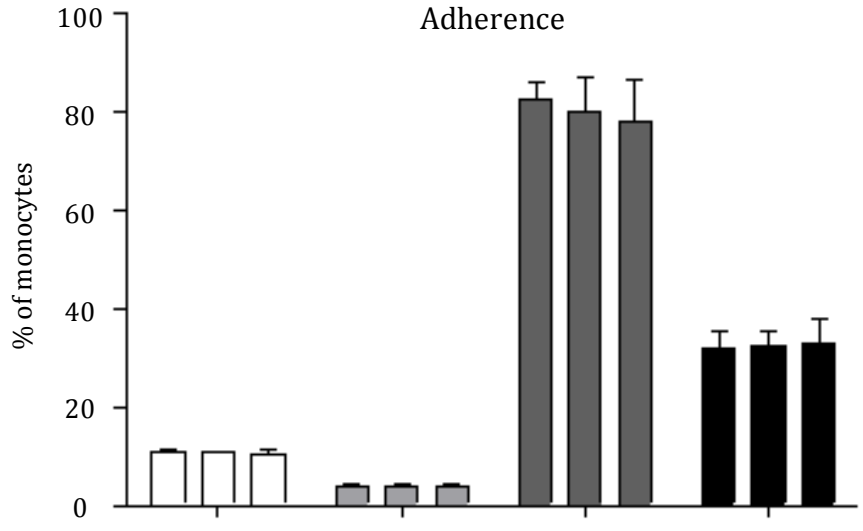

	S. uberis EF20			*S. uberis* O140J			*S. aureus*			*E. coli*		
EPS (μg/ml)	0	1	5	0	1	5	0	1	5	0	1	5
mean	11.1	10.7	10.1	4.0	3.9	3.9	84.4	79.6	77.7	31.9	32.3	33.0

Fig. 58. The percentage of monocytes with attached *S. uberis* EF20, *S. uberis* O140J, *S. aureus* and *E. coli*. The phagocytosis was inhibited by treating the MNCs with NaN_3.

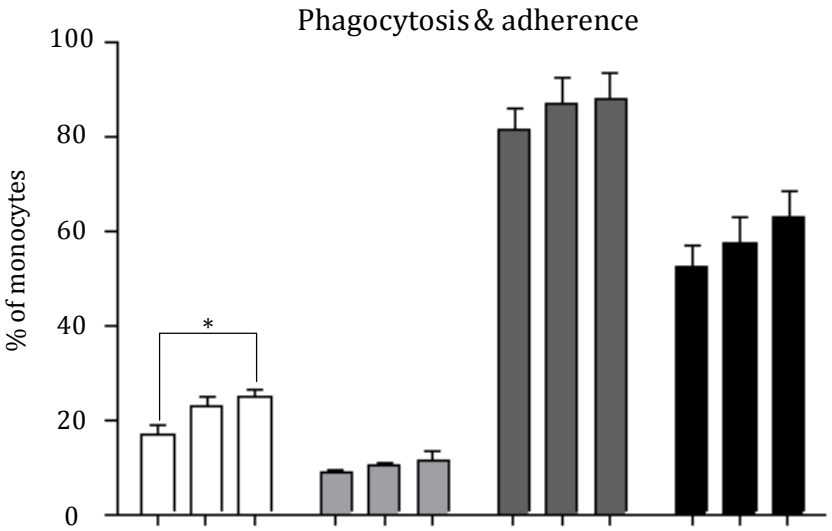

	S. uberis EF20			*S. uberis* O140J			*S. aureus*			*E. coli*		
EPS (µg/ml)	0	1	5	0	1	5	0	1	5	0	1	5
mean	16.6	22.9	24.9	8.9	10.4	11.5	81.2	86.9	87.9	52.4	57.6	63.0

Fig. 59. The percentage of monocytes which phagocytosed or/and attached *S. uberis* EF20, *S. uberis* O140J, *S. aureus* and *E. coli*. The star above the line indicating two columns refers to the significance calculated for these two biological replica (*t*-test, unpaired, *<0.05).

5. Discussion

5.1. Structures

Despite the fact that *S. uberis* is one of the major mastitis pathogens, and has been intensively studied over last five decades, its pathogenicity is not well understood. The fact, that its cell envelope components have never been investigated might be one reason for this situation. After all, the polysaccharides, present in cell envelope of bacteria, are the ones that interact with host cells, and depending on their biological activity they can or cannot start a cascade of signals leading to the elimination of the pathogen. Thus, the knowledge about the structures of these molecules is crucial in order to understand these processes.

In this study the structures of different cell envelope components were established which are discussed below.

From the cell envelope of *S. uberis* glycolipids, LTA, WTA, rhamnan, glucorhamnan, CPS and EPS were isolated.

The three glycolipids had simple structures. They consisted of diacylglycerol substituted by 1 α-Glc (G1) and 2 α-Glc linked (1→2) (kojibiose, G2), and G3 was a DGlcDAG with one phosphoglycerol unit. Such closer look at the structures of the glycolipids gave an idea about their biosynthesis: MGlcDAG (G1) is synthesized into DGlcDAG (G2) and then the phosphoglycerol units are added to this molecule (G3 contains first phosphoglycerol). These observations are in agreement with published data about the biosynthesis of LTA (Reichmann and Gründling, 2011). They are also in agreement with a structure of the isolated *S. uberis* LTA, which was composed of a lipid anchor comprised of α-Glc*p*-(1→2)-α-Glc*p*-(1→3)-1,2-diacyl-*sn*-Gro, and a hydrophilic backbone consisting of poly(*sn*-Gro-1-phosphate), randomly substituted at *O*-2 of Gro by D-Ala. The LTA obtained in this study was of type I (Greenberg et al., 1996). Kojibiose-containing anchored LTAs have been identified earlier in *Streptococcus* spp. (Fischer, 1988), *E. faecalis* (Theilacker et al., 2006) and *L. lactis* (Fischer et al., 2011). The LTA of streptococci may also possess a gentobiose-containing lipid anchor (Neuhaus and Baddiley, 2003). A poly(phospho-Gro) chain substituted non-stoichiometrically by Ala has also been identified in LTAs of *S. aureus* (Morath, 2001), *E. faecalis* (Fabretti et al., 2006), *L. lactis* (Fischer et al., 2011), *Bacillus*

subtilis (Perego et al., 1995), however, these poly(phospho-Gro) chains were additionally substituted by sugar residues.

The WTA which was isolated in this study had a rather simple structure. Like in LTA the backbone was composed of polyphosphoglycerol. The position 2 of Gro was not substituted with alanine like in LTA, but with β-Glc. The structures of WTAs are known to usually be different from LTAs, and even when they are the same, their precursors are of different origin and their chains are not stereoisomerically identical (Neuhaus and Baddiley, 2003). The reported substitutions of polyphosphoglycerol or polyphosphoribitol are D-Ala, β-GlcNAc, α-Glc (Sánchez Carballo et al., 2010; Kurokawa et al., 2011). A substitution with β-Glc has to our knowledge not been reported. The linkage to PG could not be identified. The linker between PG and WTA in *S. aureus* was composed of phosphate, *N*-acetylglucosamine and *N*-acetylmannosamine (ManNAc), and the phosphate was linked to the *O*-6 of MurNAc, and ManNAc was substituted by the first phosphoribitol unit (Xia et al., 2010). The enzymatic treatment used for the isolation of WTA of *S. uberis* should have left the disaccharide from the PG bound to the isolated molecule. However, this could not be identified, for unknown reasons.

However the structural analyses of non classical SCWPs are in their infancy, available data showed that such polysaccharides were heteropolysaccharides. One of the isolated from *S. uberis* molecules was a glucorhamnan with the structure →2)-α-L-Rha*p*-(1→3)-[α-D-Glc-(1→2)-]α-L-Rha*p*-(1→, and the other one was a homopolymer composed only of rhamnose: →2)-α-L-Rha*p*-(1→3)-α-L-Rha*p*-(1→. Both structures have not been published. Again, the linkage to the PG could not be identified. Based on the ^{31}P NMR spectrum, it was concluded that the polymers were linked to the PG *via* a pyrophosphate bridge. Such linkage of the non classical SCWP has been already reported (Schäffer et al., 2000). The spin system belonging to the signals giving cross peaks to the phosphates of the supposed pyrophosphate linkage were not assigned. Thus, further purification of the isolated material is needed in order to finish analysis.

Hyaluronic acid was postulated in 1990 to be a CPS of *S. uberis* based on the observation that the capsule was lost upon treatment with hyaluronidase (Leigh et al., 1990). Then, lectin agglutination along with TLC utilizing a synthetic hyaluronic acid as a standard was used to prove this hypothesis (Almeida and Oliver, 1993). Finally the cluster composed of the three genes *hasA, hasB, hasC* involved in the production of the hyaluronic acid capsule of *S. pyogenes* was identified also in *S. uberis* (Ward et al., 2001).

Nevertheless, we isolated and investigate the structure of the capsular polysaccharide for two reasons: 1) the NMR is a 'gold standard' in structural study, and leaves no doubts about the structure; 2) there are organisms which produce both, a CPS and an EPS, and could have been the case in *S. uberis*. The capsule was isolated using 0.9% of NaCl in order to extract a loosly bound material, and 1% of phenol to obtain more tightly bound material. Both extracts gave the same product, composed of GlcA and GlcN. The NMR spectra were solved, confirming hyaluronic acid to be a CPS.

The culture medium obtained after the cultivation of *S. uberis* was also examined for the presence of additional polysaccharides. The purified material consisted mostly of Man and traces of other sugars, from which only Glc was identified in NMR spectra. The presence of EPS has never been reported for *S. uberis*. The highly branched Man-composed EPSs have been already found to be produced by different organisms. *Phomopsis foeniculi* is a fungal pathogen of fennel and produced a polysaccharide consisted of a backbone of α-(1→6)-linked Man*p* units, substituted at C-2 by mono-, di- and trisaccharidic side chains (Corsaro et al., 1998). Then, the two Gram-negative bacteria *Pseudomonas syrinagae* pv. *ciccaronei* and *Histophilus somni* were found to produce an EPS with a very similar structure. The first bacterium is a pathogen of carob plants, and its mannan showed small differences from that one produced by *P. foeniculi*. The longest chain of the branches (3 residues) was terminated with a Glc residue or phosphorylated at C-6 of Man (Corsaro et al., 2001). *H. somni*, an opportunistic pathogen responsible for respiratory disease in cattle and sheeps produces an exopolysaccharide like *P. foeniculi*, however, the longest chain was substituted by a Gal residue (Sandal et al., 2011). The mannan isolated in this study also differed slightly from these published previously. The reducing end of the α-(1→6)-linked Man*p* main chain did not exist, since it was substituted with the cap: α-D-Man*p*-(1→3)-α-D-Man*p*-1→P←1-α-D-Man*p*-(6←. Then, as in the mannan of *P. syringae*, we could find a Glc residue, but it was not identified in the side chains. In spite of assigning its spin system, a connection of this residue with the rest of the molecule could not be found due to the low amount of Glc. Since it was not identified in the branches acetolysis, it was assumed that this residue was linked to the last Man C-6 of the main chain. Furthermore, the ^{13}C chemical shift of Glc-6 was shifted down field, indicating the substitution by a strong electronegative group. Since a substitution with the acetyl group – common non-sugar substituent – could be excluded, a sulphate group, occasionally occurring in bacterial polysaccharides (Nazarenko et al., 2003) was postulated to substitute the C-6 of Glc.

Thus, a novel EPS produced by *S. uberis* was found and its unique structure was established. However, the similar molecules were proven to be produced by different

organisms, none of which was involved in developing mastitis. Therefore, this antigen may be useful in serological assays for diagnosis of *S. uberis*.

5.2. Biological activities of *S. uberis* cells and isolated cell wall components

The study provides a comprehensive survey of genes found to be stimulated by *S. uberis* heat-inactivated cells as well as some of the cell envelope components in pbMEC and RAW264.7. Also the question how *S. uberis* avoids recognition in the udder was addressed. It should be however stressed, that the challenge of different cells by dead bacteria, differs considerably from an *in vivo* situation. The most important difference is a lack of virulence factors, actively secreted by the pathogen. The model, although not perfect, served very well for the analysis of cell type-specific mechanisms involved in the activation of immune functions.

5.2.1. *S. uberis* overcomes the TLR2 activation in the udder

It has been shown previously, that many Gram-positive bacteria are recognized by TLR2 (Thoma-Uszynski et al., 2001; Hirschfeld et al., 1999).

The activation of NF-κB which in HEK293 cells transient transfected with bovine TLR2 (boTLR2) by heat-inactivated *S. uberis* was investigated and showed that *S. uberis* did not activate NF-κB in those cells. Other Streptococci (*S. agalactiae* and *S. dysgalactiae*) did not follow this pattern and could be recognized by boTLR2. These observations were only partially in agreement with data obtained by Farhat et al., 2008. As in these studies, the recognition of *S. uberis* by transfected HEK293 cells did not occur, however, they could not observe the activation of boTLR2 by *S. agalactiae*.

Due to the often sub-clinical and chronic course of disease caused by *S. uberis*, the data presented here were confronted with those obtained by Yang et al., 2008, on *S. aureus.* This bacterium is one of the most common culprits of chronic mastitis, but it seemed that boTLR2 could properly transduce signals from *S. aureus*. Thus, it was concluded, that the

omission of TLR2 recognition in the udder is *S. uberis*-specific, and had nothing to do with the course of the disease.

5.2.2. *S. uberis* seems to be beyond the radar of pbMEC...

Mammary epithelial cells represent the dominant cell type in the healthy udder. Their main function is the production of milk during lactation. Thus, MEC are probably the first cells to be confronted with a pathogen once this enters the quarter. The immune relevance of MEC has been just recently appreciated (Pareek et al., 2005). It was shown that challenged pbMEC can develop a strong immune response by expressing the pro-inflammatory cytokines and bactericidal factors (e.g. *iNOS, LAP, SAA3*) (Günther et al., 2010). *E. coli* was shown to activate very strongly NF-κB along with expression of master cytokines (*IL-1, IL-6, TNF-α*) within first hours post-stimulation. *S. aureus* is much weaker stimulant of pbMEC, and the highest level of key cytokines was observed after 24 h from challenging (Günther et al., 2011). The activation of NF-κB in pbMEC was very slight (1.2 fold) after the stimulation with *S. uberis*. The alteration of expression of the genes encoding for the master cytokines and antimicrobial factors was not observed in challenged pbMEC. The failure in activation of IL-6, IL-8 and LAP by heat-killed *S. uberis* 233 in primary bovine mammary epithelial cells was also reported previously (Swanson et al., 2009).

The only gene, expression of which was considerably altered after the challenge was *CYP1A1*, which according to information found in Online Mendelian Inheritance in Man database (http://www.omim.org/entry/108330?search=cyp1a1&highlight=cyp1a1; derived on 20.11.2012) is involved in detoxification of xenobiotic substances. This gene is one of the key factors for oxidative metabolism of various toxic substances and showed a stimulation pattern similar to *E. coli* after challenging with *S. uberis*. Furthermore it was proven that activation of *CYP1A1* was independent from TLR signaling (Seyfert, not published). Based on these observations, we could conclude that pbMECs can notice the presence of *S. uberis* (elevated expression of *CYP1A1*), but cannot activate immune functions against it.

5.2.3. … but not macrophages

It has been already described, that infection with *S. uberis* causes an immune response in mammary tissue. The mRNA level of master cytokines in the infected gland was shown to be elevated (Swanson et al., 2009). In this work, mammary epithelial cells fail to activate immune functions when infected with *S. uberis*. Milk from a healthy quarter contains a certain amount of macrophages, therefore these cells were challenged with heat-killed bacteria. In the experiment murine macrophages RAW 264.7 were used, which were shown to be a good model in case of mastitis-causing *S. aureus* and *E. coli* (Seyfert, not published). The NF-κB induction after challenge with *S. uberis* was comparable to that one obtained from induction with *E. coli*. A strong increase of mRNA levels of genes encoding for cytokines IL-1A, IL-6 and TNF-α was observed. The expression of *CXCL2* – the murine equivalent of *IL-8* in the cow, a chemokine involved in neutrophils recruitment – was elevated either. The presence of neutrophils had been proven to be crucial in control of mastitis caused by *S. uberis* (Leigh and Field, 1991).

5.2.4. Cell wall components from *S. uberis* can activate pbMEC

Lipoteichoic acid isolated from different *S. uberis* strains was used for a challenge of HEK293 cells transfected with boTLR2. The induction of NF-κB was very low (max. induction 2.2 fold with concentration 10 µg/ml of LTA), especially when compared to the induction obtained after stimulation by *E. coli* (14.5 fold with 30 µg/ml of heat-killed bacteria). Then, pbMEC were stimulated with LTA (10 µg/ml) and significant activation of NF-κB was observed. In order to exclude the possibility of contamination, LTAs were treated with hydrogen peroxide (1%), which inactivates lipoproteins (Zähringer et al., 2008). The difference in stimulation of NF-κB in pbMEC by peroxide-treated and nontreated LTA was not significant (unpaired *t*-test, * $p < 0.05$). The isolated LTA was shown to induce the expression of all investigated pro-inflammatory genes in pbMECs. The activation of genes encoding for cyto- and chemokines as well as antimicrobial peptides by pbMEC after stimulation with LTA was already reported (Strandberg et al., 2005), however, this experiment was performed utilizing a commercial LTA preparation (often contaminated with lipoproteins), and TLR2-dependent activation was suggested. Originally, the activity of LTAs was attributed to TLR2 (Schwandner et al., 1999), but latest reports proved that LTA can bind to TLR2, but the heterodimerization into TLR2/1 or

TLR2/6 (required for signal transduction) cannot occur (Jin et al., 2007; Botos et al., 2011; Kang et al., 2009). We could show that the LTA isolated from *S. uberis* could activate pbMEC in a TLR2-independent way.

Other cell wall components – glycolipids – were isolated and also analyzed in regard of their biological activity. It was shown that none of the three isolated glycolipids could activate NF-κB in pbMEC. Additionally, the expression of pro-inflammatory and antimicrobial genes (*IL-1A, IL-6, TNF-α, IL-8, iNOS LAP, SAA3*) was investigated after the stimulation with glycolipid 1. An immune response was not observed, however, the expression of *CYP1A1* was strongly elevated. The activation pattern of this gene was comparable with that obtained in stimulation with whole *S. uberis* cells – significant induction just after 1 h from stimulation, maximum expression in the 3rd h, and returning to the base line level after 24 h. Thus, again, epithelial cells could 'sense' the presence of bacterial particle, but were not able to respond.

Since glycolipids may serve in bacterial cells as the lipid anchor of LTA, and it was shown that they could not activate the NF-κB pathway, it was assumed that either the hydrophilic part of LTA was the active one or the induction by LTA required both, long hydrophilic and hydrophobic elements. In order to clarify this, additional stimulation experiments utilizing the hydrophilic part are needed.

5.2.5. In the quest for a 'magic hood'

We could show that *S. uberis* could not be recognized by boTLR2, as well as by pbMECs. It is worth to mention that the other streptococcal species, namely *S. agalactiae* and *S. dysgalactiae* activated the NF-κB pathway by TLR2-dependant way. Furthermore, the LTA isolated from three different strains of *S. uberis* induced the immune response in mammary epithelial cells. Thus, the question 'what is masking the active particles of this bacterium?' arose. Our first idea was a capsular polysaccharide, since these molecules are well known to represent a hood preventing the pathogen from recognition by immune system (Whitfield, 1988). Despite the fact that it was shown that the mutant impaired in capsule production (Ward et al., 2001) was still able to develop infection and clinical mastitis *in vivo* (Field et al., 2003), it was decided to investigate whether the immune response in pbMEC vary between encapsulated strain and noncapsulated mutant (*ΔHasA*).

The investigations showed no differences in NF-κB activation neither in HEK293 transfected with boTLR2 nor in pbMEC. Also immune genes expression in mammary epithelial cells after stimulation with heat-inactivated *ΔHasA* mutant or the wild type did not differ. These observations suggested that the *ΔHasA* mutant could possibly produce another polysaccharide. Similarly, it was reported that *Lactococcus lactis* produced a very complexed capsule (Hanuszkiewicz, 2008), and then, whereas trying to isolate this polysaccharide later again, another one was found (Fischer et al., 2012). It was suggested that the laboratory strain lost the ability to produce the capsule, but instead overproduced a teichoic acid, which took over the covering function. In order to investigate, whether such situation had occurred in *S. uberis*, the *HasA* mutant was treated in the same manner as for a capsule isolation (3.2.2.4), but no polysaccharide was found in any of the extracts.

From the sterile culture medium, after cultivation of *S. uberis*, the EPS was isolated. EPSs are released to the culture medium and maintain only limited association with the bacterial surface. They were reported to play a role in bacterial attachment, adhesion and biofilm formation (Bazaka et al., 2011). Just recently, M. Houde and colleagues revealed, that the capsule of *S. suis* type 2 provides protection from phagocytosis (Houde et al., 2011). Interestingly, the protection was not due to a 'simple' masking of the cells, but to the active destabilization of lipid rafts, preventing from phagocytosis by macrophages and dendritic cells. In the sight of these informations, an experiment was planned which aimed at the antiphagocitic effect of isolated EPS. Bovine monocytes were incubated with heat-killed *S. uberis* O140J and EF20 with or without addition of EPS. The results showed no inhibiting effect of EPS on attachment or phagocytosis. Furthermore, strain EF20 was significantly more efficiently phagocytosed after addition of 5 µg/ml of EPS. It needs to be stressed, that the used model was very artificial. First of all, *in vivo* the EPS, although loosely, is associated to the cell. In the mentioned article from Houde e*t al*. the capsular polysaccharide had to coat the examined material (bacteria or beads) in order to prevent it from phagocytosis. In the experiment performed here, the EPS had no contact with bacterial cells. Then, in the experiment performed before, it was shown that murine macrophages were strongly activated by heat-killed *S. uberis* (5.2.3), whereas here, the monocytes could not efficient uptake heat-killed *S. uberis*, when compared to phagocytosis of *S. aureus* and *E. coli.* It should be, however, stressed that the monocytes differ considerably from the macrophages. (e.g. with distribution of receptors). Last, but not least, the monocytes could be activated as strong as macrophages, and still be unable to perform the phagocythosis, since the activation of the immune functions and phagocytosis can but do not have to go in parallel. Taken together, it became clear that the biological function of EPS should be taken under closer investigation. Treatment of bovine

macrophages by EPS-coated material would give a clear answer whether or not the EPS is an important virulent factor in bovine mastitis caused by *S. uberis.*

5.3. Mutant O140J::IS*S1*P'(*sub0538* & *sub0539*)

The resistance on antibiotic treatment of recurrent and chronic mastitis is one of the nightmares of the people involved in the dairy industry. Various reports show that the mastitis pathogens remain susceptible against common antimicrobial agents *in vitro* (Erskine et al., 2002). In spite of it, the result of mastitis therapy remains often disappointing since the health status of the udder does not improve or, after a short lag period from improvement, deteriorates again. The ability of many bacteria to grow in biofilms in infected tissues is responsible for the development of an innate resistance to most therapeutic agents (Melchior et al., 2006). The biofilm formation of pathogenic bacteria is composed of four steps, and each step is characterized by different gene expression pattern. The first step – initial attachment to the eukaryotic cells – is considered as a first step of infection by many pathogens. Then follow: cellular aggregation, clumping and production of extracellular polysaccharides (CPS or/and EPS) and finally, after maturation, detachment of planctonic cells (Donlan, 2001).

The role of glycolipids in adherence to epithelial cells and biofilm formation was studied by Theilacker *et al* (Theilacker et al., 2009). In that study the *bgsA* gene encoding for a glycosyltransferase synthesizing DGlcDAG from MGlcDAG in *E. faecalis* was inactivated. The results clearly demonstrated that the knock-out strain was almost completely impaired in biofilm formation on plastic surfaces and adherence to Caco-2 cells. In the model of mouse bactaeremia, the *ΔbgsA* mutant was faster cleared from the blood stream than the wild type strain. In the same study it was observed that the overexpression of *bgsA* resulted in increased biofilm production (Theilacker et al., 2009). Later, the same group knocked out the *bgsB,* gene encoding for a glucosyltransferase that synthesizes MGlcDAG from diacylglycerol. The changes in adhesion, adherence and biofilm formation of this mutant were comparable to those observed in *ΔbgsA* (Theilacker et al., 2011). Another group was using a mutant of *S. agalactiae* in the *iagA* gene (*iagA* is a functional homolog of *bgsA*) and they could show, that this gene was critical for bacterial invasion in brain microvascular endothelial cells (Doran et al., 2005).

The pathogenicity of the discussed mutants was strongly reduced. Here it was investigated if the *S. uberis* mutant, impaired in production of DGlcDAG from MGlcDAG would arrest biofilm formation.

The gene *sub0538* of *S. uberis* was identified using BLAST. Its product shares a high similarity to BgsA of *E. faecalis* (58%) and IagA of *S. agalactiae* (72%). We used the established method of genotyping selection of the mutant from the mutant bank, possessing insert built in the gene of interest (Taylor et al., 2003). The mutant bank consisted of 9000 mutants and was generated utilizing the method of transposon mutagenesis with plasmid pGh9::IS*S1* in 2001 by the group of J. Leigh (Ward et al., 2001). The insertion of the transposable element IS*S1* was reported to be random with a lesion every ~ 200 bp. The size of *sub0538* was 999 bp, therefore the theoretical by expected amount of mutants with insertion in the gene of interest to be found in the mutant bank was 5. Despite the fact, that the mutant bank was screened in both directions (expecting that the insert can build in 5'→3' or 3'→5') only one candidate was found which turned out to have an insert in the non-coding sequence, upstream the *sub0538*. Later attempts to obtain the mutant utilizing the targeted mutagenesis failed also. Based on those two facts it was postulated that the knock out of the *S. uberis sub0538* gene was lethal for the bacterium.

Thus, a closer look was taken at the only mutant obtained, and it was found out that the insertion occurred in the -35 cassette of the promoter region (Fig. 27). The element -35 is an attribute of strong promoters, which allow a high level gene expression. Mutations in this region result in a decreased genes expression level (Cooper, 2000). Moreover, it was found that *sub0538* was in a cluster together with *sub0539,* the product of which is a functional homolog of BgsB in *E. facealis*. The expression of the *sub0538* was measured and it was shown that it was more than 5 times lower than in the wild type. Additionally, the glycolipids from the mutated strain were isolated and analyzed by TLC plate. The experiment was repeated 3 times and the result was always the same, i.e. much lower intensity of the bands corresponding to MGlcDAG (G1) and DGlcDAG (G2) in case of the mutated strain, when compared to the wild type and other *S. uberis* strains. The colony morphology of the mutant did not differ from that of the wild type.

Then, it was investigated whether the lower expression of *sub0538* and probably *sub0539* (we did not examine the expression of this gene) influenced the biofilm formation. It was demonstrated that the mutant almost arrested the production of the biofilm on the plastic surfaces (the difference to the control was not significant, *t*-test, unpaired * $p < 0.05$).

There was a significant difference in biofilm production between the mutant and wild type. However, it was observed that strain O140J was the worst biofilm producer compared to the other clinical isolates (T1-18, 233). The avirulent strain EF20 showed a similar ability to form a biofilm as O140J, a fact that had already been reported (Crowley et al., 2011).

Thus, it was confirmed that the glycolipids were involved in biofilm formation. Furthermore, it was shown that already their decreased amounts in the cell membrane negatively influenced this process in *S. uberis*. The *E. faecalis ΔbgsA* mutant was shown to be more rapidly removed from the system in a mouse model. We do not yet know whether the O140J::IS*S1*P'(*sub0538* & *sub0539*) mutant could develop the infection in the udder, neither if the immune system of the cow could manage the mutant better than the wild type. If it was the case, then an inhibitor of the glucotransferase encoded by the *sub0538* could be a target for a drug of the *S. uberis* mastitis.

6. Summary

Mastitis, namely infection and inflammation of the udder in cattle, is of prime economic importance in dairy industry and one of its most important pathogen is *Streptococcus uberis*. So far there is no effective vaccination against *S. uberis* available on the market, no rapid diagnostic tests and the classical antibiotic treatment leaves much to be desired. Despite the fact, that many virulence factors have been proposed, the pathogenicity of the bacterium remains not clear.

To make further progress in this field of research, the main goal of this thesis was to isolate cell envelope components, determine their structures and to investigate their biological functions.

Six different cell envelope components were isolated and their structures were determined. The structures of the glycolipids and lipoteichoic acid (LTA) isolated from *S. uberis* are quite common among Gram-positive bacteria. The wall teichoic acid (WTA) possessed a simple structure of repeating unit, namely phosphoglycerol substituted non-stoichiometrically by β-Glc, still this substitution in WTA has to our knowledge never been reported. The neutral polysaccharides from Gram-positive bacteria have not been studied very intensively, therefore it cannot be judged if the presence of two rhamnans is specific only for *S. uberis* or occurs also in other bacteria. The structures of rhamnans have not been published before. The presence of capsular polysaccharide (CPS) in *S. uberis* has been known for at least 23 years, and it was conjectured that it was composed of hyaluronic acid. This study confirmed this presumption by analyzing the molecule utilizing NMR spectroscopy. Additionally, a mannose-rich, highly branched exopolysaccharide (EPS) was produced by *S. uberis*. Its structure was, however, similar to some exopolysaccharides produced by other microbes, but differed from them to some extend, making it unique.

This study provides also a comprehensive survey of pro-inflammatory genes found to be stimulated by *S. uberis* heat-inactivated cells and cell envelope components in bovine mammary epithelial cells and murine macrophages. *S. uberis* could not be recognized by the bovine TLR2 receptor and remained invisible the primary bovine mammary epithelial cells (pbMEC), the most abundant cells in the udder. The failure to elicit the immune response seemed to be pbMEC-specific, since the induction of immune genes occurred in a murine macrophages cell line (RAW 264.7). On the other hand it was shown that the LTA (isolated from various strains of *S. uberis*) was a strong stimulus of pbMEC. The

stimulation with LTA occurred through a TLR2-independent way. Therefore, it was concluded that active or passive mechanisms mask PAMPs and/or prohibit an adequate response. On the search of the 'magic hood' of *S. uberis* it was proven that not the CPS (composed of hyaluronic acid) act in this role. Then, a novel EPS, never reported to be produced by *S. uberis*, was found and examined for its antiphagocytic effect. The results obtained from the phagocytosis assay did not prove this hypothesis, but it became clear that the repetition of the experiment in a more complex form is needed.

It was also found that the glycolipids were involved in biofilm formation. Deletion of the gene encoding for the glycosyltransferase synthesizing DGlcDAG seemed to be lethal for *S. uberis*. A mutant with a reduced expression (5.77 times) of this gene was impaired in biofilm formation.

Thus, this study gave much information about the immune capacity of MEC during infection with *S. uberis* and it provided novel knowledge about the cell envelope components of this bacterium, their biological activity and possible functions. Furthermore, this knowledge can be exploited for *S. uberis* diagnosis and therapy. The novel EPS could find a potential application as a target for rapid diagnostic tests whereas the inhibitor of DGlcDAG glycotransferase (if the biofilm plays an important role in *S. uberis* mastitis) could be an additive to antibiotic treatment.

7. References

Aderem, A., and Ulevitch, R.J. (2000). Toll-like receptors in the induction of the innate immune response. Nature *406*, 782–787.

Akers, R.M., and Nickerson, S.C. (2011). Mastitis and its impact on structure and function in the ruminant mammary gland. Journal of Mammary Gland Biology and Neoplasia *16*, 275–289.

Akira, S., and Takeda, K. (2004). Toll-like receptor signalling. Nature Reviews Immunology *4*, 499–511.

Akira, S., Uematsu, S., and Takeuchi, O. (2006). Pathogen recognition and innate immunity. Cell *124*, 783–801.

Alluwaimi, A.M. (2004). The cytokines of bovine mammary gland: prospects for diagnosis and therapy. Research in Veterinary Science *77*, 211–222.

Almeida, R.A., and Oliver, S.P. (1993). Growth curve, capsule expression and characterization of the capsular material of selected strains of *Streptococcus uberis*. Journal of Veterinary Medicine, Series B *40*, 697–706.

Altman, E., Schäffer, C., Brisson, J.R., and Messner, P. (1996). Isolation and characterization of an amino sugar-rich glycopeptide from the surface layer glycoprotein of *Thermoanaerobacterium thermosaccharolyticum* E207-71. Carbohydr. Res. *295*, 245–253.

Amano, K., Araki, Y., and Ito, E. (1980). Effect of *N*-Acyl substitution at glucosamine residues on lysozyme-catalyzed hydrolysis of cell-wall peptidoglycan and its oligosaccharides. European Journal of Biochemistry *107*, 547–553.

Araki, Y., and Ito, E. (1989). Linkage units in cell walls of gram-positive bacteria. Crit. Rev. Microbiol. *17*, 121–135.

Atilano, M.L., Pereira, P.M., Yates, J., Reed, P., Veiga, H., Pinho, M.G., and Filipe, S.R. (2010). Teichoic acids are temporal and spatial regulators of peptidoglycan cross-linking in *Staphylococcus aureus*. Proc. Natl. Acad. Sci. U.S.A. *107*, 18991–18996.

Baldassarri, L., Cecchini, R., Bertuccini, L., Ammendolia, M.G., Iosi, F., Arciola, C.R., Montanaro, L., Rosa, R.D., Gherardi, G., Dicuonzo, G., et al. (2001). *Enterococcus* spp. produces slime and survives in rat peritoneal macrophages. Med Microbiol Immunol *190*, 113–120.

Bannerman, D.D. (2009). Pathogen-dependent induction of cytokines and other soluble inflammatory mediators during intramammary infection of dairy cows. J ANIM SCI *87*, 10–25.

Bannerman, D.D., Paape, M.J., Goff, J.P., Kimura, K., Lippolis, J.D., and Hope, J.C. (2004). Innate immune response to intramammary infection with *Serratia marcescens* and *Streptococcus uberis*. Veterinary Research *35*, 681–700.

Barlow, J. (2011). Mastitis therapy and antimicrobial susceptibility: a multispecies review with a focus on antibiotic treatment of mastitis in dairy cattle. Journal of Mammary Gland Biology and Neoplasia *16*, 383–407.

Bazaka, K., Crawford, R.J., Nazarenko, E.L., and Ivanova, E.P. (2011). Bacterial extracellular polysaccharides in bacterial adhesion, D. Linke, and A. Goldman, eds. (Springer Netherlands), pp. 213–226.

Belardelli, F., and Ferrantini, M. (2002). Cytokines as a link between innate and adaptive antitumor immunity. Trends in Immunology *23*, 201–208.

Bera, A., Biswas, R., Herbert, S., Kulauzovic, E., Weidenmaier, C., Peschel, A., and Götz, F. (2007). Influence of wall teichoic acid on lysozyme resistance in *Staphylococcus aureus*. J. Bacteriol. *189*, 280–283.

Berghaus, L.J., Moore, J.N., Hurley, D.J., Vandenplas, M.L., Fortes, B.P., Wolfert, M.A., and Boons, G.-J. (2010). Innate immune responses of primary murine macrophage-lineage cells and RAW 264.7 cells to ligands of Toll-like receptors 2, 3, and 4. Comp. Immunol. Microbiol. Infect. Dis. *33*, 443–454.

Bitton, G., and Freihofer, V. (1977). Influence of extracellular polysaccharides on the toxicity of copper and cadmium toward *Klebsiella aerogenes*. Microb Ecol *4*, 119–125.

Blowey, R., and Edmondson, P. (2010). Mastitis control in dairy herds (CABI).

Botos, I., Segal, D.M., and Davies, D.R. (2011). The structural biology of Toll-like receptors. Structure *19*, 447–459.

Bougarn, S., Cunha, P., Harmache, A., Fromageau, A., Gilbert, F.B., and Rainard, P. (2010). Muramyl dipeptide synergizes with *Staphylococcus aureus* lipoteichoic acid to recruit neutrophils in the mammary gland and to stimulate mammary epithelial cells. Clin. Vaccine Immunol. *17*, 1797–1809.

Bradley, A.J. (2002). Bovine mastitis: an evolving disease. The Veterinary Journal *164*, 116–128.

Van Calsteren, M.-R., Gagnon, F., Lacouture, S., Fittipaldi, N., and Gottschalk, M. (2010). Structure determination of *Streptococcus suis* serotype 2 capsular polysaccharide. Biochemistry and Cell Biology *88*, 513–525.

Cartwright, K. (2002). Pneumococcal disease in western Europe: burden of disease, antibiotic resistance and management. Eur J Pediatr *161*, 188–195.

Cava, F., De Pedro, M.A., Schwarz, H., Henne, A., and Berenguer, J. (2004). Binding to pyruvylated compounds as an ancestral mechanism to anchor the outer envelope in primitive bacteria. Mol. Microbiol. *52*, 677–690.

Cieslewicz, M.J., Chaffin, D., Glusman, G., Kasper, D., Madan, A., Rodrigues, S., Fahey, J., Wessels, M.R., and Rubens, C.E. (2005). Structural and genetic diversity of group B *Streptococcus* capsular polysaccharides. Infect. Immun. *73*, 3096–3103.

Ciuffreda, P., Casati, S., and Manzocchi, A. (2007). Complete ^{1}H and ^{13}C NMR spectral assignment of alpha- and beta-adenosine, 2'-deoxyadenosine and their acetate derivatives. Magn Reson Chem *45*, 781–784.

Clarke-Sturman, A.J., Archibald, A.R., Hancock, I.C., Harwood, C.R., Merad, T., and Hobot, J.A. (1989). Cell wall assembly in *Bacillus subtilis*: partial conservation of polar wall material and the effect of growth conditions on the pattern of incorporation of new material at the polar caps. J. Gen. Microbiol. *135*, 657–665.

Cooper, G.M. (2000). Transcription in *Prokaryotes*.

Corsaro, M.M., De Castro, C., Evidente, A., Lanzetta, R., Molinaro, A., Mugnai, L., Parrilli, M., and Surico, G. (1998). Chemical structure of two phytotoxic exopolysaccharides produced by *Phomopsis foeniculi*. Carbohydrate Research *308*, 349–357.

Corsaro, M.M., Evidente, A., Lanzetta, R., Lavermicocca, P., and Molinaro, A. (2001). Structural determination of the phytotoxic mannan exopolysaccharide from *Pseudomonas syringae pv. ciccaronei*. Carbohydrate Research *330*, 271–277.

Crowley, R.C., Leigh, J.A., Ward, P.N., Lappin-Scott, H.M., and Bowler, L.D. (2011). Differential protein expression in *Streptococcus uberis* under planktonic and biofilm growth conditions. Appl. Environ. Microbiol. *77*, 382–384.

D'Elia, M.A., Millar, K.E., Beveridge, T.J., and Brown, E.D. (2006). Wall teichoic acid polymers are dispensable for cell viability in *Bacillus subtilis*. J. Bacteriol. *188*, 8313–8316.

DeAngelis, P.L., Papaconstantinou, J., and Weigel, P.H. (1993). Molecular cloning, identification, and sequence of the hyaluronan synthase gene from group A *Streptococcus pyogenes*. J. Biol. Chem. *268*, 19181–19184.

Delcour, J., Ferain, T., Deghorain, M., Palumbo, E., and Hols, P. (1999). The biosynthesis and functionality of the cell-wall of lactic acid bacteria. Antonie Van Leeuwenhoek *76*, 159–184.

Dinarello, C.A. (2000). Proinflammatory Cytokines. CHEST *118*, 503–508.

Donlan, R.M. (2001). Biofilm formation: a clinically relevant microbiological process. Clin Infect Dis. *33*, 1387–1392.

Doran, K.S., Engelson, E.J., Khosravi, A., Maisey, H.C., Fedtke, I., Equils, O., Michelsen, K.S., Arditi, M., Peschel, A., and Nizet, V. (2005). Blood-brain barrier invasion by group B *Streptococcus* depends upon proper cell-surface anchoring of lipoteichoic acid. Journal of Clinical Investigation *115*, 2499–2507.

Endl, J., Seidl, H.P., Fiedler, F., and Schleider, K.H. (1983). Chemical composition and structure of cell wall teichoic acids of staphylococci. Archives of Microbiology *135*, 215–223.

Erskine, R.J., Walker, R.D., Bolin, C.A., Bartlett, P.C., and White, D.G. (2002). Trends in antibacterial susceptibility of mastitis pathogens during a seven-year period. Journal of Dairy Science *85*, 1111–1118.

Eskola, J., Peltola, H., Takala, A.K., Käyhty, H., Hakulinen, M., Karanko, V., Kela, E., Rekola, P., Rönnberg, P.R., and Samuelson, J.S. (1987). Efficacy of *Haemophilus influenzae* type B polysaccharide-diphtheria toxoid conjugate vaccine in infancy. N. Engl. J. Med. *317*, 717–722.

Fabretti, F., Theilacker, C., Baldassarri, L., Kaczynski, Z., Kropec, A., Holst, O., and Huebner, J. (2006). Alanine esters of enterococcal lipoteichoic acid play a role in biofilm formation and resistance to antimicrobial peptides. Infect. Immun. *74*, 4164–4171.

Farhat, K., Sauter, K.-S., Brcic, M., Frey, J., Ulmer, A.J., and Jungi, T.W. (2008). The response of HEK293 cells transfected with bovine TLR2 to established pathogen-associated molecular patterns and to bacteria causing mastitis in cattle. Veterinary Immunology and Immunopathology *125*, 326–336.

Fernebro, J., Andersson, I., Sublett, J., Morfeldt, E., Novak, R., Tuomanen, E., Normark, S., and Normark, B.H. (2004). Capsular expression in *Streptococcus pneumoniae* negatively affects spontaneous and antibiotic-induced lysis and contributes to antibiotic tolerance. J Infect Dis. *189*, 328–338.

Field, T.R., Ward, P.N., Pedersen, L.H., and Leigh, J.A. (2003). The hyaluronic acid capsule of *Streptococcus uberis* is not required for the development of infection and clinical mastitis. Infection and Immunity *71*, 132–139.

Finch, J.M., Winter, A., Walton, A.W., and Leigh, J.A. (1997). Further studies on the efficacy of a live vaccine against mastitis caused by *Streptococcus uberis*. Vaccine *15*, 1138–1143.

Fischer, K., Stein, K., Ulmer, A.J., Lindner, B., Heine, H., and Holst, O. (2011). Cytokine-inducing lipoteichoic acids of the allergy-protective bacterium *Lactococcus lactis* G121 do not activate *via* Toll-like receptor 2. Glycobiology *21*, 1588–1595.

Fischer, K., Vinogradov, E., Lindner, B., Heine, H., and Holst, O. (2012). The structure of the extracellular teichoic acids from the allergy-protective bacterium *Lactococcus lactis* G121. Biological Chemistry *393*, 749-755.

Fischer, W. (1988). Physiology of lipoteichoic acids in bacteria. Adv. Microb. Physiol. *29*, 233–302.

Fontaine, M.C., Perez-Casal, J., Song, X.-M., Shelford, J., Willson, P.J., and Potter, A.A. (2002). Immunisation of dairy cattle with recombinant *Streptococcus uberis* GapC or a chimeric CAMP antigen confers protection against heterologous bacterial challenge. Vaccine *20*, 2278–2286.

Fournier, J.M., Bouvet, A., Mathieu, D., Nato, F., Boutonnier, A., Gerbal, R., Brunengo, P., Saulnier, C., Sagot, N., and Slizewicz, B. (1993). New latex reagent using monoclonal antibodies to capsular polysaccharide for reliable identification of both oxacillin-susceptible and oxacillin-resistant *Staphylococcus aureus*. J. Clin. Microbiol. *31*, 1342–1344.

Graham, F.L., Smiley, J., Russell, W.C., and Nairn, R. (1977). Characteristics of a human cell line transformed by DNA from human adenovirus type 5. J Gen Virol *36*, 59–72.

Greenberg, J.W., Fischer, W., and Joiner, K.A. (1996). Influence of lipoteichoic acid structure on recognition by the macrophage scavenger receptor. Infect. Immun. *64*, 3318–3325.

Griesbeck-Zilch, B., Meyer, H.H.D., Kühn, C., Schwerin, M., and Wellnitz, O. (2008). *Staphylococcus aureus* and *Escherichia coli* cause deviating expression profiles of cytokines and lactoferrin messenger ribonucleic acid in mammary epithelial cells. Journal of Dairy Science *91*, 2215–2224.

Günther, J., Esch, K., Poschadel, N., Petzl, W., Zerbe, H., Mitterhuemer, S., Blum, H., and Seyfert, H.-M. (2011). Comparative kinetics of *Escherichia coli*- and *Staphylococcus aureus*-specific activation of key immune pathways in mammary epithelial cells demonstrates that *S. aureus* elicits a delayed response dominated by interleukin-6 (IL-6) but not by IL-1A or tumor necrosis factor alpha. Infect. Immun. *79*, 695–707.

Günther, J., Koczan, D., Yang, W., Nürnberg, G., Repsilber, D., Schuberth, H.-J., Park, Z., Maqbool, N., Molenaar, A., and Seyfert, H.-M. (2009). Assessment of the immune capacity of mammary epithelial cells: comparison with mammary tissue after challenge with *Escherichia coli*. Veterinary Research *40*, 31.

Günther, J., Liu, S., Esch, K., Schuberth, H.-J., and Seyfert, H.-M. (2010). Stimulated expression of TNF-α and IL-8, but not of lingual antimicrobial peptide reflects the concentration of pathogens contacting bovine mammary epithelial cells. Veterinary Immunology and Immunopathology *135*, 152–157.

Harada, A., Sekido, N., Akahoshi, T., Wada, T., Mukaida, N., and Matsushima, K. (1994). Essential involvement of interleukin-8 (IL-8) in acute inflammation. J Leukoc Biol *56*, 559–564.

Heinrich, P.C., Behrmann, I., Haan, S., Hermanns, H.M., MüLler-Newen, G., and Schaper, F. (2003). Principles of interleukin (IL)-6-type cytokine signalling and its regulation. Biochemical Journal *374*, 1-20.

Hirschfeld, M., Kirschning, C.J., Schwandner, R., Wesche, H., Weis, J.H., Wooten, R.M., and Weis, J.J. (1999). Cutting Edge: Inflammatory signaling by *Borrelia burgdorferi* lipoproteins is mediated by Toll-like receptor 2. J Immunol *163*, 2382–2386.

Hirschfeld, M., Weis, J.J., Toshchakov, V., Salkowski, C.A., Cody, M.J., Ward, D.C., Qureshi, N., Michalek, S.M., and Vogel, S.N. (2001). Signaling by Toll-like receptor 2 and 4 agonists results in differential gene expression in murine macrophages. Infect. Immun. *69*, 1477–1482.

Holst, O. (2000). Deacylation of lipopolysaccharides and isolation of oligosaccharide phosphates. In Bacterial Toxins: Methods and Protocols, O. Holst, and J.M. Walker, eds. (Humana Press), pp. 345–353.

Hölzl, G., and Dörmann, P. (2007). Structure and function of glycoglycerolipids in plants and bacteria. Progress in Lipid Research *46*, 225–243.

Houde, M., Gottschalk, M., Gagnon, F., Van Calsteren, M.-R., and Segura, M. (2011). *Streptococcus suis* capsular polysaccharide inhibits phagocytosis through destabilization of lipid microdomains and prevents lactosylceramide-dependent recognition. Infection and Immunity *80*, 506–517.

Huebner, J., Wang, Y., Krueger, W.A., Madoff, L.C., Martirosian, G., Boisot, S., Goldmann, D.A., Kasper, D.L., Tzianabos, A.O., and Pier, G.B. (1999). Isolation and chemical characterization of a capsular polysaccharide antigen shared by clinical isolates of *Enterococcus faecalis* and vancomycin-eesistant *Enterococcus faecium*. Infect. Immun. *67*, 1213–1219.

Jarosch, M., Egelseer, E.M., Mattanovich, D., Sleytr, U.B., and Sára, M. (2000). S-layer gene sbsC of *Bacillus stearothermophilus* ATCC 12980: molecular characterization and heterologous expression in *Escherichia coli*. Microbiology *146*, 273–281.

Jin, M.S., Kim, S.E., Heo, J.Y., Lee, M.E., Kim, H.M., Paik, S.-G., Lee, H., and Lee, J.-O. (2007). Crystal structure of the TLR1-TLR2 heterodimer induced by binding of a tri-acylated lipopeptide. Cell *130*, 1071–1082.

Jorasch, P., Warnecke, D.C., Lindner, B., Zähringer, U., and Heinz, E. (2000). Novel processive and nonprocessive glycosyltransferases from *Staphylococcus aureus* and *Arabidopsis thaliana* synthesize glycoglycerolipids, glycophospholipids, glycosphingolipids and glycosylsterols. European Journal of Biochemistry *267*, 3770–3783.

Kang, J.Y., Nan, X., Jin, M.S., Youn, S.-J., Ryu, Y.H., Mah, S., Han, S.H., Lee, H., Paik, S.-G., and Lee, J.-O. (2009). Recognition of lipopeptide patterns by Toll-like receptor 2-Toll-like receptor 6 heterodimer. Immunity *31*, 873–884.

Karakawa, W.W., Sutton, A., Schneerson, R., Karpas, A., and Vann, W.F. (1988). Capsular antibodies induce type-specific phagocytosis of capsulated *Staphylococcus aureus* by human polymorphonuclear leukocytes. Infect. Immun. *56*, 1090–1095.

Kinjo, Y., Illarionov, P., Vela, J.L., Pei, B., Girardi, E., Li, X., Li, Y., Imamura, M., Kaneko, Y., Okawara, A., et al. (2011). Invariant natural killer T cells recognize glycolipids from pathogenic Gram-positive bacteria. Nature Immunology *12*, 966–974.

Koch, H.U., and Fischer, W. (1978). Acyldiglucosyldiacylglycerol-containing lipoteichoic acid with a poly(3-O-galabiosyl-2-O-galactosyl-sn-glycero-1-phosphate) chain from *Streptococcus lactis* Kiel 42172. Biochemistry *17*, 5275–5281.

Kocourek, J., and Ballou, C.E. (1969). Method for fingerprinting yeast cell wall mannans. J. Bacteriol. *100*, 1175–1181.

Kohler, T., Weidenmaier, C., and Peschel, A. (2009). Wall teichoic acid protects *Staphylococcus aureus* against antimicrobial fatty acids from human skin. J. Bacteriol. *191*, 4482–4484.

Koskiniemi, S., Sellin, M., and Norgren, M. (1998). Identification of two genes, *cpsX* and *cpsY*, with putative regulatory function on capsule expression in group B streptococci. FEMS Immunology & Medical Microbiology *21*, 159–168.

Kumar, H., Kawai, T., and Akira, S. (2009). Toll-like receptors and innate immunity. Biochem. Biophys. Res. Commun. *388*, 621–625.

Kumar, H., Kawai, T., and Akira, S. (2011). Pathogen recognition by the innate immune system. International Reviews of Immunology *30*, 16–34.

Kurokawa, K., Gong, J.-H., Ryu, K.-H., Zheng, L., Chae, J.-H., Kim, M.-S., and Lee, B.L. (2011). Biochemical characterization of evasion from peptidoglycan recognition by *Staphylococcus aureus*

D-alanylated wall teichoic acid in insect innate immunity. Developmental & Comparative Immunology *35*, 835–839.

Lahouassa, H., Moussay, E., Rainard, P., and Riollet, C. (2007). Differential cytokine and chemokine responses of bovine mammary epithelial cells to *Staphylococcus aureus* and *Escherichia coli*. Cytokine *38*, 12–21.

Leigh, J.A. (1999). *Streptococcus uberis*: a permanent barrier to the control of bovine mastitis? Vet. J. *157*, 225–238.

Leigh, J.A., Egan, S.A., Ward, P.N., Field, T.R., and Coffey, T.J. (2010). Sortase anchored proteins of *Streptococcus uberis* play major roles in the pathogenesis of bovine mastitis in dairy cattle. Veterinary Research *41*, 63.

Leigh, J.A., and Field, T.R. (1991). Killing of *Streptococcus uberis* by bovine neutrophils following growth in chemically defined media. Vet Res Commun *15*, 1–6.

Leigh, J.A., Field, T.R., and Williams, M.R. (1990). Two strains of *Streptococcus uberis*, of differing ability to cause clinical mastitis, differ in their ability to resist some host defence factors. Res. Vet. Sci. *49*, 85–87.

Lin, S.C., Lo Y.C., and Wu H. (2010). Helical assembly in the MyD88-IRAK4-IRAK2 complex in TLR/IL-1R signaling. Nature *465*, 885-891.

Melchior, M.B., Vaarkamp, H., and Fink-Gremmels, J. (2006). Biofilms: A role in recurrent mastitis infections? The Veterinary Journal *171*, 398–407.

Mesnage, S., Fontaine, T., Mignot, T., Delepierre, M., Mock, M., and Fouet, A. (2000). Bacterial SLH domain proteins are non-covalently anchored to the cell surface *via* a conserved mechanism involving wall polysaccharide pyruvylation. EMBO J. *19*, 4473–4484.

Milne, M.H., Biggs, A.M., Barrett, D.C., Young, F.J., Doherty, S., Innocent, G.T., and Fitzpatrick, J.L. (2005). Treatment of persistent intramammary infections with *Streptococcus uberis* in dairy cows. Veterinary Record *157*, 245–250.

Molenaar, C., Wiesmeijer, K., Verwoerd, N.P., Khazen, S., Eils, R., Tanke, H.J., and Dirks, R.W. (2003). Visualizing telomere dynamics in living mammalian cells using PNA probes. The EMBO Journal *22*, 6631–6641.

Moore, G.E., and Woods, L.K. (1977). Culture media for human cells—RPMI 1603, RPMI 1634, RPMI 1640 and GEM 1717. Tca Manual *3*, 503–509.

Morath, S. (2001). Structure-function relationship of cytokine induction by lipoteichoic acid from *Staphylococcus aureus*. Journal of Experimental Medicine *193*, 393–398.

Nazarenko, E.L., Komandrova, N.A., Gorshkova, R.P., Tomshich, S.V., Zubkov, V.A., Kilcoyne, M., and Savage, A.V. (2003). Structures of polysaccharides and oligosaccharides of some Gram-negative marine *Proteobacteria*. Carbohydrate Research *338*, 2449–2457.

Neuhaus, F.C., and Baddiley, J. (2003). A Continuum of Anionic Charge: Structures and Functions of d-Alanyl-Teichoic Acids in Gram-Positive Bacteria. Microbiol Mol Biol Rev *67*, 686–723.

Nolan, T., Richmond, P., Marshall, H., McVernon, J., Alexander, K., Mesaros, N., Aris, E., Miller, J., Poolman, J., and Boutriau, D. (2011). Immunogenicity and safety of an investigational combined *Haemophilus influenzae* type B-*Neisseria meningitidis* serogroups C and Y-tetanus toxoid conjugate vaccine. Pediatr. Infect. Dis. J. *30*, 190–196.

Oku, Y., Kurokawa, K., Matsuo, M., Yamada, S., Lee, B.-L., and Sekimizu, K. (2009). Pleiotropic roles of polyglycerolphosphate synthase of lipoteichoic acid in growth of *Staphylococcus aureus* cells. J. Bacteriol. *191*, 141–151.

Oliver, S.P., Almeida, R.A., and Calvinho, L.F. (1998). Virulence factors of *Streptococcus uberis* isolated from cows with mastitis. Journal of Veterinary Medicine, Series B *45*, 461–471.

Pareek, R., Wellnitz, O., Van Dorp, R., Burton, J., and Kerr, D. (2005). Immunorelevant gene expression in LPS-challenged bovine mammary epithelial cells. J. Appl. Genet. *46*, 171–177.

Pedersen, C.M., Figueroa-Perez, I., Boruwa, J., Lindner, B., Ulmer, A.J., Zähringer, U., and Schmidt, R.R. (2010). Synthesis of the core structure of the lipoteichoic acid of *Streptococcus pneumoniae*. Chemistry – A European Journal *16*, 12627–12641. Identification of genes and regulation. J. Biol. Chem. *270*, 15598–15606.

Peschel, A. (1999). Inactivation of the *dlt* operon in *Staphylococcus aureus* confers sensitivity to defensins, protegrins, and other antimicrobial peptides. Journal of Biological Chemistry *274*, 8405–8410.

Peschel, A., Vuong, C., Otto, M., and Götz, F. (2000). The D-alanine residues of *Staphylococcus aureus* teichoic acids alter the susceptibility to vancomycin and the activity of autolytic enzymes. Antimicrob. Agents Chemother. *44*, 2845–2847.

Pum, D., Schuster, B., Sara, M., and Sleytr, U.B. (2004). Functionalisation of surfaces with S-layers. Nanobiotechnology, IEE Proceedings - *151*, 83 – 86.

Raschke, W.C. (1980). Transformation by Abelson Murine Leukemia Virus: Properties of the transformed cells. Cold Spring Harb Symp Quant Biol *44*, 1187–1194.

Reichmann, N.T., and Gründling, A. (2011). Location, synthesis and function of glycolipids and polyglycerolphosphate lipoteichoic acid in Gram-positive bacteria of the phylum *Firmicutes*. FEMS Microbiology Letters *319*, 97–105.

Riollet, C., Rainard, P., and Poutrel, B. (2001). Cell subpopulations and cytokine expression in cow milk in response to chronic *Staphylococcus aureus* infection. Journal of Dairy Science *84*, 1077–1084.

Riollet, C., Rainard, P., and Poutrel, B. (2002). Cells and cytokines in inflammatory secretions of bovine mammary Gland. In Biology of the Mammary Gland, J.A. Mol, and R.A. Clegg, eds. (Springer US), pp. 247–258.

Rosenberger, C.M., Scott, M.G., Gold, M.R., Hancock, R.E.W., and Finlay, B.B. (2000). *Salmonella typhimurium* infection and lipopolysaccharide stimulation induce similar changes in macrophage gene expression. J Immunol *164*, 5894–5904.

Sánchez Carballo, P.M., Vilen, H., Palva, A., and Holst, O. (2010). Structural characterization of teichoic acids from Lactobacillus brevis. Carbohydrate Research *345*, 538–542.

Sandal, I., Inzana, T.J., Molinaro, A., De Castro, C., Shao, J.Q., Apicella, M.A., Cox, A.D., St Michael, F., and Berg, G. (2011). Identification, structure, and characterization of an exopolysaccharide produced by *Histophilus somni* during biofilm formation. BMC Microbiology *11*, 186.

Sára, M. (2001). Conserved anchoring mechanisms between crystalline cell surface S-layer proteins and secondary cell wall polymers in Gram-positive bacteria? Trends Microbiol. *9*, 47–49; discussion 49–50.

Sava, I.G., Zhang, F., Toma, I., Theilacker, C., Li, B., Baumert, T.F., Holst, O., Linhardt, R.J., and Huebner, J. (2009). Novel interactions of glycosaminoglycans and bacterial glycolipids mediate binding of enterococci to human cells. Journal of Biological Chemistry *284*, 18194–18201.

Schäffer, C., Graninger, M., and Messner, P. (2001). Prokaryotic glycosylation. Proteomics *1*, 248–261.

Schäffer, C., Kählig, H., Christian, R., Schulz, G., Zayni, S., and Messner, P. (1999). The diacetamidodideoxyuronic-acid-containing glycan chain of *Bacillus stearothermophilus* NRS 2004/3a represents the secondary cell-wall polymer of wild-type *B. stearothermophilus* strains. Microbiology *145*, 1575–1583.

Schäffer, C., and Messner, P. (2001). Glycobiology of surface layer proteins. Biochimie *83*, 591–599.

Schäffer, C., and Messner, P. (2005). The structure of secondary cell wall polymers: how Gram-positive bacteria stick their cell walls together. Microbiology *151*, 643–651.

Schäffer, C., Müller, N., Mandal, P.K., Christian, R., Zayni, S., and Messner, P. (2000). A pyrophosphate bridge links the pyruvate-containing secondary cell wall polymer of *Paenibacillus alvei* CCM 2051 to muramic acid. Glycoconj. J. *17*, 681–690.

Schleifer, K.H., and Kandler, O. (1972). Peptidoglycan types of bacterial cell walls and their taxonomic implications. Bacteriol Rev *36*, 407–477.

Schmidt, R.R., Pedersen, C.M., Qiao, Y., and Zähringer, U. (2011). Chemical synthesis of bacterial lipoteichoic acids: An insight on its biological significance. Org. Biomol. Chem. *9*, 2040–2052.

Schröder, N.W.J., Heine, H., Alexander, C., Manukyan, M., Eckert, J., Hamann, L., Göbel, U.B., and Schumann, R.R. (2004). Lipopolysaccharide binding protein binds to triacylated and diacylated lipopeptides and mediates innate immune responses. J Immunol *173*, 2683–2691.

Schukken, Y.H., Günther, J., Fitzpatrick, J., Fontaine, M.C., Goetze, L., Holst, O., Leigh, J., Petzl, W., Schuberth, H.-J., Sipka, A., et al. (2011). Host-response patterns of intramammary infections in dairy cows. Veterinary Immunology and Immunopathology *144*, 270–289.

Schwandner, R., Dziarski, R., Wesche, H., Rothe, M., and Kirschning, C.J. (1999). Peptidoglycan- and lipoteichoic acid-induced cell activation is mediated by Toll-like receptor 2. J. Biol. Chem. *274*, 17406–17409.

Shaw, G., Morse, S., Ararat, M., and Graham, F.L. (2002). Preferential transformation of human neuronal cells by human adenoviruses and the origin of HEK293 cells. FASEB J *16*, 869–871.

Silhavy, T.J., Kahne, D., and Walker, S. (2010). The bacterial cell envelope. Cold Spring Harb Perspect Biol *2*,.

Steindl, C., Schäffer, C., Smrecki, V., Messner, P., and Müller, N. (2005). The secondary cell wall polymer of *Geobacillus tepidamans* GS5-97T: structure of different glycoforms. Carbohydr. Res. *340*, 2290–2296.

Steindl, C., Schäffer, C., Wugeditsch, T., Graninger, M., Matecko, I., Müller, N., and Messner, P. (2002). The first biantennary bacterial secondary cell wall polymer and its influence on S-layer glycoprotein assembly. Biochem. J. *368*, 483–494.

Strandberg, Y., Gray, C., Vuocolo, T., Donaldson, L., Broadway, M., and Tellam, R. (2005). Lipopolysaccharide and lipoteichoic acid induce different innate immune responses in bovine mammary epithelial cells. Cytokine *31*, 72–86.

Swanson, K.M., Stelwagen, K., Dobson, J., Henderson, H.V., Davis, S.R., Farr, V.C., and Singh, K. (2009). Transcriptome profiling of *Streptococcus uberis*-induced mastitis reveals fundamental differences between immune gene expression in the mammary gland and in a primary cell culture model. Journal of Dairy Science *92*, 117–129.

Taylor, D.L., Ward, P.N., Rapier, C.D., Leigh, J.A., and Bowler, L.D. (2003). Identification of a differentially expressed oligopeptide binding protein (OppA2) in *Streptococcus uberis* by representational difference analysis of cDNA. J. Bacteriol. *185*, 5210–5219.

Theilacker, C., Holst, O., Lindner, B., Huebner, J., and Kaczyński, Z. (2012). The structure of the wall teichoic acid isolated from *Enterococcus faecalis* strain 12030. Carbohydrate Research *354*, 106–109.

Theilacker, C., Kaczynski, Z., Kropec, A., Fabretti, F., Sange, T., Holst, O., and Huebner, J. (2006). Opsonic antibodies to *Enterococcus faecalis* strain 12030 are directed against lipoteichoic acid. Infection and Immunity *74*, 5703–5712.

Theilacker, C., Sanchez-Carballo, P., Toma, I., Fabretti, F., Sava, I., Kropec, A., Holst, O., and Huebner, J. (2009). Glycolipids are involved in biofilm accumulation and prolonged bacteraemia in *Enterococcus faecalis*. Molecular Microbiology *71*, 1055–1069.

Theilacker, C., Sava, I., Sanchez-Carballo, P., Bao, Y., Kropec, A., Grohmann, E., Holst, O., and Huebner, J. (2011). Deletion of the glycosyltransferase *bgsB* of *Enterococcus faecalis* leads to a complete loss of glycolipids from the cell membrane and to impaired biofilm formation. BMC Microbiology *11*, 67.

Thoma-Uszynski, S., Stenger, S., Takeuchi, O., Ochoa, M.T., Engele, M., Sieling, P.A., Barnes, P.F., Rollinghoff, M., Bolcskei, P.L., Wagner, M., et al. (2001). Induction of direct antimicrobial activity through mammalian Toll-like receptors. Science *291*, 1544–1547.

Tuomanen, E.I. (1996). Surprise? Bacteria glycosylate proteins too. J Clin Invest *98*, 2659–2660.

Uhlinger, D.J., and White, D.C. (1983). Relationship between physiological status and formation of extracellular polysaccharide glycocalyx in *Pseudomonas atlantica*. Appl. Environ. Microbiol. *45*, 64–70.

Updyke, E.L., and Nickle, M.I. (1954). A dehydrated medium for the preparation of type specific extracts of group A streptococci. Appl Microbiol *2*, 117–118.

Van Calsteren, M.-R., Gagnon, F., Lacouture, S., Fittipaldi, N., and Gottschalk, M. (2010). Structure determination of *Streptococcus suis* serotype 2 capsular polysaccharide. Biochemistry and Cell Biology *88*, 513–525.

Vergara-Irigaray, M., Maira-Litran, T., Merino, N., Pier, G.B., Penades, J.R., and Lasa, I. (2008). Wall teichoic acids are dispensable for anchoring the PNAG exopolysaccharide to the *Staphylococcus aureus* cell surface. Microbiology *154*, 865–877.

Vogel, S., and Wainwright, S.A. (1969). A functional bestiary - Laboratory studies about living systems.

Vollmer, W. (2008). Structural variation in the glycan strands of bacterial peptidoglycan. FEMS Microbiology Reviews *32*, 287–306.

Vollmer, W., Blanot, D., and De Pedro, M.A. (2008). Peptidoglycan structure and architecture. FEMS Microbiology Reviews *32*, 149–167.

Vu, B., Chen, M., Crawford, R.J., and Ivanova, E.P. (2009). Bacterial extracellular polysaccharides Involved in Biofilm Formation. Molecules *14*, 2535–2554.

Ward, J.B. (1981). Teichoic and teichuronic acids: biosynthesis, assembly, and location. Microbiol Rev *45*, 211–243.

Ward, P.N., Field, T.R., Ditcham, W.G.F., Maguin, E., and Leigh, J.A. (2001). Identification and disruption of two discrete loci encoding hyaluronic acid capsule biosynthesis. Genes *hasA*, *hasB*, and *hasC* in *Streptococcus uberis*. Infect. Immun. *69*, 392–399.

Watts, J.L. (1988). Etiological agents of bovine mastitis. Veterinary Microbiology *16*, 41–66.

Weidenmaier, C., McLoughlin, R.M., and Lee, J.C. (2010). The zwitterionic cell wall teichoic acid of *Staphylococcus aureus* provokes skin abscesses in mice by a novel CD4+ T-cell-dependent mechanism. PLoS ONE *5*, e13227.

Whitfield, C. (1988). Bacterial extracellular polysaccharides. Canadian Journal of Microbiology *34*, 415–420.

Wu, D., Fujio, M., and Wong, C.-H. (2008). Glycolipids as immunostimulating agents. Bioorganic & Medicinal Chemistry *16*, 1073–1083.

Xia, G., Kohler, T., and Peschel, A. (2010). The wall teichoic acid and lipoteichoic acid polymers of *Staphylococcus aureus*. International Journal of Medical Microbiology *300*, 148–154.

Yang, W., Molenaar, A., Kurtsebert, B., and Seyfert, H. (2006). NF-κB factors are essential, but not the switch, for pathogen-related induction of the bovine β-defensin 5-encoding gene in mammary epithelial cells. Molecular Immunology *43*, 210–225.

Yang, W., Zerbe, H., Petzl, W., Brunner, R.M., Günther, J., Draing, C., Von Aulock, S., Schuberth, H.-J., and Seyfert, H.-M. (2008). Bovine TLR2 and TLR4 properly transduce signals from *Staphylococcus aureus* and *E. coli*, but *S. aureus* fails to both activate NF-κB in mammary epithelial cells and to quickly induce TNFα and interleukin-8 (CXCL8) expression in the udder. Molecular Immunology *45*, 1385–1397.

Yother, J. (2011). Capsules of *Streptococcus pneumoniae* and other bacteria: paradigms for polysaccharide biosynthesis and regulation. Annual Review of Microbiology *65*, 563–581.

Zadoks, R., and Fitzpatrick, J. (2009). Changing trends in mastitis. Ir Vet J *62*, S59–S70.

Zadoks, R.N., Gillespie, B.E., Barkema, H.W., Sampimon, O.C., Oliver, S.P., and Schukken, Y.H. (2003). Clinical, epidemiological and molecular characteristics of *Streptococcus uberis* infections in dairy herds. Epidemiology and Infection *130*, 335–349.

Zähringer, U., Lindner, B., Inamura, S., Heine, H., and Alexander, C. (2008). TLR2 – promiscuous or specific? A critical re-evaluation of a receptor expressing apparent broad specificity. Immunobiology *213*, 205–224.

Zajonc, D.M., and Kronenberg, M. (2009). Carbohydrate specificity of the recognition of diverse glycolipids by natural killer T cells. Immunological Reviews *230*, 188–200.

8. Acknowledgements

There are many people whom I wish to thank and without whom this thesis would not have been the same.

First and foremost I would like to thank Prof. Dr. Otto Holst for giving me the opportunity to prepare my doctoral thesis in the Research Center Borstel. I am very grateful for his support in the project, many fruitful discussions and advices; on the other hand he gave me the chance to work with the high degree of autonomy. In this way the high interdisciplinary of this thesis was possible.

My special thanks go to Dr. Katarzyna Duda, who not only introduced me to all analytical methods described in this thesis, but was also sharing with me her knowledge about NMR analyses. She was always there when I needed her advice.

I am also very thankful for the fruitful cooperation with Prof. Hans-Martin Seyfert and Dr. Juliane Günther from the Leibniz-Institute for Farm Animal Biology (FBN), Molecular Biology Research Unit, Dummerstorf, Germany, who performed all stimulation experiments on HEK293, pbMEC and RAW 264.7 cells. Prof. Seyfert was also acting as my co-supervisor and was always willing to answer my questions regarding the immune response of examined cells.

Furthermore I wish to thank Prof. James Leigh and Dr. Sharon Egan from The University of Nottingham, The School of Veterinary Medicine and Science, UK, for their hospitality and help in isolating the *S. uberis* mutant. The time spent in Nottingham was of great importance for my knowledge and skills. Thank you very much for the discussions during and after my stay.

In regard of the isolated *S. uberis* mutant I appreciate the help of PD Dr. Norbert Reiling and Julius Brandenburg from Microbial Interface Biology, Research Center Borstel for investigating the *sub0538* gene expression.

I would like to thank Prof. Dr Hans-Joachim Schuberth and Jamal Hussen from University of Veterinary Medicine, Immunology Unit, Hannover, Germany, for phagocythosis and adherence experiments on bovine mononuclear cells.

For mass spectrometry I wish to thank PD Dr. Buko Lindner.

Special thanks go to Regina Engel for her help in isolation of the glycolipids and her support during the whole time of my thesis.

I am also very grateful to Hermann Moll for GLC-MS and great discussions on the structural studies of bacterial carbohydrates.

I would like to acknowledge Dr. Nicolas Gisch and Heiko Käßner for NMR recording.

I appreciate the help obtained from Dr. Uwe Mamat with anion-exchange chromatography.

I would like to thank all my other colleagues from the group of Structural Biochemistry for the friendly atmosphere in the lab, and for their help supporting my work.

The financial support by the Pfizer Animal Health is gratefully acknowledged.

Last, but not least, I wish to thank my family and my friends for their support and presence when I needed them the most.

Curriculum Vitae

List of publications

Printed publications

Structural analysis of the lipoteichoic acids isolated from bovine mastitis *Streptococcus uberis* 233, *Streptococcus dysgalactiae* 2023 and *Streptococcus agalactiae* 0250.
Czabanska, A., Neiwert, O., Lindner, B., Leigh, J., Holst, O., and Duda, K.A.
Carbohydrate Research, 2012, *361*, 200–205.

Chemical structures of the secondary cell wall polymers (SCWPs) isolated from bovine mastitis *Streptococcus uberis.*
Czabanska A., Holst O., Duda K.A.
Carbohydrate Research, 2013, *377*, 58–62.

Poster presentations

Characterization of glycolipids isolated from *Streptococcus uberis* and their role in biofilm formation.
Czabanska A., Egan S., Leigh J., Brandenburg J., Reiling N., Duda K.A., and Holst O.
4th Annual Interdisciplinary Symposium 2013 "Inflammation at Interfaces; Gene to Target - Target to Function - Function to Clinic", February 22-23rd 2013, Hamburg, Germany

Structural characterization of glycolipids isolated from various *Streptococcus uberis* strains.
Czabanska A., Seyfert H-M., Lindner B., and Holst O.
5th Baltic Meeting on Microbial Carbohydrates, September 2-6th, 2012, Suzdal, Russia

Structural investigations of the lipoteichoic acid isolated from *Streptococcus uberis* 233.
Czabanska A., Duda K.A.., and Holst O.
Physiology and Genomics of Mastitis, October 31st – November 2nd, 2011, Tutzing, Germany

Structural investigations of the lipoteichoic acid isolated from *Streptococcus uberis* 233 – structure of the lipid anchor.
Czabanska A., Duda K.A.., and Holst O.
XVI European Carbohydrate Symposium, July 3-8th, 2011, Sorrento, Italy

Erklärung

Die vorliegende Arbeit wurde von April 2010 bis Januar 2013 unter der Betreuung von Herrn Prof. Dr. Otto Holst am Forschungszentrum Borstel in der Forschergruppe Strukturbiochemie angefertigt. Ich versichere, dass ich die Dissertation ohne fremde Hilfe angefertigt und keine anderen als die angegebenen Hilfsmittel verwendet habe. Weder vorher noch gleichzeitig habe ich andernorts einen Zulassungsantrag gestellt oder diese Dissertation vorgelegt. Ich habe mich bisher noch keinem Promotionsverfahren unterzogen.

Anna Czabanska